UNIVERSITÁ DEGLI STUDI DI GENOVA

Dipartimento di Medicina Sperimentale (DIMES)

Dottorato in Biotecnologie in Medicina Traslazionale

Curriculum Medicina Rigenerativa e Ingegneria dei Tessuti

XXXII ciclo

Articular cartilage regenerative strategies based on platelet derivatives with perspective view in 3D-bioprinting technology

Coordinator:

Prof. Rodolfo Quarto

Tutor:

Prof.ssa Chiara Gentili

PhD Student

Simonetta Carluccio

Accademic Year 2019-20

Table of contents

Introduction

Articular cartilage is an unique and highly specialized connective tissue adapted to bear compressive loads and shear forces in synovial joints, which is a crucial function during body's motion. In adult joints, articular cartilage is composed by chondrocytes immersed in an intricate extracellular matrix, displaying a complex multi-zonal organization. Despite a relatively low metabolic activity within a harsh physical environment, chondrocytes are active in maintaining the matrix, thus allowing healthy tissue to sustain itself and carry out its functions.

Damage to tissue high level of organization and molecular architecture is a major source of morbidity for articular cartilage, thus it is usually susceptible to malfunction following acute injury or chronic diseases such as osteoarthritis. Cartilage has poor intrinsic repair and regenerative capacity, although it has been demonstrated to contain a subset of progenitors even in adults. These cells have shown to react to injury, but do not seem to be able to mount an effective tissue reparative or regenerative action when needed.

Hence, much effort has been devoted to finding ways by which articular cartilage repair could be induced and enhanced. Surgical techniques and bioengineered treatment options developed over recent decades have led to several clinical treatment modalities for acutely injured or osteoarthritic joints. To prevent progressive cartilage degeneration or to replace damaged tissue, the surgical treatment is often the only option, but it does not ensure full tissue function recovery. Therefore, regenerative medicine has emerged as an important field of research in the treatment of cartilage disorders. In this context, the medical community have shown great interest in therapeutic strategies based on the use of platelet-derived products, such as platelet rich plasma (PRP) and platelet lysate (PL). Since these derivatives are a mix of growth factors, cytokines and chemokines normally involved in tissue healing, the rationale behind their application is the re-activation of latent endogenous regenerative mechanisms.

PRP therapeutic use in musculoskeletal disorders have led to promising outcomes, although mechanism of action and efficacy of platelet products in orthopaedics still need to be elucidate.

The main objective of this PhD thesis is to study the effects of platelet derivatives on cartilage cell behaviour, including chondrocytes and chondro-progenitors, in order to highlight potentialities and even identify limits concerning their use, both useful in better direct biomedical applications in the field of articular cartilage therapy. Indeed, a better understanding of the events that could induce cartilage repair by PRP or PL may allow to clarify current experimental outcomes and offer the

opportunity to conceive innovative strategies or tools in cell therapy approach and in the latest tissue engineering technologies.

In this regard, it will be beneficial to find alternative options to cell transplantation (based on mesenchymal stem cells or chondrocytes) aimed in achieving cartilage regeneration, planning interventions focused on *in situ* stimulation of resident cell population or local progenitor niche in the joint, that are developmentally endowed with greater chondrogenic potential than traditional cell sources.

In parallel, the research in the field of tissue engineering continues to be active and innovative strategies for the fabrication of enhanced bioengineered grafts are recently emerging by the spreading of 3D-printing technology. 3D-bioprinting especially represents a developmental biology inspired alternative to classic scaffold-based approaches in the field, since it shows the ability to assemble biological components replicating complex native-like tissue architecture more faithfully than traditional methods of assembly as well as patient customization. In this context, bioprinted constructs may provide a solution for cartilage injuries and defects, despite 3D-bioprinting is still a technology in progress and consequently some challenges have to be overcome before its translation to clinical applications.

The research tasks of this work and the main obtained results are:

1) the *in vitro* characterization of human articular chondrocyte responses at PL treatment with focus on the recruitment/re-activation of a chondro-progenitor cell population from PL-treated cartilage explant cultures.

Stem cell-based therapies to achieve articular cartilage regeneration attract great interest. Stem cell niches are located within the joint, where they could participate directly in tissue homeostasis and repair processes. It is reasonable that exploiting local chondro-progenitors for cartilage repair may be a better and more efficient cell-based therapeutic strategy compared to the use of mesenchymal stem cell from different sources, given that they are developmentally primed for differentiation into chondrocytes. Furthermore, in the field of regenerative medicine therapeutic strategies targeting stem cells *in situ* could be more attractive and more advantageous than stem cell transplantation. According to this approach, endogenous stem cells could be recruited to the injury site by administration of bioactive factors. Thus, in the last decades, among a wide range of products, PRP has spread as a clinical treatment tool for musculoskeletal diseases. Several studies have investigated PRP or PL roles both *in vitro* and *in vivo*, highlighting their capacity to exert anti-

inflammatory and proliferating effects on cells, as well as to stimulate resident progenitors or to recruit circulating ones.

Primary cultures of human articular chondrocytes and cartilage chips were set up from donor biopsies and were treated *in vitro* with PL. Proliferation, clonogenic potential and phenotype of chondrocytes and chondro-progenitor cells derived from explant cultures in PL were characterized. Tri-lineage differentiation potential were tested *in vitro* and scaffold-assisted chondrogenesis of these cells were studied in nude mice. Moreover, secretory profile of chondro-progenitors were analysed together with their migratory capabilities by mimic osteoarthritis *in vitro*. Finally, it was reported that *ex vivo* treatment of human articular cartilage with PL induced activation and outgrowth of cells showing features of stemness, such as clonogenicity and expression of nestin. The stimulation of nestin-positive progenitor cells induced by PL in articular cartilage is of particular interest for the future development of therapeutic strategies given the involvement of these cells in tissue regenerative processes. In addition, their high proliferation capacity with concurrent chondrogenic potential maintenance further sustain the potential of PL-mobilized chondro-progenitor cells as promising tool in the field of cartilage tissue engineering. Moreover, PL-induced effects on phenotype of mature articular chondrocytes were further characterized, showing that they can revert to an earlier stage similar to chondro-progenitor one.

2) Embedding and re-differentiation of primary human articular chondrocytes in PRP-based hydrogel suitable for 3D-bioprinting.

Although the implantation of cultured chondrocytes intended for injured cartilage therapy is performed worldwide, there are still unresolved challenges associated with the maintenance of their chondrogenic phenotype. The expansion of chondrocytes *in vitro* is associated with de-differentiation, which is a reduction in the expression of cartilage-specific markers. Accordingly, such cells often produce fibrocartilage rather than native hyaline cartilage when used in clinical procedures. Several strategies to counteract this phenomenon have been adopted, such as 3D-culture of chondrocytes encapsulated in biomaterials. Adoption of hydrogels attracts particular interest in cartilage regeneration since they provide a highly hydrated environment similar to that of native tissue. In this context, progresses are expected thanks to the application of the 3D-bioprinting. However, the field of biofabrication often strongly focuses on the biomaterial rheology to allow controlled production, taking less care of its inherent impact on cellular phenotype. The combination of both aspects can be achieved by incorporation of biological components in printable hydrogels that often lack of bioactivity.

Primary human articular chondrocytes derived from previous monolayer culture expansion were bioprinted by embedding them in a commercial available alginate-based ink and their ability to regain the chondrogenic potential both *in vitro* and *in vivo* was evaluated. Interestingly, an improved ability to sustain cell viability, proliferation and a certain degree of chondrogenic phenotype rescue were found inside the bioprointed constructs by adding PRP as a source of biological agents in the ink formulation.

This thesis is organized as follows:

- the **chapter 1** introduces functions and composition of articular cartilage. Given the peculiar nature of the tissue, injuries to articular cartilage could progress toward chronic diseases. Thus an overview of cartilage disorders, including tissue defects and the inflammatory pathology of osteoarthritis is reported. Finally, therapeutic strategies for injured or pathological cartilage are described from symptomatic treatments and surgical procedures to the approaches inspired by progresses in regenerative medicine (cell therapy) and tissue engineering (scaffold-assisted methods).
- the **chapter 2** delves into the emerging technology of 3D-bioprinting, which is the additive manufacturing method intended to generate 3D-living constructs through the layer-by-layer apposition of a special ink made of cells encapsulated in biomaterials. An overview of 3D-bioprinting typologies is reported, each based on different available bioinks, process resolution and performances. The main biomaterial eligible for cell encapsulation is represented by hydrogels, but they need of some essential properties to be 3D-printed. The criteria for good printability are explained as well as a series of printable hydrogels are listed. Finally, the potential of 3D-bioprinting applied to the field of articular cartilage restoration are outlined.
- the **chapter 3** describes the finding of MSC-like progenitor cells within human articular cartilage explants after PL treatment *in vitro*, whose involvement in tissue regenerative applications is suggested.
- the **chapter 4** reports the 3D-bioprinting of human articular chondrocytes embedded in a PRP-activated hydrogel promoting cell re-differentiation. Such bioprinted constructs can be exploited as *in vitro* model for cartilage-related studies or graft prototype for tissue engineering.

1 Cartilage biology, tissue damage and related therapeutic strategies

1.1 Hints on cartilage as special connective tissue: subtypes and functions

Cartilage is a special connective tissue with a mesodermal origin, composed of chondrocytes immersed within an abundant extracellular matrix (ECM) rich in polysaccharides, fibrous proteins and water. Depending on ECM composition, cartilage in humans is classified into three subtypes: hyaline, fibro- and elastic cartilage (Figure 1.1). During fetal development hyaline cartilage forms the template for the skeleton (endochondral ossification) and in adulthood it persists at level of articular surfaces, ribs, ears and the tracheobronchial tree. Hyaline cartilage is the predominant type in the human body and the best characterized of the cartilage subtypes. It forms all diarthrotic articular surfaces, the most peripheral part of the nucleus pulposus of the intervertebral disk, portions of the ribs and tracheobronchial tree. Fibrocartilage is present in the temporomandibular and sternoclavicular joints and the annulus fibrosus of the intervertebral disk as well as the meniscus at the knee and the labrum of the shoulder. Finally, elastic cartilage is largely restricted to the external ear and a few other sites [1,2].

All subtypes of cartilage are structurally adapted to resist compressive forces. However, the presence of type I collagen in fibrocartilage and elastin in elastic cartilage also allows these tissue to resist tension. In general, cartilage functionally plays important roles in skeletal development, growth and repair, joint articulation, lubrication and patency of the respiratory tract.

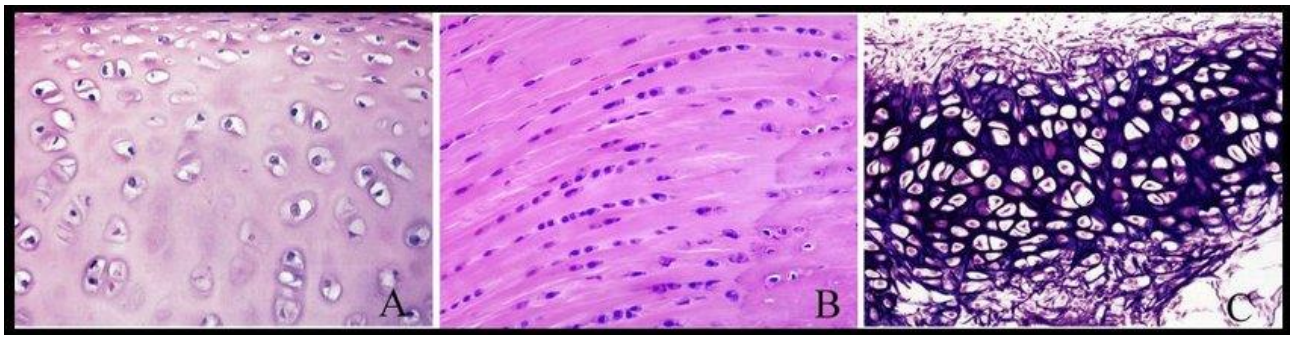

Figure 1.1: Different subtypes of cartilage. (**A**) Hyaline cartilage. (**B**) fibrocartilage. (**C**) elastic cartilage. Image taken from *http://medcell.med.yale.edu*.

1.2 Hyaline articular cartilage: composition and structure

Glass-like in appearance (from the Greek *hyalos* meaning “glass or transparent stone”), hyaline articular cartilage lines the ends of articulating bones. Its principal function is to provide a smooth, lubricated surface for articulation and to facilitate the transmission of loads with a low frictional coefficient. Articular cartilage lacks blood vessels, lymphatics and nerves and is subjected to a hard biomechanical environment. Its ECM is rich in glycosaminoglycans (GAGs) and collagen fibers (mainly type II collagen), altogether known as ground substance. GAGs are covalently linked as lateral chains to a core protein to form proteoglycans, among which aggrecan represents the most abundant [3,4].

In general, articular cartilage shows a zonal structure, which consists of superficial (tangential), middle (transitional), deep (radial) and calcified zones (Figure 1.2). The transition among the first three zones is gradual, but the deep and calcified zones are separated by a distinct front of mineralization known as tidemark. The organization of the ECM components as well as the shape, phenotype and orientation of the chondrocytes change depending on the zone. Thus, collagen fibers (primarily, type II and IX collagen) are oriented parallel to the surface in the superficial zone and the chondrocytes, present in relatively high number, are flattened and disposed in the same direction. This arrangement is responsible for resisting the shear forces of joint movement at the surface. The transitional zone contains thicker collagen fibers disposed obliquely, proteoglycans and a low density of spherical chondrocytes. The deep zone contains the largest diameter collagen fibers in a radial disposition, perpendicular to the joint line, along with chondrocytes typically arranged in parallel columnar orientation. The transitional and the deep zones provide resistance to compressive forces. The calcified zone ensures the anchorage of the cartilage to the subchondral bone and chondrocytes are enlarged but very sparse in this area. Proteoglycan concentration varies with depth in articular cartilage, being the lowest at the surface and the highest around chondrocytes in the deep zone. Conversely, the highest collagen content is in the superficial zone [1,2].

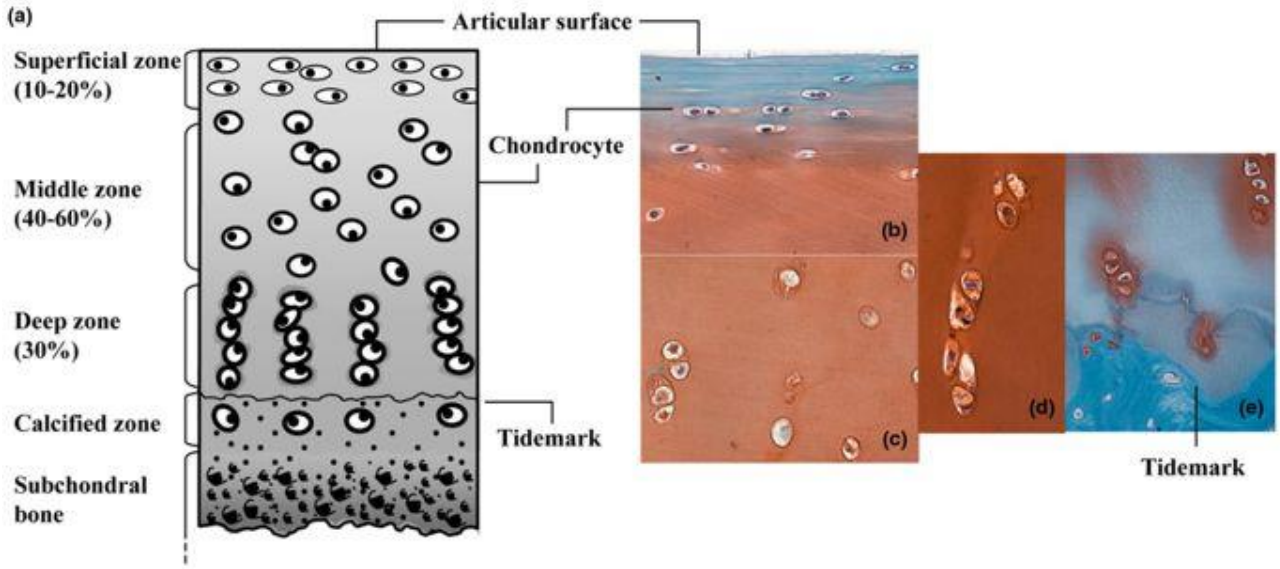

Figure 1.2: Schematic representation of articular cartilage zonal organization. (**a**) Illustration of articular cartilage zones showing cell shape, morphology, orientation and pericellular matrix deposition. Micrographs of the (**b**) superficial zone, (**c**) middle (transitional) zone, (**d**) deep zone chondrocytes and (**e**) deep zone and calcified zone stained with safranin O. Image taken from [5].

1.2.1 Embryonic development of articular cartilage

The musculoskeletal system originates during development from precursor cells of the mesenchyme that differentiate into osteogenic, myogenic and chondrogenic lineages, giving raise to bone, muscle and cartilage, respectively. In particular, migration and condensation of mesoderm cells, or chondro-progenitors, producing ECM rich in fibronectin, hyaluronan, tenascin and type I collagen, are involved in limb formation. Pre-cartilaginous condensation and differentiation of these cells into chondrocytes lead to a change in the local ECM composition, which becomes richer in cartilage specific proteins including type II collagen and aggrecan. Further differentiation events of these chondrocytes, such as hypertrophy with expression of type X collagen, lead to the process of endochondral ossification. Osteoblasts, carried by invading blood vessels during vascularization, replace these terminally differentiated chondrocytes and gradually cause mineralization that is necessary for proper long bone development [6]. Several recent studies, as described below, have demonstrated that a progenitor-like cell population still exists in adult hyaline cartilage tissue [7,8].

1.2.2 Extracellular matrix composition in articular cartilage

The ECM of mature articular cartilage is produced and maintained by chondrocytes, which control the homeostasis of the tissue and participate in its repair. The composition of articular cartilage

ECM varies spatiotemporally, from the more superficial layer, in contact with the synovial fluid in the joint cavity, to the deepest layer, in contact with the subchondral bone, and during tissue development. In addition to variations in structure of the ECM depending on the zone, it can be further distinguished into pericellular, territorial, and interterritorial regions based on proximity to chondrocytes and composition (see review [9]).

In general, mature articular cartilage ECM consists predominantly of water (66-78%) with the remaining dry weight composed of proteoglycans, collagen and additional specialized proteins [10]. The highest concentration of water is present at the articular surface [11]. Proteoglycans, thanks to their hydrophylic nature, are directly responsible for the high water content of cartilage. Proteoglycans account for ~40% of the dry weight of cartilage and demonstrate a remarkable hierarchy (Figure 1.3). At the highest level of organization, multiple proteoglycans are no-covalently attached to a central hyaluronic acid moiety, stabilized by a small protein known as link protein. A proteoglycan is composed of a protein backbone to which long, sulphated, carbohydrate side chains are covalently attached. A single proteoglycan may be glycosylated with 100-150 such side chains, resulting in an organization similar to a bottle brush. The predominant proteoglycan in cartilage is aggrecan and the most common carbohydrate side chains are chondroitin sulphate and keratan sulphate [12]. These sulphated carbohydrate side chains confer charge to the proteoglycans, thus they attract water, expand in volume and act as a shock-absorber. Since proteoglycans are able to extrude and re-imbibe water in response to load, they are fundamental in cartilage's ability to resist compression [13]. Moreover, this movement of water in and out of the cartilage matrix with joint compression and the phenomenon of diffusion ensure nutrition to chondrocytes, which are not supplied from blood circulation.

In addition to the above mentioned structural components, cartilage contains numerous other minor proteins that have both structural and regulatory roles. Structural proteins include other proteoglycans, fibronectin, thrombospondin-1, -3 and -5, cartilage intermediate layer protein, matrilin-1 and -3, and tenascin-C. Regulatory proteins, which influence cell metabolism, include galectin, chondromodulin-I and -II, cartilage-derived retinoic acid-sensitive protein, chitinase-3-Like Protein 1, matrix Gla protein as well as catabolic and growth promoting factors such as bone morphogenic proteins and transforming growth factor-β (TGF-β) [10,14].

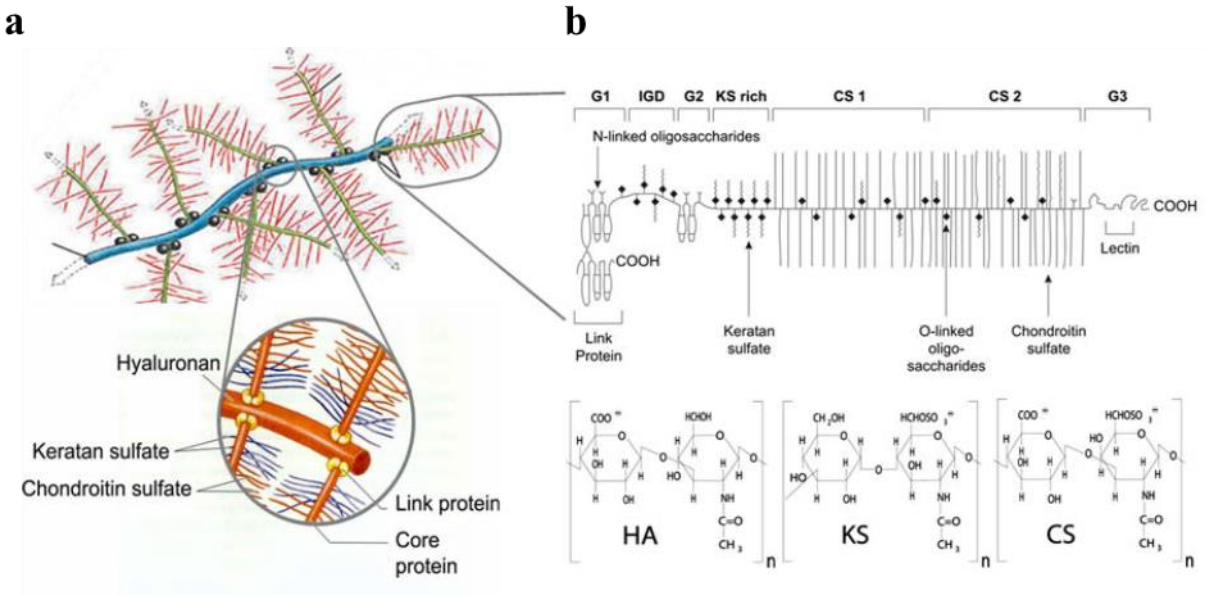

Figure 1.3: Hierarchical structure of proteoglycans in articular cartilage. (**a**) Schematic illustration of the brushed organization and (**b**) chemical structure of the most relevant polysaccharides in cartilage proteoglycans [hyaluronic acid (HA), keratan sulphate (KS) and chondroitin sulfate (CS)]. Image taken from [15].

Collagens represent ~50% of the dry weight of the cartilage ECM. They are comprised of repeating amino acid sequences (e.g., glycine, proline, hydroxyproline) and exhibit a characteristic triple helix structure (Figure 1.4). In articular cartilage, type II collagen predominates and confers tensile stiffness and strength to the matrix [16]. Apart from type II collagen, less abundant collagens, including type IV, VI, IX, X, XI, XII, XIII, and XIV are present in the ECM, being essential for the mechanical properties, organization and shape of articular cartilage as well as fulfilling specific biological functions [17]. Thus, type VI collagen is present in the pericellular matrix and lesser amount of type IX and XI collagen are deposited in the interterritorial matrix. In particular, type IX collagen interacting with type II collagen functions as a fitting molecule contributing to the biomechanical properties of the tissue. Type XI collagen is present within the fibres of type II collagen, regulating their thickness. The collagen fibres display differential organisation in the different layers of cartilage, as already mentioned, that depends on the direction of the mechanical stimulation and confers cartilage with tensile properties [13]. Finally, collagen X is present only in the hypertrophic cartilage, in the calcified layer [16].

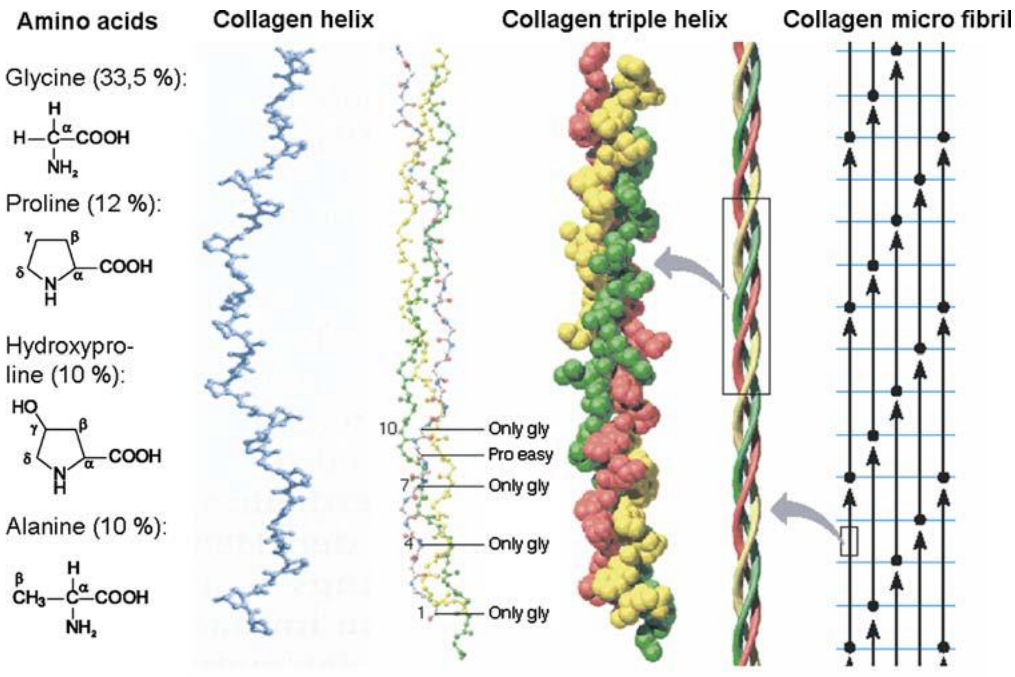

Figure 1.4: Illustration showing collagen structure. From left to right: the single amino acids that constitute each three polypeptide chains in the right-handed triple helix with a (Gly-X-Y) repeat structure characteristic of all collagen types. The X and Y position is often occupied by proline and hydroxyproline. The three chains are supercoiled around a central axis in a right-handed manner to form the triple helix. Multiple helices are associated to forming fibrils. Image taken from [15].

1.2.3 Cells in articular cartilage

Chondrocytes have been traditionally considered the only cell type within articular cartilage, until the presence of cells with stemness features in this tissue started to be reported by several research groups as already mentioned [7,8].

1.2.3.1 Chondrocytes

Chondrocytes are considered the terminally differentiated cell unit in cartilage present at different densities throughout the depth of the tissue. When compared to other tissues in the body, articular cartilage is sparsely populated by cells (chondrocytes represent only 1% of the total tissue volume [2]), but chondrocytes are pivotal for its homeostasis since they are responsible for the synthesis and maintenance of the matrix components and regulatory molecules including growth factors, enzymes and inflammatory mediators.

As reported above, the precursor cells of chondrocytes during development synthesise abundant ECM. With the increasing amount of matrix produced, the cells become separated from each other and embedded within cavities known as *lacunae*. In mature cartilage, chondrocytes within the *lacunae* organise themselves in isogenous groups derived from the division of the same progenitor. Isogenous groups are more abundant in the middle and transitional zones compared to the superficial and deep zones of the articular cartilage. In the deep zone, chondrocytes are hypertrophic and synthesise type X collagen supporting the mineralisation of cartilage in this region [13,16].

Importantly, chondrocytes may also differentiate from adult mesenchymal stem cells (MSCs), at least *in vitro* [18], a finding that has received much attention as possible treatment for degenerative joint disease. At the molecular levels, several key regulatory proteins play roles in chondrocyte differentiation, including the transcription factor SOX9 considered as the master regulator of this process from precursor cells [19].

Articular chondrocytes from the superficial, middle and deep zones have specific morphologies and expression profiles. Cell diameters range from 10-13 μm, with superficial zone cells being smaller than middle/deep zone cells [20]. In general, middle/deep zone cells possess greater synthetic activity for the major molecular constituents of cartilage than superficial zone cells when cultured *in vitro* [21]. Chondrocytes from these two zonal populations also have different mechanical, elastic and viscoelastic properties [22]. These variations are likely caused by the different strain levels that cells experience within the zones of cartilage. Tissue near the surface is compressed more than that in the bulk of the cartilage [23], and hence those cells might need to be stiffer to survive the high strains.

Chondrocytes are known to lose their phenotypic markers *in vitro* as evidenced by loss of morphologic characteristics and changes in metabolic activities of cells when cultured in monolayer [24]. In this condition, chondrocytes flatten over the course of days and begin to proliferate, rapidly losing their typical expressions. However, chondrocytes cultured in agarose retain morphological characteristics and the ability to synthesize proteoglycans [21]. This is likely due to the three-dimensional environment, which forces a rounded cell morphology and facilitate the synthesis of cartilage-specific molecules. Additionally, the application of mechanical stimuli such as stress, strain, and pressurization can affect their phenotypic expression and ECM production through a phenomenon termed mechanotrasduction [25,26].

Chondrocytes control the turnover and remodeling of the articular cartilage not only by secreting ECM but also by producing proteinases that degrade ECM constituents. The main proteinases are the metalloproteinases (collagenase, gelatinase, and stromelysin), which degrade collagens,

fibronectin, elastin, and aggrecan, and the disintegrin-metalloproteinases with thrombospondin motifs (ADAMTS), which cleavage proteoglycans. The cathepsins (cathepsin B and D), which degrade aggrecan, and the elastases, which hydrolyse elastin, fibronectin, laminin and other molecules, are also involved in the cleavage of the ECM but to a lesser extent [27,28].

1.2.3.2 Cartilage stem/progenitor cells (CSPCs)

Stem cells are defined functionally as characterized by the ability to self-renew as well as the potency to differentiate in multiple lineages [29]. Embryonic stem cells, derived from the inner cell mass of blastocysts, are considered pluripotent because of their ability to progress along the endodermal, mesodermal and ectodermal lineages [30]. During development, the potency of stem cells becomes gradually more restricted, and some of them remain in certain adult tissues as progenitor cells, where they contribute to tissue renewal and homeostasis [31].

In the case of articular cartilage, chondro-progenitor cells have been shown to exist not only in developing tissue, but also in fully developed adult cartilage.

The developmental origin of human cartilage stem/progenitor cells (CSPCs) has not been well-defined because of the lack of stable markers for tracing their lineage, nevertheless some indications are available. Two coexisting cell sub-populations of cartilage-forming cells were detected in human developing cartilage: one composed of multipotent cartilage stem cells (CSCs) with the capacity to undergo multilineage differentiation, including chondrogenesis; and other population composed of oligopotent chondrogenic cartilage progenitor cells (CPCs) which are able to undergo only chondrogenesis [32].

The existence of such a stem/progenitor cell population within adult articular cartilage tissue suggests that it may have the biological repertoire to be used for the cell-based therapy of cartilage defects and perhaps even degenerative joint diseases. This endogenous stem/progenitor population in articular cartilage has shown to respond to tissue damage [33], although repair is not ensured as confirmed by the distinctive inability of hyaline cartilage to heal after injury.

Many studies have shown that CSPCs are present in both human and animal cartilage, with the articular hyaline cartilage being the earliest and most well-studied source of CSPCs to date [34]. Increasing evidences suggest the existence of CSPCs in other types of cartilages, including the intervertebral disk [35], auricular [36], nasoseptal [37], tracheal [38] and costal [39] tissues in the order of decreasing frequency and across a variety of species.

Since articular cartilage develops in an appositional fashion [40], it has been suggested that the articular surface may contain a progenitor population capable of proliferating and expanding the cartilage tissue. Several studies have reported that these progenitors represent approximately 0.1% of all cells that can be extracted from the superficial zone of articular cartilage tissue [41,42].

However, a recent study has demonstrated the existence of progenitors within the deep zone of human [43] and bovine articular cartilage [44]. Like the articular surface, the joint synovium is known to be an abundant source of progenitors capable of successfully differentiating along the chondrogenic lineage [45]. While these synovium-derived progenitor cells technically do not reside within cartilage tissue, their presence in the joint may facilitate their migration toward the superficial zone of cartilage in response to articular surface injury.

Various CSPCs isolation methods have been adopted, from differential adhesion to fibronectin [7,8], to selection based on set of surface markers [46,47], as well as identifying migratory subpopulations [33,48,49]. These cells were then characterized according to properties of adult stem cells, such as self-renewal capacity, multilineage differentiation potential [50], the presence of a repertoire of bone-marrow-derived MSCs-related surface markers [46], and migratory activity [33] (Figure 1.5).

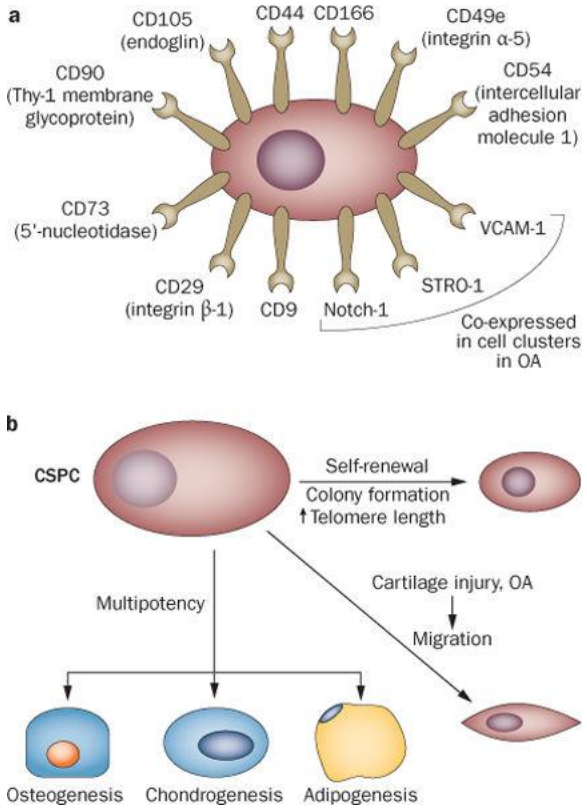

Figure 1.5: Stem cell-like properties of CSPCs. (**a**) Expression of stem cell-related surface markers (individually or in combination); (**b**) properties such as clonogenicity, multipotency and migratory activity of CSPCs in response to injury or osteoarthritis (OA). Image taken from [34].

Interestingly, the colony forming efficiency of chondro-progenitors has no correlation with the age of the patient from which they were isolated [8], suggesting that these cells exhibit a self-renewal capacity that is unrestricted by the patient's age.

Phenotypic analysis detects the expression of various stem cell-related surface markers, individually and in combination, including CD9 [47], CD29 (integrin β-1) [49], CD44 [49], CD49e (integrin α-5) [8], CD54 (intercellular adhesion molecule 1) [47], CD73 (5'-nucleotidase) [49], CD90 (Thy-1 membrane glycoprotein) [49], CD105 (type I membrane glycoprotein endoglin) [46,49], CD166 (activated leukocyte cell adhesion molecule) [43,46], Notch-1 (neurogenic locus notch homologue protein 1) [51] and STRO-1 [41], among others.

Although CSPCs in human cartilage are studied by different research groups, no single cell-specific surface marker is available yet to directly identify CSCs/CPCs either *in vitro* or *in vivo* [52]. This difficulty could be not only due to the lack of a well-defined marker to enable specific purification of these cells, but also to changes in the cellular phenotype upon isolation and monolayer expansion of chondrocytes [53]. Indeed, during *in vitro* monolayer culture, stem cell surface markers such as

Notch-1 and STRO-1 are not well maintained [54,55]. Furthermore, many of the MSCs markers (e.g. CD73 and CD49e) have also been found to be positive in mature chondrocytes, indicating lack of specificity [53]. It has also been reported that the distribution of some stem cell markers within the cartilage tissue, including Notch-1, STRO-1 and vascular cell adhesion protein 1 (VCAM-1) is not consistent with the stem cell content detected, concluding that these surface molecules may not be useful for specifically identifying CSPCs [41]. Thus, if CSPCs become crucial for future cartilage therapeutic strategies, more efficient and specific isolation techniques will be necessary for their isolation and purification.

However, an intrinsic feature of chondro-progenitors may consist in the expression of the transcription factor SOX9, a well-known marker of cells committed to the chondrogenic lineage [56]. SOX9 is not highly expressed in MSCs, which are the precursors of chondro-progenitors since they are not yet fully committed to the chondrogenic lineage. Conversely, clonal population of chondro-progenitors isolated from bovine and human articular cartilage has been shown to continually express SOX9 during expansion and retain the capacity for re-differentiation [56]. Moreover, articular chondro-progenitors, unlike bone marrow-derived mesenchymal stem cells (BM-MSCs), do not generate a type X collagen-rich matrix or express RUNX2 transcription factor protein upon chondrogenic differentiation, but produce an extracellular matrix that is predominantly hyaline in nature [8].

Chondrocytes traditionally secrete cartilage ECM when cultured in a 3D environment, but their de-differentiation following expansion limits their use for cartilage regeneration [57]. In contrast, CSPCs are considered as a promising renewable cell source for this purpose thanks to their niche-specific lineage preference for chondrogenesis [58] and since they show to be implicated in migration and tissue reparative activities in response to native articular cartilage injury [33,49]. However, it is still not clear whether CSPCs maintain themselves within their niche in native cartilage to promote repair through extracellular signalling factors or differentiate to maintain the cartilage tissue itself.

Although chondro-progenitors are highly capable of chondrogenic differentiation, it has been demonstrated that they can undergo osteogenesis and, to a certain extent, adipogenesis [8]. As such, the potential for chondrogenic, osteogenic and adipogenic differentiation has become a defining feature of chondro-progenitors that distinguish them from mature chondrocytes.

Finally, it has been observed that CSPCs exhibit detectable telomerase activity and undergo delayed telomeric erosion during *in vitro* monolayer culture compared to chondrocytes [8,56].

1.3. Cartilage injuries and degeneration towards OA development

In 1743 William Hunter affirmed "If we consult the standard Chirurgical Writers from Hippocrates down to the present age, we shall find, that an ulcerated cartilage is universally allowed to be a very troublesome disease; that it admits of a cure with more difficulty than carious bone; and that, when destroyed, it is not recovered" [59]. Articular cartilage has very limited healing potential and poor regenerative capacity: once articular cartilage is damaged, full recovery of its structure, function and biomechanical properties is unlikely and it is usually a step towards progression of osteoarthritis (OA).

A hallmark of cartilage defects, injuries and degeneration is the loss of cartilage matrix as a consequence of an imbalance between catabolic and anabolic processes, that usually influence the normal cartilage turnover [13].

In general, injurious impact and repeated loading, torsional loading and joint malalignment lead to cartilage injuries, that are classified according to the depth of the lesion as cartilage microfractures, chondral and osteochondral (full thickness) defects. Cartilage physiology, size, depth and location of the defect together with aging directly affect the efficacy of the self-repair mechanisms and therefore the outcomes for cartilage injuries as well as the progression towards OA. Furthermore, the lack of vasculature and the nature of the tissue result in few cells available to mount an adequate healing response.

In cartilage microfractures, the damage to the collagen network induces superficial GAGs loss [60] and alters load distribution, resulting in local stress increase that can cause further damage or a greater proportion of forces borne by the bone. These loading alterations, as well as fractures to the calcified layer can occur leading to eventual thickening of the subchondral bone [61]. Since cartilage is aneural, repeated loading of microfractured cartilage can continue without pain, leading to further degeneration [62].

Chondral fissures are defects that do not extend to the subchondral bone. Chondral defects can proceed from cartilage microfractures or from trauma, improper loading or foreign bodies. Without blood supply, the intrinsic metabolic activity after such an injury is insufficient to result in an adequate repair, leading to the eventual development of osteochondral fissures [62]. Osteochondral fissures are lesions that cross the tidemark and penetrate the underlying bone. Although large number of progenitor cells are recruited from the bone vasculature to mount a repair process, there is an impaired functionality of the repaired tissue, with a mix of fibrocartilage and hyaline cartilages, resulting in eventual tissue degeneration towards OA [63]. With age, both chondrocytes

and progenitor cells decrease in number and metabolic activity, thus contributing to the cartilage healing problem.

OA in western countries is a leading cause of pain and disability especially in elderly persons. It compromises overall health and quality of life of affected patients, representing a huge economic burden to the public health system [64]. Since OA is characterized by degeneration of articular cartilage, synovial inflammation and changes in periarticular and subchondral bone, it is considered a disease of the entire joint (Figure 1.6) [65]. Initially, changes associated with joint capsule such as thickening and frequent adherence to the underlying bone are seen, with increased vascularization [66]. Destruction of the cartilage surface in OA occurs with fibrillation, surface erosion and fissures at the beginning of the disease. From this point on, proteoglycan content decreases and the tidemark begins to appear irregular and punctuated with blood vessels. At a later time, articular cartilage undergoes to surface wear and irregularity with vertical and horizontal fissures. These patterns of increased tissue fragmentation and decreased content in ECM components continues until the cartilage, completely devoid of its abilities to withstand load, is worn away to expose the subchondral bone [67]. The subchondral bone remodels with thickening as it becomes unprotected from the load borne by cartilage [68]. Along with the thickening, new bone formation (osteophytes) is observed.

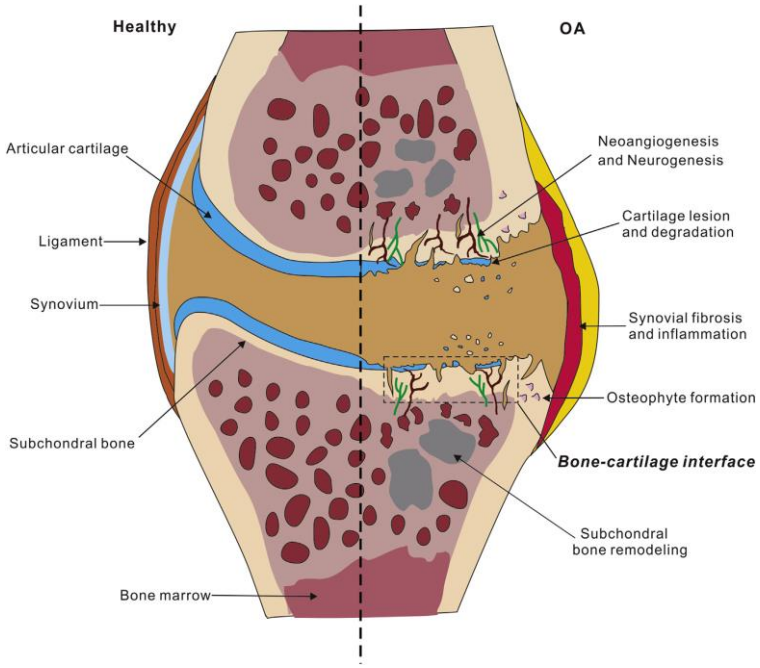

Figure 1.6: Comparison between normal and osteoarthritic joints. Image taken from [69].

At molecular and cellular levels, the processes involved in cartilage destruction during OA include cell death, degradation of the extracellular matrix, calcification, and production of inflammatory mediators. In particular, OA is characterized by an increase in serum and synovial fluid of pro-inflammatory cytokines, such as IL-6, IL-1β and TNF-α, which working in concert reduce in chondrocytes the synthesis of ECM proteins, including aggrecan and type II collagen, enhance the gene expression of proteinases MMPs (MMP-3 and MMP-13) and ADAMTS (ADAMTS5), inhibit the production of natural protease inhibitors (TIMPs), up-regulate the synthesis of eicosanoids (E2 prostaglandins), and promote apoptosis to further degrade joint tissues [70,71].

In addition, it has been hypothesized that also senescence of cells within joint tissues may contribute to the pathology OA. Indeed, the profile of catabolic and inflammatory mediators found during the pathogenesis of OA resembles very closely the one observed in 'classical' senescent cells. During OA, chondrocytes display an up-regulation of several senescence markers, including senescence-associated beta-galactosidase (SA-βgal) activity, accumulation of MMPs induced by pro-inflammatory cytokines, ROS secretion, activated DNA damage response, telomere attrition, and accumulation of $p16^{Ink4a}$ [72]. Thus, senescence of chondrocytes leads to a further shift of the balance between ECM synthesis and degradation, while the senescence of stem or progenitor cells could compromise tissue repair as described in the next section.

1.3.1 CSPCs in articular cartilage injuries and OA

Similar to other tissue-specific stem cell populations that exhibit a remarkably ability to migrate to sites of injury, chondro-progenitors can migrate across the articular surface to sites that have suffered trauma. Migratory chondrogenic progenitor cells have been detected in degenerated cartilage sites in late-stage OA [49] or emerged and migrated to the site of injury following blunt impact in healthy cartilage explants [33]. In the latter case, soluble factors released after injury are thought to initiate such migration, since CSPCs showed a similar behaviour in presence of dead-cell debris and medium conditioned by injured cartilage. Other soluble factors could also enhance the chemotactic activity of CSPCs, such as insulin-like growth factor 1 (IGF-1) in serum, platelet-derived growth factor (PDGF) in synovial fluid [48] or post-traumatic bleeding [73]. Thus migration of CPCs is likely to be regulated by multiple tissue-injury-related signals.

The functional role of the migratory cells is not clearly understood. Interestingly, the cells described above also showed a high level of lubricin (proteoglycan 4) compared with BM-MSCs from the same donor [33]. Since lubricin is an important superficial zone protein responsible for lubrication

and protection of the articular cartilage surface in the joint cavity, migratory CSPCs probably contribute to the biological resurfacing of this tissue after injury. In some clinical cases, a very thin, protective, cartilage-like layer can be found on the surface of the abnormal subchondral bone, probably as a result of chondrocyte aggregation with lubricin production [74]. Although the mechanisms responsible for this joint-resurfacing activity in such late-stage OA are unknown, the involvement of CSPCs is highly probable and it could represent a target for OA therapy.

Available evidences strongly suggest that the phenotype of CSPCs in OA correlates with the degree of ECM degeneration in the articular cartilage, but the function of these cells remains unclear and is likely to be different at different stages of the pathology. In early OA, which is characterized by loss of the superficial zone and structural changes in the internal matrix, despite an increase in cell number and the formation of cell clusters, the cells remain embedded within the ECM [75]. In later OA, the matrix undergoes further loss of organization and the cells seem to be able to migrate freely [49]. Thus any therapeutic strategies that target CSPCs must take into consideration the stage-specific nature of cells.

Cell proliferation and stem cell surface markers increase in OA tissue, evidenced by the finding that the proportion of $CD105^{+}/CD166^{+}$ cells in OA cartilage was ~8% compared with ~4% in normal cartilage [46]. A possible explanation is that CSPCs residing within adult articular cartilage start to replicate in response to cartilage injury and give rise to daughter cells. Thus, one of the daughter cells may remain a progenitor while the other one undergoes further replication and differentiation along the chondrogenic lineage. All these events are subject to regulation and, therefore, defects in any of these events may affect cartilage repair [76].

Other data indicate that CSPCs are involved in all stages of OA. In early OA, cell clusters were found in and near the fissures of the articular cartilage; within these clusters, both anabolic and catabolic markers were detected and most cells expressed Notch-1, STRO-1 and VCAM-1. In proximity to the cell clusters, positive staining for these three stem cell markers was also found in the middle zone of OA cartilage [5,75]. These findings suggest that CSPCs might be involved in ECM remodelling in early OA, but more studies are needed to confirm this.

In a recent study, it has been reported that CSPCs in cellular clusters, hallmark of the OA disease, may even contribute to its pathogenesis, being a novel cell target for OA therapy [77].

In late OA, Koelling *et al*. [49] reported a migratory population of chondrogenic progenitor cells in degenerated cartilage sites. These cells were located in areas of tissue repair and could have been local cells or cells that had migrated from neighbouring bone tissue, or both, as the cartilage tidemark was broken and neovascularization underneath the cartilage tissue was evident. This

disruption of the cartilage ECM in late OA probably alters the mode and extent of communication between the articular cartilage and the subchondral bone, synovium and other neighbouring tissues; perhaps these migratory cells could act as a messenger-cell population that shuttles between tissues. CSPCs from diseased states have shown to regenerate cartilage at least *in vitro*, but their susceptibility to various inflammatory mediators such as NF-k B and ILβ1 in late stages of OA may hamper their utility *in vivo* [78,79].

Finally, a recent study shows that the increase in progenitor frequency in OA tissue is concurrent with the emergence of a divergent progenitor sub-population that can be separated on the basis of proliferative potential and capacity for telomere maintenance. Upon culture expansion, OA-CPCs could be separated into two groups: an early-senescent one and another classified as late-senescent population [80]. OA is an age-related disease and cellular senescence is predicted to be a significant component of the pathological process, as mentioned above. Deranged progenitors that have adopted a senescence-associated secretory phenotype following replicative exhaustion may cause long-term deleterious effects and be a significant contributor to the progressive degradation of cartilage within the osteoarthritic tissue.

1.4. Current therapeutic approaches for articular cartilage repair

Traumatic and degenerative pathologies of the articular cartilage are currently treated through several therapeutic approaches developed by clinicians and researches, including symptomatic treatments and restoration procedures both clinically available and under development [81].

Symptomatic treatments consists of systemic treatment (usually pain killers and anti-inflammatory drugs) and local intra-articular injections, such as injections of corticosteroids or platelet-rich plasma. Among clinically available cartilage repair procedures, surgical approaches (microfracture and mosaicplasty) and those based on regenerative medicine (implantation of expanded autologous chondrocytes) are the most representative to be mentioned. Moreover, experimentations of regenerative approaches based on tissue engineering field and involving different combinations of biomaterials and stem cells are in progress.

1.4.1 Clinical orthopaedic approaches: intra-articular injections and surgery

Intra-articular injection is a minimally invasive procedure used to directly deliver compounds, such as corticosteroids, hyaluronic acid (HA) and platelet-rich plasma (PRP), to an affected joint.

The Osteoarthritis Research Society International (OARSI) guidelines recommend the treatment with corticosteroids as an anti-inflammatory agents to reduce joint pain [82]. However, these drugs should be given at low doses and for a short period of time, given that high doses and long treatment result in chondrocyte toxicity, cartilage damage and accelerated progression of OA [83].

The so-called viscosupplementation therapy is based on intra-articular injections of HA in OA synovial fluid with the aim to restore its normal concentration and molecular weight levels [84]. Since HA is considered a critical component of normal synovial fluid and an important contributor to joint homeostasis [85], this type of treatment received United States Food and Drug Administration (FDA) approval 20 years ago. However, a significant effect of intra-articular injections of HA compared to intra-articular injections of a placebo did not emerge from a meta-analysis of randomized clinical trials for the treatment of OA [86].

PRP is a concentrate of platelets derived from blood, whose growth factors and cytokines are thought to activate a variety of signalling pathways promoting tissue repair [87,88]. Despite the lack of knowledge and long-term data about its action in arthritic joints [87,88], the use of PRP intra-articular injections in degenerative OA reports improvements in pain and functional outcome scores [89]. The topic of therapeutic use of platelet derivatives will be explored in the next sections (see 1.4.4).

In the surgical field, microfracture and chondroplasty are the most common procedures for damaged cartilage repair (Figure 1.7). Microfracture together with abrasion and drilling techniques work by disrupting the subchondral bone integrity to create channels between the defect in the cartilage and the underlying bone marrow [90]. The recruitment of bone marrow-derived progenitor cells through these channels leads to subsequent formation of cartilage-like tissue in the defect region. Despite its minimal invasiveness and low cost, this strategy has revealed a relatively short-term functional improvement (< 24 months) due to the formation of fibrocartilage rather than hyaline articular cartilage [91]. Mosaicplasty represents another surgical approach in the treatment of cartilage defects and it provides for the use of tissue grafts, i.e. osteochondral allo- or auto-grafts. [92]. In the latter case, small cylindrical plugs are harvested from patient's own non-weight-bearing cartilage areas and then fitted into the defects. Although cartilage restoration *via* mosaicplasty often produces a good functional outcome, some drawbacks, such as donor-site soreness and limited availability of donor tissue, remain and often limit its feasibility [93].

1.4.2 Regenerative medicine approaches: cell-based therapies

Regenerative medicine focuses on new therapies to replace lost or damaged tissue with the final goal to restore tissue function.

Because of the lack of blood supply and subsequent wound healing response, damage to cartilage results in an incomplete attempt at repair by local chondrocytes. To prevent progressive cartilage degeneration or to replace damaged cartilage, the surgical treatment is often the only option, but it rarely restores full function of the injured tissue. Therefore, regenerative medicine for the generation of functional cartilage tissue has emerged as an important field of research. There are different approaches for cartilage regeneration that may help to replace, repair or promote tissue healing. The use of cells including chondrocytes and stem cells may represent a promising approach.

1.4.2.1 Chondrocytes-based cartilage therapy

The first cell-based approach to cartilage regeneration, autologous chondrocyte implantation (ACI), was developed by Brittberg and colleagues in 1994 [94] and involves harvesting small tissue biopsies from the patient's own cartilage, followed by the expansion of chondrocytes *in vitro* and subsequent injection of them into the defect (Figure 1.7). In the original procedure, the injected cells were covered with an autologous periosteal patch, while in the second-generation ACI chondrocytes were put in contact with an absorbable collagen membranes, to prevent their outflow into the joint cavity upon transplantation [95]. Compared to microfracture (first-choice treatment for lesions < 2.5 cm^2) or mosaicplasty, ACI allows repair of larger cartilage defects (full-thickness chondral defects) [96]. The main limitations to this approach include its high cost [97], as well as the invasiveness of harvesting (two-stage operations), the formation in most cases of fibrocartilage and graft hypertrophy [95,98]. Since chondrocytes reside within an ECM that provide specific mechanical properties, a further development of ACI is the implementation of the matrix-induced autologous chondrocyte implantation (MACI) for cartilage regenerative purposes [99]. This procedure involves transplantation into the cartilage defect of a special three dimensional (3D)-scaffold with mechanical properties resembling those of the native ECM and containing autologous chondrocytes (previously expanded *in vitro*) (Figure 1.7). A large number of commercial products suitable for this type of biomedical application is already available [100].

Although the implantation of mature cultured chondrocytes is performed worldwide, there are still unresolved challenges associated with the maintenance of these chondrocytes in a stable state. The

expansion of autologous chondrocytes *in vitro* to obtain a sufficient number of cells is associated with chondrocyte de-differentiation, a reduction in the expression of cartilage-specific markers (type II collagen and aggrecan) with an increase in the synthesis of non-specific type I collagen [101]. Accordingly, such cells often produce fibrocartilage rather than the native hyaline cartilage. On the other hand, mature differentiated chondrocytes do not proliferate and cannot therefore be easily expanded *in vitro* [24]. One way to counteract chondrocyte dedifferentiation during *in vitro* expansion is to re-differentiate them by 2D- or 3D-culture in media supplemented with chondrogenic growth factors [102,103]. Thus, the proper balance between chondrocytes proliferation and differentiation represents an open issue that has yet to be fully resolved.

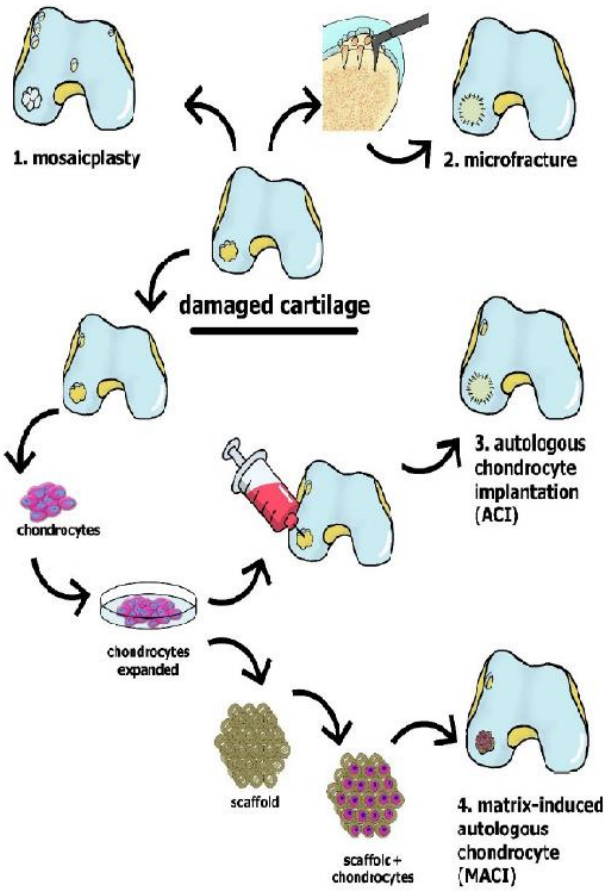

Figure 1.7: Schematic illustration of the clinically developed approaches for cartilage tissue restoration. Image taken from [81].

1.4.2.2 Stem cell-based cartilage therapy

Another strategy involves the use of an alternative cell type that maintains its inherent proliferative capacity, such as MSCs or CSPCs.

BM-MSCs are a pluripotent stem cell population that can be isolated from bone marrow and expanded for therapeutic use thanks to their differentiation ability along bone, cartilage and adipose tissue lineages [104]. Despite several preclinical [105] and clinical studies [106] have demonstrated the efficacy of using MSCs as a cell-based therapy for cartilage defects and OA, they are mostly prone to hypertrophy or differentiate completely along the osteogenic lineage, therefore conferring a lack of stability in their commitment to a desired tissue lineage (in this case cartilage) [107]. This should be taken into account especially when treating an OA joint where there is a dysregulation of cytokines, chemokines and growth factors underlying the disrupted tissue homeostasis. Therefore, it would be advantageous to utilize instead a population of progenitors that is lineage restricted to achieve the same goal, like CSPCs.

CSPCs can be obtained from local cartilage and they have sufficient clonability for expansion without losing their chondrogenic differentiation potential. Moreover, CSPCs from native cartilage are believed to be further along in their commitment or to be primed to the chondrogenic lineage making them a logical choice for cell implantation into cartilage defects, contrary to immature stromal cells from bone marrow- and adipose-derived progenitors. Nevertheless, using autologous chondro-progenitors to fill cartilage defects has also some limitations. For instance, CSPCs represent a very rare population of cells, since they are significantly less than even 1% of all cells in adult articular cartilage [5,42]. The search of alternative sources of progenitors with chondrogenic potential has brought much attention to pluripotent progenitors that can be derived from various tissue types including that of the joint synovium and infrapatellar fat pads [108]. Nonetheless, the major challenge of identifying an accessible and abundant source of expandable chondro-progenitors is still a limiting factor for their utilization for cartilage repair.

Thus, each source of cells has its own advantages and drawbacks, and a further evaluation of their potential and especially of their long-term outcomes is required.

1.4.3 Tissue-engineering approach

The goal of tissue engineering is to develop tissue or organ replacement strategies through the use of specific scaffolds. They represent templates for cell adhesion and cell recruitment into a defect site as well as provide mechanical supports during tissue regeneration. Biomimetic scaffolds create

an environment close to the natural ECM of a specific tissue, in which cells could be guided to organize a new one with appropriate biomechanical characteristics and functions.

Tissue engineering for the restoration of damaged articular cartilage involves several different scenarios. The basic scenario utilizes synthetic or natural scaffolds that mimic the ECM of native cartilage [109]. In an advanced one, tissue-engineered constructs are loaded with living cells and/or growth factors which facilitate the integration of the implant into the host tissue [110].

The polymers utilized for the articular cartilage engineering can be synthetic or natural [81]. Natural polymers (such as alginate, gelatin, agarose, HA, fibrin and collagen) are both biodegradable and biocompatible, but their composition varies from batch to batch. Conversely, synthetic polymers (such as some polyesters, polyethers, Pluronic®, polyurethane and self-assembling peptides) are more easily reproducible and their synthesis is precisely controlled. Nonetheless, natural polymers are the most widely used in ongoing clinical studies, with collagen being the most common. Overall, the requirements for a tissue engineering scaffold must be tissue-like mechanical properties, biocompatibility and resistance to wear. Recently, a number of commercially available tissue-engineered constructs, both synthetic and based on natural polymers, demonstrated favourable clinical outcomes [111]. However, several limitations still impede the complete and sustained repair of damaged articulate cartilage tissue.

Scaffolds are produced using various techniques, including 3D-bioprinting. Layer-by-layer 3D-bioprinting is based on computer-aided design (CAD) and allows the construct to be customized to the shape of the individual defect [112]. The use of hydrogel-based bioinks enables the homogenous incorporation of cells and biological factors during production, while retaining mechanical support [113]. Importantly, the water content of hydrogels (~80 wt%) is similar to that of articular cartilage. The polymers used in hydrogels are often naturally occurring. Among them, alginate or gelatin take favour with a low biodegradation rate and compatibility with chondrocytes, although, at the same time, their low adhesiveness and bio-inertness limit the regenerative potential. The bioink can also be rendered bioactive by incorporating various functional components [113]. Collagen and HA, inherent components of articular cartilage, support cell attachment and stimulate formation of the ECM, but exhibit little mechanical stability and are subject to intense biodegradation [114,115]. Synthetic polymers are superior to these natural ones in terms of controllable biodegradation and biomechanics, but often demonstrate poor biocompatibility and require modifications to provide specific biological functions. Thus, hybrid bioinks are often combinations of polymers with different desirable properties. The next chapter will explore the topic further.

1.4.4 Platelet derivatives in the treatment of injured articular cartilage

Along with macrophages and MSCs, platelets participate in tissue regenerative processes. Upon wounding, platelets coagulate and degranulate releasing bioactive factors that, with a fine spatiotemporally regulation, promote inflammation and thus neutrophil and macrophage activation, as well as migration and proliferation of fibroblast, smooth muscle cells, endothelial cells and MSCs, collagen synthesis and angiogenesis, resulting in tissue regeneration [116].

Given the avascular nature of cartilage tissue, traditional inflammatory factors involved in tissue repair process are hindered in reaching the locally affected area and therefore do not contribute to the healing response in the setting of cartilage injury, especially in the full-thickness defects. Thus the rationale for the use of platelet products is that the supraphysiological direct delivery of platelet-derived factors to the site of cartilage injury or disease can stimulate the natural healing cascade and tissue regeneration. The term "platelet-rich plasma" (PRP) indicates autologous blood containing such platelets in higher amount than normal concentrations, typically obtained via differential centrifugation [117]. A further derivate is represented by "platelet lysate" (PL), that is usually prepared by several freeze-thaw cycles of platelet concentrates and subsequent centrifugal separation of the debris from all the bioactive platelet factors.

Proteomic studies have shown that platelets contain more than 1,500 protein-based bioactive factors [118], including immune system messengers, growth factors, enzymes and their inhibitors, which together can participate in tissue repair and wound healing. Platelets also store proteins with antibacterial and fungicidal effects, coagulation factors and membrane glycoproteins that influence inflammation by modulating the synthesis of interleukins (ILs) and chemokines. Furthermore, platelets' granules contain and release adenoside diphosphate, adenoside triphosphate, calcium ions, histamine, serotonin and dopamine, which contribute to tissue homeostasis. PDGF, epidermal growth factor (EGF), IGF-1, TGFβ-I, vascular endothelial growth factor (VEGF), hepatocyte growth factor (HGF) and basic fibroblast growth factor (bFGF) should be mentioned among platelet-derived growth factors [119].

In particular, the release of the aforementioned growth factors and hundreds of others after platelet activation could promote cartilage matrix synthesis, cell growth, migration and phenotype changes, and facilitate protein transcription within chondrocytes [120,121]. Among them, TGF-β plays a significant role in regulating chondrocyte homeostasis from early to terminal stages [122]. In particular, TGF-β acts as inhibitor of terminal hypertrophic differentiation in post-natal chondrocytes and promotes their anabolism, by enhancing matrix production, cell proliferation and

osteochondrogenic differentiation. Furthermore, *in vivo* short-term intra-articular injections showed beneficial effects on osteochondrogenesis [123].

Evidences support also PRP or PL anti-inflammatory properties. The transcription of many degradative cytokines, including IL-1β, tumor necrosis factor-α (TNF-α), and IL-6, are under the upstream control of nuclear factor-κB (NF-κB), which is activated in OA. Platelet α-granules contain several factors able to inhibit this pro-inflammatory and catabolic pathway preventing the detrimental effects of persistent inflammation on OA articular cartilage [124]. In this context, activated PRP increases *in vitro* levels of HGF, which enhances cellular IκBα expression and subsequently disrupts the NF-κB transactivating activity [125]. Moreover, it has been reported from *in vitro* studies on several cell systems (including human keratinocytes, osteoblasts, articular chondrocytes, and murine BM-MSCs) an early and transiently enhanced PL-induced activation of the pro-inflammatory NF-κB pathway in an inflammatory milieu [126–129]. In such conditions, after the early inflammatory burst, PL inhibits the activation of NF-κB showing a pro-resolving activity. It's likely that platelet-released factors exert an immediate pro-inflammatory effect causing a rapid antimicrobial response by the tissue, as demonstrated by the release of antimicrobial proteins such as neutrophil gelatinase-associated lipocalin (NGAL) and the migration of neutrophils and macrophages that engulf contaminant microorganisms and remove the devitalized tissue. At later time, these factors exert an opposite effect by inhibiting NF-κB activation and promoting resolution of the inflammatory phase.

Since the use of platelet derivatives shows beneficial effects at molecular level, there has been a great increase in the number of randomized trials and meta-analyses that evaluate whether these promising findings *in vitro* can be translated to the clinical practice. Thus, these studies, as previously discussed, have shown that PRP injections in joint lead to a reduction in pain scores and an improvement in the function of the repaired tissue at several follow-up times [130,131].

With the development of tissue engineering technology, treatment with cultured autologous cartilage cells and engineered construct for repairing articular cartilage defects has also spread in clinical practice. Since cell therapy requires a large chondrocyte numbers, suitable protocols for *in vitro* cell expansion have been developed. The standard method for cartilage cell expansion involves culture medium with fetal bovine serum (FBS) or serum-free medium. Furthermore, the low number of human articular chondrocytes obtained from cartilage biopsies along with their limited proliferation potential and the de-differentiation process during monolayer culture have promoted research aimed at the discovery of alternative and more efficient culture procedures. Thus, while FBS may contain undesired xenogeneic pathogens and raises safety concerns when

used in clinical-grade preparations and serum-free medium is expensive, substitutes for these supplements are represented by human platelet derivatives, effective also thanks to their mitogenic power [132–134].

In this context, several studies have confirmed that PL stimulates proliferation of chondrocytes [128,135], but controversial results have been reported on its impact on chondrogenic differentiation and cartilage matrix accumulation [136–139].

Nevertheless, acellular repair technology has greatly used in recent years based on the use of PRP gel, the solid state of PRP, or PRP in combination with scaffolds such as HA or hydrogel to imitate the native cartilage environment. For instance, it has been reported that the combination of a polyglycolic acid (PGA)-hyaluronan scaffold with PRP after subchondral drilling can lead to the formation of hyaline-like cartilage in the knee at 1-year follow-up [109].

Although PRP and PL are used in orthopaedics, sports medicine, dentistry and maxillary surgery for the treatment of several disorders, their efficacy is still controversial due mainly to the lack of consensus on its preparation methods. Furthermore, the platelet concentration in the blood is highly variable from individual to individual and within the same individual it can vary over time. Thus, products with distinct platelet concentration and variable composition of growth factors and cytokines can be produced, making difficult the comparison of the results obtained by different laboratories. This variability leads also to different therapeutic outcomes given that some of the soluble factors contained in these products have the ability to maintain the phenotype of chondrocytes while others lack this property. Hence, a standardized PRP/PL-production procedure, starting from pools of human-certified buffy coats has been proposed to reduce variability and to obtain a platelet products with a well-defined platelet and growth factor concentration [132–134].

2 Three-dimensional (3D) bioprinting as emerging tool in cartilage tissue engineering

2.1 3D-bioprinting basics, spreading and applications

Bioprinting is an emerging additive manufacturing (AM) technique that is having a growing impact on medical and pharmaceutical sciences, and hence is gaining significant attention worldwide [140]. It dates back to 1988, when Klebe [141] described with the term ‘cytoscribing’ a technique for the precise positioning of cells on a 2D substrate using a computer-controlled ink jet printer or graphics plotter. Since several research groups joined, the technique evolved and the first international workshop on bioprinting was held in 2004 at the University of Manchester [142]. Between 2012 and 2015, the number of papers referring to bioprinting increased fourfold [143] and to date the field is rapidly expanding.

Bioprinting consists of the simultaneous writing of living cells and biomaterials with a predetermined layer-by-layer stacking organization using a computer-aided transfer process for the fabrication of bioengineered constructs [144]. Bioprinting technology has a broad utility in various application areas such as tissue engineering, regenerative medicine, transplantation, clinics, drug screening and high throughput assays and cancer research (Figure 2.1).

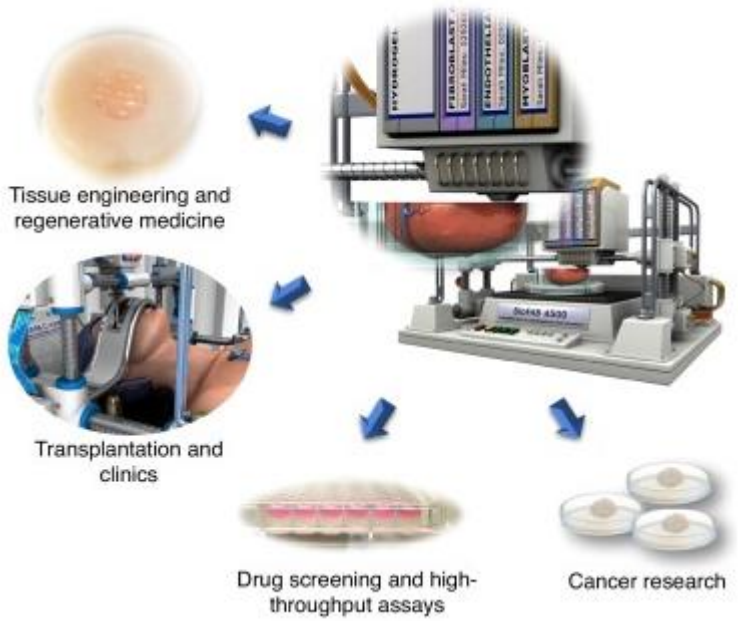

Figure 2.1: Application areas of bioprinting technology. Image taken from [145].

In biomedical area, 3D bioprinting allows the development of 3D tissue models that can replace current 2D cell culture and animal models for drug discovery and toxicology, and for the study of tissue pathological processes. Recent research has greatly increased awareness of the dramatic differences between 2D and 3D-culture systems, since the latter provides a more physiologically relevant environment to guide cell behaviour [146,147]. In addition, great efforts have been made to develop 3D biofabrication techniques that can generate complex, functional 3D architectures with appropriate biomaterials and cell types suitable in mimic tissues such as tracheal splints, heart tissue, vascular grafts, multilayered skin, cartilaginous structures and bone in view of future clinical applications for regenerative purposes [148]. Due to a scarcity of patient-compatible donor tissue and organs, the demand for tissue engineering solutions, including 3D-bioprinted tissues, is constantly increasing. In this context, the advantage provided by 3D-printing is that personalized tissues can be fabricated starting from anatomical 3D image analysis and computed tomography techniques. In comparison to traditional tissue engineering strategies, this technique allows also a homogeneous distribution of cells [148], which is achieved even when they have to fill large tissue scaffolds.

Bioprinting devices have the ability to print cell aggregate, cell encapsulated in hydrogels or viscous fluids, or cell-seeded microcarriers, all of which can be referred to as bioink, as well as cell-free polymers that provide mechanical structure [149]. However, the technique is still at its early stage and many challenges have to be faced for transplantation and other applications.

The 3D bioprinting process can be divided into three crucial technological steps: pre-processing, processing (actual printing) and post-processing. Pre-processing is a blueprint of tissue or organ design using imaging and computer-aided design (CAD) techniques. Subsequently, after the blueprint is designed, the actual printing is processed through a bioprinter, and a bioprinted cell-laden construct is rapidly obtained. Being 3D bioprinting an AM technique, deposition of biomaterials (either encapsulating cells or loaded with cells later on) in micrometer scale to form subtle structures, is provided in most cases by a three-axis mechanical platform that controls the movements of extruders printing the bioink in the required shape. This platform's movement is governed by coordinates created by the designer and saved in a file format such as g-code that could be easily followed by the printer. As the third step, the bioprinted construct must then undergo the process of cell proliferation, tissue remodelling and maturation.

3D bioprinting has advantages such as precise deposition, cost-effectiveness, simplicity and cell distribution controllability. As a result of increasing interest in 3D bioprinting, need for new bioinks

providing required properties for successful printing, such as printability, printing fidelity, and mechanical properties has been rising, leading to development of new materials.

2.2 Classification of 3D-bioprinting technologies

For the fabrication of 3D-bioprinted constructs, the bioink and bioprinter are key elements. Important factors such as strength, resolution and shape depend on the fabrication method. The main bioprinting technologies, as discussed below, are droplet-based, extrusion-based, laser-induced forward transfer and stereolithography (Figure 2.2).

2.2.1 Droplet-based bioprinting (DBB)

DBB is an agile technique in which droplets are layered in a controlled way on the top of a substrate without contact between the nozzle and the substrate. DBB is highly versatile as it is compatible with many biological materials and it can print low viscous inks (3.5–12 mPa s^{-1}) with high speed and resolution [150]. However, it has to face some challenges, such as inconsistent encapsulation of cells [150], lack of droplet uniformity as well as poor mechanical and structural integrity of the printed constructs [151]. DBB can be further subdivided into three categories: inkjet, acoustic and micro-valve bioprinting.

- ***Inkjet bioprinting***

As the most common form of DBB, this technology includes continuous-inkjet, drop-on-demand inkjet and electrodynamic inkjet bioprinting. In continuous-inkjet bioprinting, a stream of bioink solution is extruded through a nozzle and breaks up into droplets due to the Rayleigh-Plateau instability [151]. The drop-on-demand (DOD) inkjet technique generates droplets using thermal or piezoelectric actuators or electrostatic forces. Briefly, in the thermal DOD typology, a voltage pulse is applied to locally heat the bioink solution and produce a vapour bubble that then expands rapidly and bursts. The pressure produced by this pulse will at some point overcome the surface tension at the nozzle orifice, causing droplet ejection. In piezoelectric-induced droplet formation, a piezoelectric actuator causes deformation in the fluid chamber and a following pressure wave, which overcomes the surface tension at the nozzle orifice leading to droplet ejection. The third subset of inkjet bioprinting, electrohydrodynamic inkjet bioprinting, uses an electric field to pull the droplet through the nozzle orifice [151].

- ***Acoustic bioprinting***

In acoustic-droplet ejection bioprinters, the bioink is not exposed to stressors like heat, high pressure, high voltage or shear stress as in inkjet bioprinting. Rather, the bioink is kept in an open pool and droplets are produced through acoustic waves. The bioink in the reservoir is held in place due to the surface tension at a small exit microfluidic channel. The acoustic actuator consists of a piezoelectric substrate with interdigitated gold rings placed upon it, which generate acoustic waves on demand on the surface. The generated circular waves move from the air–bioink interface down toward the exit channel to form an acoustic focal point. When the force of this focal point exceeds the surface tension at the exit channel, a droplet will be ejected [151].

- ***Micro-valve bioprinting***

In a micro-valve bioprinter, droplets are generated by the opening and closing of a microvalve under pneumatic pressure [152]. The printer contains a solenoid coil and a plunger that blocks the orifice. When a voltage pulse is applied, the valve coil at the top of the print head will generate a magnetic field which pulls the plunger upwards, unblocking the exit. When the back pressure in the bioink chamber is large enough and exceeds the surface tension, the bioink is ejected [151].

2.2.2 Extrusion-based bioprinting (EBB)

EBB is the most common and affordable bioprinting technique [150]. It is able to fabricate 2D and 3D structures by continuous dispersion of a hydrogel containing cells through a micro-nozzle. Extrusion-based printers disperse the bioink through a pneumatic or mechanical system and the 2D patterns are created by physically or chemically solidifying the hydrogels. By stacking these 2D patterns, 3D structures can be created [152]. The advantages of this technique are the ability to deliver multiple cells and materials and the high material selectivity. It has the ability to disperse highly viscous bioinks with high cell densities, cell pellets, tissue spheroids, and tissue strands. Furthermore, the production is scalable and synthetic polymers can be used. A great advantage is the high cell viability, even above 90% [152]. The technique however has a downside, as it has a relatively low resolution (>100 μm). Several tissue types have already been explored for extrusion-based bioprinting, including cartilage [113,153].

2.2.3 Laser-induced forward transfer (LIFT) bioprinting

LIFT bioprinting was first used for the deposition of inorganic materials and then adapted for bioprinting [154]. The system contains a donor layer and an energy-absorbing layer (gold or titanium), sensible to laser stimulation. During printing, a laser pulse is applied on the donor layer, heating a small portion that evaporates and creates a high-pressure bubble. In turn, the high-pressure bubble puts pressure on the bioink layer suspended on the bottom of the donor one and propels the bioink towards the substrate**,** where it will then immediately be cross-linked [155].

2.2.4 Stereolithography

Instead of heating a donor layer as in LIFT printing, stereolithography uses a laser or digital light projector to layer by layer photo-cross-link the bioinks. Advantages of stereolithography are its high resolution (<100 μm), short printing time (<1 h), and high cell viabilities [155].

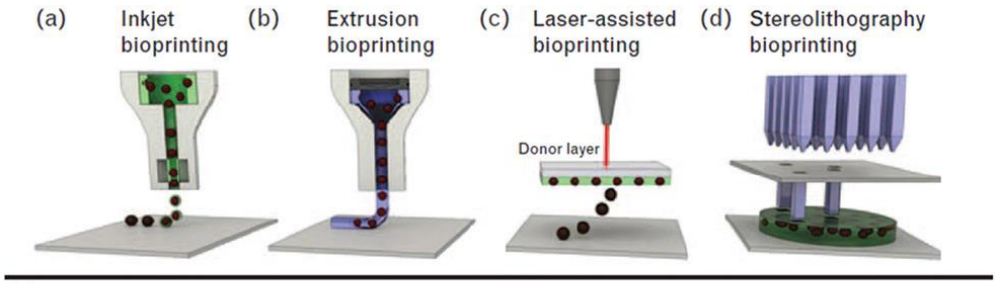

(e) Comparison of 3D bioprinting modalities

	Inkjet	Extrusion	Laser assisted	Stereolithography
Ink viscosity	3.5–12 mPa/s	Up to 6 x 10^7 mPa/s	1–300 mPa/s	No limitation
Cell density	Low, <10^6 cells/ml	No limitation	Medium, <10^8 cells/ml	No limitation
Resolution	High	Moderate	High	High
Print speed	Fast	Slow	Medium	Fast
Cost	Low	Medium	High	Low

Figure 2.2: Schematic representation of bioprinting technologies. (**a**) Inkjet bioprinting includes continuous, drop-on-demand, and electrohydrodynamic jetting. (**b**) Extrusion-based printing. (**c**) Laser-assisted (also known as laser-induced forward transfer) bioprinting. (**d**) Stereolithography. (**e**) Comparison of the techniques **a–d**. Image taken from [156].

2.3 Bioink typologies

3D bioprinting allows fabrication of living tissue/organ-like structures throughout the deposition of bioink. In this context, an ideal bioink should resemble the mechanical, rheological and biological properties of the target tissues in order to ensure correct functionality of the bioprinted tissues and organs. Two main bioink types have been developed: scaffold-based and scaffold-free [144]. The former type is composed of cells and biomaterials (hydrogels or similar exogenous materials) which are mixed and released together in order to produce a construct. The biomaterial acts as scaffold that provide an environment suitable for cell growth and differentiation with the final goal of tissue formation. The latter type is instead characterized by aggregates such as cell pellets, tissue strands or spheroids bioprinted without the use of an exogenous biomaterial in a scaffold-free process mimicking embryonic development. The scaffold-based approach is the most common, but it has been suggested that both approaches can complement each other to help cover the broad spectrum of tissue engineering/regenerative medicine applications.

Regarding scaffold-based bioink, a wide array of biomaterials have been developed for tissue engineering and regenerative medicine [157], but most of them are not compatible with existing bioprinting technologies. Some important features of an ideal bioink material are printability, tunable mechanical properties, insolubility in cell culture medium, post-printing maturation, biocompatibility, non-immunogenicity, and the ability to promote cell adhesion. In addition, bioink materials should be easily manufactured and processed, affordable and commercially available. Finally, bioprinted constructs are expected to keep their designed shape, structural strength and integrity, maintain 3D architecture for a defined period of time *in vitro*, easily engraft with the host and degrade over time *in vivo* at a rate appropriate to the regenerating tissue [158].

2.3.1 Hydrogels in 3D-bioprinting

Hydrogel is generally referred as a class of insoluble cross-linked polymeric substances, of natural or synthetic origin, capable of absorbing and retaining large quantities of water [159]. Since hydrogels are highly hydrated and also permeable to oxygen, nutrients and other water-soluble compounds, they are attractive biocompatible materials for fabrication of tissue constructs [160]. In contrast to polymeric scaffolds used in tissue engineering where cells are generally seeded on the surface, hydrogels provide an appropriate environment for embedding cells when undergo gelation (cross-linking), which enables them to migrate in any direction in 3D and communicate with each

other through a porous flexible network [161]. A disadvantage of hydrogels, however, is their weak mechanical properties, which preclude them from maintaining their designed shape [162].

The suitability of a hydrogel for a specific bioprinting process mainly depends on its physicochemical properties (Figure 2.3), including rheological properties and cross-linking mechanisms [163,164]. However, the specific processing parameters, such as nozzle gauge, will consequently determine the shear stress the embedded cells are exposed to, as well as the maximal time required for fabrication of a construct.

Finally, once the hydrogel precursors and cells have been printed, the construct has to possess, develop or be endowed with shape fidelity and sufficient mechanical stability, for example by post-processing gelation as a result of cross-linking. These parameters are important for the different biofabrication technologies: thus, DBB is generally limited to low maximum viscosities and requires rapid gelation to allow fabrication of an intricate 3D structure; while EBB bioinks with higher viscosities can be processed and the maintenance of the initial shape is facilitated allowing for gelation of the generated structures post-fabrication, as well as building large constructs in the x, y, z directions.

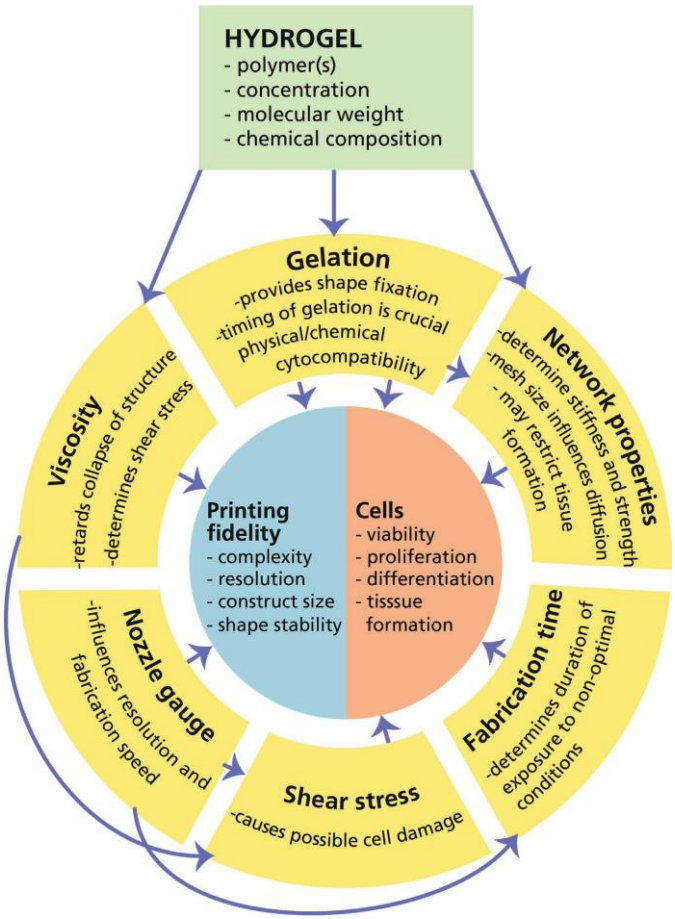

Figure 2.3: Crucial variables and relations in hydrogel-based 3D bioprinting. Hydrogel features (polymer types, concentration, molecular weight and chemical composition) directly influence the viscosity, gelation, and mechanical properties of the final gel. This, in combination with processing parameters, such as nozzle gauge and fabrication time, influence the printing fidelity and viability of embedded cells. Image taken from [164].

2.3.1.1 Rheology of bioprinted hydrogels: viscosity, shear thinning and yield stress

Rheology is highly relevant to biofabrication (Figure 2.4) since it represents the study of the flow of matter under application of an external force. Some of the rheological parameters of a hydrogel, including viscosity, shear thinning and yield stress, are discussed below.

Viscosity is the resistance of a fluid to flow upon application of stress. It depends mainly on polymer concentration and molecular weight of the selected material, but also solubility parameter, shear rate and temperature can contribute. In biofabrication, a high viscosity hinders both surface tension-driven droplet formation and the collapse of deposited structures. Thus, viscosity of the bioink directly influences shape fidelity after deposition [165]. Printing fidelity generally increases with increasing viscosity, but it implies an increase of the applied shear stress, which may be

harmful for the suspended cells [166]. However, cell viability in printed hydrogels used so far was generally not severely affected although a (negative) influence of shear stress has been observed for EBB [167]. Shear stress is influenced by the geometry of the dispensing setup (dimensions of channels, nozzles and/or orifices) and flow rates. Consequently, shear stresses may be reduced at the cost of loss of resolution (larger nozzles/orifices) or at the cost of flow rate.

Shear thinning refers to the non-Newtonian behaviour in which the viscosity decreases as shear rate increases [168]. It is caused by shear-induced reorganization of the polymer chains to a more stretched conformation, which leads to decreased entanglements and, therefore, viscosity. This phenomenon is, to a variable extent, exhibited by most polymeric systems. Particularly, shear thinning is observed for solution of polymers with high molecular weight. Sodium alginate is an example of a polymer that shows strong shear thinning behaviour [169]. Before starting the bioprinting, polymer chains form a temporary network in the syringe and induce gel-like viscosity. Upon dispensing through a needle, the temporary network is broken up by shear and all polymer chains align, reducing the viscosity by orders of magnitude. Directly after removal of shear stress, the temporary network is restored, viscosity increases (resulting in a high printing fidelity) and the plotted filament solidifies instantly.

Yield stress is stress that must be overcome to initiate flow. Generally, interactions between polymer chains result in the formation of a fragile, physically cross-linked network, which is broken by shear forces (above the yield stress) and slowly reforms when the shear is removed. Where high viscosity only delays collapse of a deposited 3D structure, the presence of a yield stress can potentially prevent flow and collapse. Besides improving printing fidelity, the presence of a yield stress also prevents cell settling in the hydrogel precursor reservoir. Hydrogel systems that exhibit yield stress and shear thinning have been developed more specifically for delivering cells or bioactive molecules into the body by injection from a syringe [168].

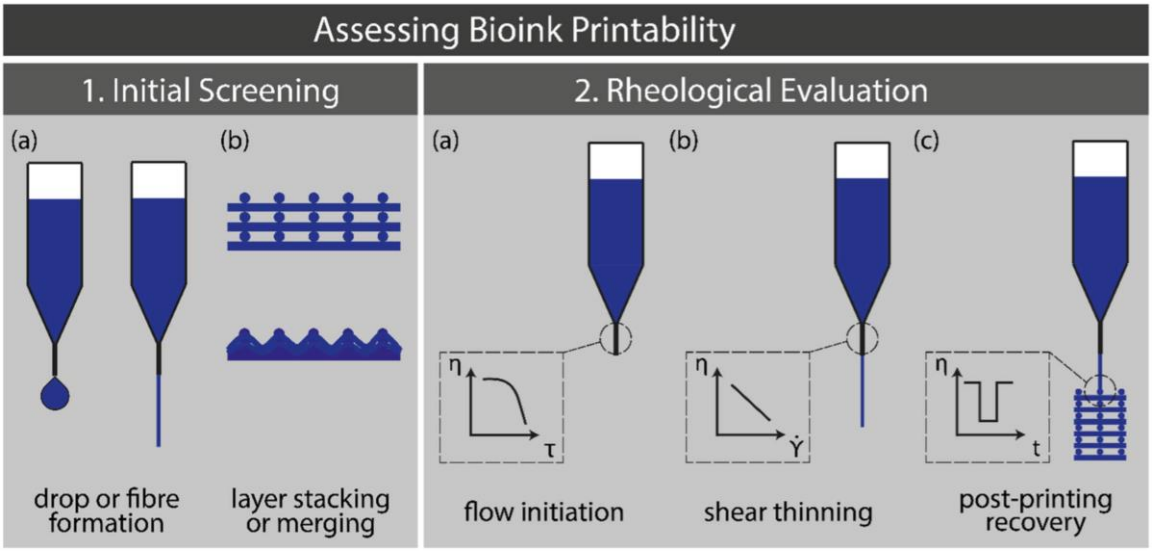

Figure 2.4: Parameters to assess bioink printability in EBB. 1. Initial screening of ink formulation that must show (**a**) fibre formation and (**b**) layer stacking. 2. Rheological evaluations of the ink regarding (**a**) the flow initiation properties and yield stress, (**b**) degree of shear thinning and (**c**) post-printing recovery. Image taken from [170].

2.3.1.2 Cross-linking mechanisms of bioprinted hydrogels

As discussed above, cross-linking or gelation of a printed hydrogel structure is necessary to preserve its shape, which otherwise could collapse at some point. The gelation can either be physical (based on reversible interaction), chemical (based on formation of covalent chemical bonds), or a combination of both processes, and it is achieved by intervention of an external stimulus, such as light, temperature, or ion concentration.

Physical cross-linking consist on non-covalent interactions, including hydrogen bonds, ionic interactions, hydrophobic interactions and thermal response. Physically cross-linked gels are very common in biofabrication since they do not require harmful chemical cross-linking agents and consequently are compatible with cells and biomolecules [164]. However, one disadvantage of these hydrogels is the lack of stability due to the fact that the reactions are reversible and can be disrupted by changes in ion concentrations, pH or temperature.

Chemical cross-linking leads to hydrogel formation by newly formed covalent bonds between gel precursors (i.e. low molecular weight monomers). Chemical cross-linking mechanisms include radical polymerization, chemical reaction of complementary groups, high energy irradiation and enzymatic reactions. Chemically cross-linked hydrogels are more stable than physically cross-linked hydrogels. Moreover, their mechanical strength can be controlled by the cross-linking

density. Among the disadvantages of these methods, the toxicity of the cross-linking agents and the potential unwanted reactions with the bioactive substances should be taken into account [164].

2.3.2 Hydrogel types used in 3D-bioprinting

Hydrogels are classified into two groups: naturally-derived hydrogels, such as gelatin, fibrin, collagen, HA and alginate, and synthetically-derived hydrogels such as Pluronic® or polyethylene glycol (PEG) [171]. Naturally-derived hydrogels can be further categorized based on where they have been derived from. Hydrogels such as collagen, fibrin, and gelatin are generally derived from vertebrates and so they possess inherent signaling molecules for cell adhesion, whereas hydrogels like alginate are derived from other living organisms such as algae or sea weeds and lacks these signalling molecules. Both natural and synthetic hydrogels have some limitations. Natural hydrogels generally have weak mechanical properties while synthetic counterparts lack bioactive signals for cell adhesion or migration [160]. In next sections, examples of hydrogels belonging to these two categories exploited in 3D bioprinting are described (Figure 2.5).

2.3.2.1 Natural hydrogels

- ***Agarose***

Agarose is a naturally-derived polysaccharide molecule which undergoes gradual gelation at low temperatures and liquefies at temperatures ranging from 20 to 70 °C, depending on the hydroxyethylation [172]. Low cell adhesion and spreading suggest that agarose is a poor material for cell culture; however, its biological properties can be improved by blending with other hydrogels such as collagen [173]. Agarose provides superior stability and construct thickness in EBB compared to collagen/agarose blends. Although cell viability was maintained, they retained a round as opposed to a spread morphology [173]. Since agarose has a thermally-reversible behaviour, it can be used as a sacrificial material in a bulky scaffold of a thermally stable hydrogel. It can be liquefied and drained, leaving a hollow, perfusable structure [174]. In general, its viscous nature does not allow inkjet bioprinting as it can easily clog the nozzle. Agarose is a promising candidate for laser-based bioprinting due to its viscoelastic nature and rapid gelation mechanism.

- ***Alginate***

Alginate is a popular hydrogel used in bioprinting processes due its biocompatibility, various choices of cross-linking and bioprinting methods, low price and ease of use in the creation of 3D structures [175]. It is a polysaccharide made of alternating β-D-mannuronate (M) and its C-5 epimer

α-L-guluronate (G) units [176], where the G subunits are responsible for forming the gel phase. Alginate undergoes ionic cross-linking in calcium chloride ($CaCl_2$) or calcium sulfate ($CaSO_4$) solutions. The divalent calcium ions form a bridge due to the attraction of negatively charged carboxylic acid groups between two neighbouring alginate chains. Alginate has been widely used for cell encapsulation, including articular chondrocytes [177]. EBB of alginate has been one of the most popular techniques in the field. Alginate in 2–4% (w/v) is extrudable, structurally stable and biologically acceptable and, after contacting the cross-linker, solidifies rapidly and maintains its 3D shape [178,179]. The concentration of alginate determines the viscosity of the solution, porosity and cross-linking time. It is possible to form pre-cross-linked alginate by mixing with low concentrations of the cross-linker, which increases its printability [180].

- ***Type I collagen***

As one of the major components of connective tissues in mammals, type I collagen is a triple helical biocompatible protein which has been extensively used in tissue engineering applications [181]. Collagen matrix facilitates cell adhesion and growth due to abundant integrin-binding domains. Although type I collagen has been used in bioprinting, it has limitations as it remains in a liquid state at low temperatures and forms a fibrous structure at a slow gelation rate and with increased temperature (complete gelation can take up to half an hour at 37 °C). Thus, before gelation takes place, 3D printed collagen structure loses its shape as well as embedded cells are pulled down by gravity and consequently not homogeneously distributed. EBB has utilized collagen alone as a bioink [182], but low mechanical properties together with the abovementioned issues necessitate the use of supportive hydrogels (mixing it with Pluronic® has generated better results [183]). Droplet-based bioprinting also takes advantage of collagen as a bioink material; however, collagen needs to be deposited before the onset of cross-linking [184].

- ***Fibrin***

Fibrin is a hydrogel formed by the enzymatic reaction between thrombin and fibrinogen, the key proteins involved in blood clotting. It plays a significant role in wound healing and has been used in fabrication of skin grafts [185]. Due to the no shear thinning nature of fibrinogen and thrombin, fibrin is rarely extruded. However, bioprinting of the two components of fibrin is an ideal option for DBB [151], while it can be mixed with other compatible hydrogels in laser-based bioprinting [186].

- ***Gelatin***

Gelatin is a denatured form of collagen protein, whose strands self-associate to form helical structures in a gel-like state at low temperatures and reverts back to a random coil conformation as temperature increases [187]. Gelatin retains the Arg–Gly–Asp (RGD) sequence from its precursor, and promotes cell adhesion, differentiation, migration and proliferation [188]. Gelatin is rarely bioprinted in its native form due to its poor mechanical properties. To employ gelatin for bioprinting, it has been chemically cross-linked by the addition of agents such as glutaraldehyde [189]. Gelatin is, however, not a popular hydrogel for DBB. Some studies have been performed by blending gelatin with other hydrogels such as alginate [190]. Gelatin has been successfully used in laser-based bioprinting due to its viscoelastic properties, stability and ability to hold cells in precise positions without damaging them [191].

- ***HA***

HA, a linear non-sulfated glycosaminoglycan, is ubiquitous in almost all connective tissues and a major ECM component of cartilage. It is comprised of repeating disaccharide units of D-glucuronic acid and N-acetyl-D-glucosamine moieties linked by alternating β-1,4 and β-1,3 glycosidic linkages [192]. HA has slow gelation rate and poor mechanical properties, thus, chemical modifications of the aforementioned groups are often carried out to enhance its rheological properties [114]. Hyaluronic acid has been used in EBB blended (chemically linked) with other hydrogels to enhance its bioprintability and solidification ability. Use of HA in DBB has not been demonstrated so far due to its viscous nature and slow gelation rate; however, it has been employed in laser-based bioprinting when combined with other hydrogels such as fibrin [186] to facilitate faster cross-linking.

2.3.2.2 Synthetic hydrogels

- ***Methacrylated gelatin (GelMA)***

GelMA consists in gelatin with methacrylate groups conjugated to its amine side groups. It has been used for tissue engineering due to its tunable mechanical characteristics [193]. GelMA is frequently used in EBB studies, including bioprinting of chondrocytes [165]. It is easy to extrude since it has low viscosity at room temperature, furthermore it forms a hydrogel that is mechanically strong when cross-linked in the presence of a photo-initiator. Its cross-linking rate can be also manipulated by the length of exposure to UV light.

- ***Pluronic® F-127***

Pluronic® F-127 is a trade name for a synthetic poloxamer-based polymeric compound. It exhibits a polymeric architecture consisting of two hydrophilic blocks between a hydrophobic block making it an effective surfactant [194]. Pluronic® undergoes reverse gelation as it starts to cross-link with increasing temperature. However, its copolymer structure erodes quickly and cannot hold structural integrity for longer than a few hours. Despite this issue, Pluronic® in combination with other hydrogels such as PEG, is useful for drug delivery and controlled release applications [195]. The reversible properties of Pluronic® can be useful in fabrication of complex constructs: if Pluronic® in solid form (at room temperature) is surrounded by a second type of hydrogel, it liquefies after the construct is placed at 4 °C. This procedure creates perfusable channels within bulky cell-laden constructs [196]. The thermosensitive nature and high viscosity of Pluronic® is problematic for DBB and the lack of viscoelasticity preclude from its use in laser-based bioprinting.

- ***PEG***

PEG has been widely used in medical and pharmaceutical products [197]. One of the major limitations of PEG is its poor mechanical strength, which can be overcome by addition of diacrylate (DA) of methacrylate (MA) moieties. However, additives such as DA and MA require photo-induced cross-linking by UV-light exposure for a specific time to obtain the desired mechanical properties. Excessive exposure to UV-light can dramatically reduce cell viability. PEG-DA and PEG-MA hydrogels are used in all types of bioprinting modalities: EBB [198], DBB [199] and laser-based technologies [200].

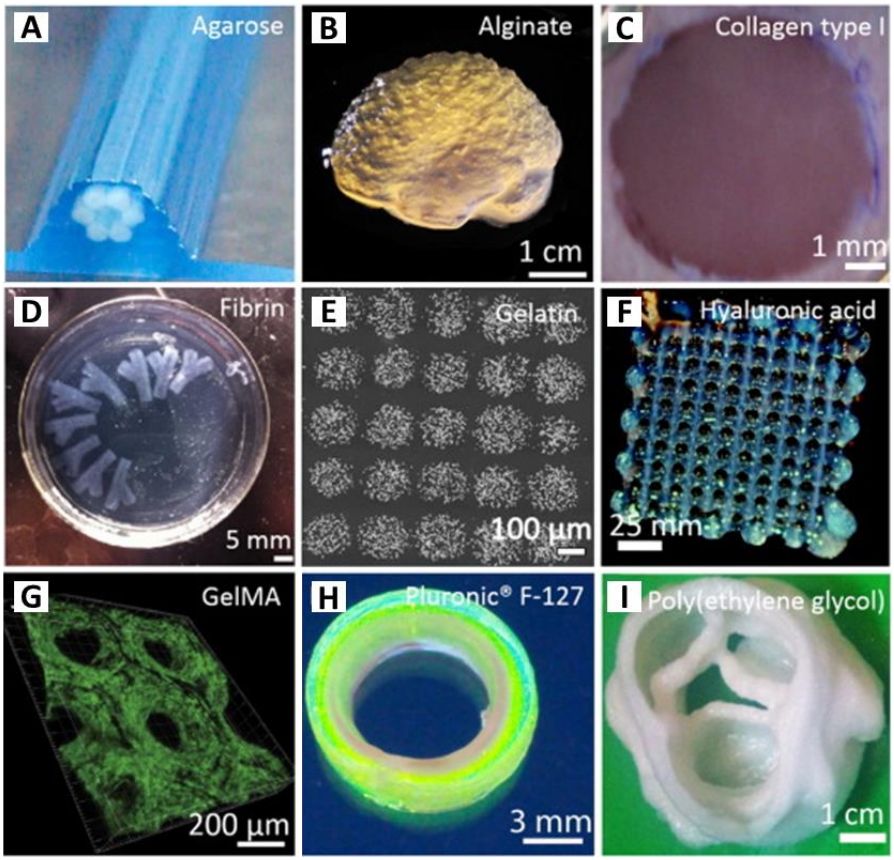

Figure 2.5: 3D-bioprinted structures of naturally- and synthetic-derived hydrogels. (**A**) Agorose filaments; (**B**) alginate in brain shape; (**C**) type I collagen construct inserted in a wound; (**D**) tubular scaffolds of fibrin; (**E**) gelatin with embedded cells; (**F**) HA grid; (**G**) GelMA scaffold with embedded cells; (**H**) Pluronic® F-127 tube; (**I**) PEG aortic valve construct. Image taken from [158] with some modifications.

2.4 3D-bioprinting for cartilage regeneration purposes and perspectives

3D bioprinting has the potential to replicate complex native-like tissue architecture more faithfully than traditional tissue engineering methods of assembly, consisting of nonspecific cell seeding of scaffolds [201]. This emerging technology represents a developmental biology inspired alternative to classic scaffold-based approaches in tissue engineering and has the ability to assemble biological components in prescribed 3D structure as well as patient customization [202]. Many tissue engineering and 3D bioprinting researches to date have focused on cartilage since it theoretically should be a simple tissue type to replicate as it is avascular and aneural. Although significant improvements in reparative cartilage treatments, as already discussed, have been achieved over the past few decades, full cartilage restoration remains a significant challenge.

Since bioprinting technology is rapidly gaining interest in the field of regenerative medicine, bioprinted constructs may provide a solution for cartilage injuries and defects. However, it is still an emerging technology and consequently some challenges have to be overcome before its translation to clinical applications.

EBB is the most suitable and used technique for the fabrication of viable constructs of several centimeters in size and with high cell densities [164]. However, the resolution of the printed fiber thickness is limited by the extrusion process to ~100 μm. In contrast, inkjet and laser-based printing allow the deposition of smaller volumes and are, thus, more suitable for the accurate deposition of micropatterns, down to the level of single cells. Despite these considerations, inkjet bioprinting, in combination with electrospinning, has been used *in vitro* to generate layered cartilage constructs able to maintain suitable mechanical and structural properties and to support cell function [203]. Currently, the most promising bioinks for cell-based 3D bioprinting are based on hydrogels, as they provide a highly hydrated and mechanically supportive 3D environment for cell encapsulation.

So far, in cartilage bioprinting research, the focus has predominantly been on the use of chondrocytes as cell source. Nevertheless, when using autologous chondrocytes, obtaining sufficient cell numbers remains a challenge, especially since expansion in monolayer culture causes dedifferentiation of the cells toward a fibroblastic phenotype [204]. An alternative cell type is the multipotent MSC population, which can be derived from multiple tissues, including bone marrow, adipose tissue and muscle [205]. These cells can be differentiated towards chondrogenic lineage in presence of specific growth factors, such as the TGF-β, although some of them are often less efficient in terms of chondrogenic commitment [206]. However, other cues to control MSC fate have to be provided, as these cells have the tendency to progress into hypertrophic chondrogenesis and to give rise to bone formation via the endochondral pathway once implanted *in vivo* [207]. Therefore, alternative cell populations with regenerative potential are being investigated, including subpopulations of chondro-progenitor cells, which can be harvested from mature cartilage and can be expanded in monolayer culture without losing their chondrogenic phenotype [34].

Additionally, in order to generate bioactive constructs based on 3D-printing technologies, the embedding of biological cues that stimulate encapsulated cells or attracts and/or stimulates cells from the host can be pursued. Overall, hydrogel-based bioinks allow for the incorporation of growth factors, bioactive proteins, peptides, chemicals and matrix components [208], and printing procedures have not shown any negative effects on the activity of these biological cues [113,209]. In this context, since one of the limitations of the synthetic or natural biomaterials currently used for cartilage repair is their poor capacity to mimic the complexity of natural ECM, decellularized ECM

(dECM) has been recently printed to provide microenvironments able to promote cells engraftment, survival and growth of cartilage tissue [210].

Moreover, multiple inks consisting of different biomaterials, bioactive factors, and cells can be loaded in a bioprinter to fabricate complex anatomical architectures with multiple tissue types. Printing with multiple bioinks also allows for the inclusion of tissue interfaces in the construct. This is of particular importance in the orthopaedic field, where osteochondral constructs can be fabricated through suitable bioinks that mimic bone and cartilage regions [211].

3D bioprinting may be a unique tool to achieve also the appropriate zone-specific compositional and mechanical heterogeneity present in articular cartilage. It could be pursued by mimic its specific fiber arrangement or depth dependent differences in cell densities and phenotypes, as it has been obtained by gradient bioprinting method [212] and incorporation of biological cues and matrix components [213] respectively.

Finally, bioprinting can contribute to the automation of the implant production process. Besides printing into a cell dish, constructs could also be printed directly into a bioreactor, minimizing handling and, thus, infection risks. Potentially, cartilage defects could also be filled *in situ*, by printing the implant directly into the lesion. In line with this, steps exploring the feasibility of *in situ* bioprinting have been taken for calvarial defects in living mice [214]. Additionally, a bio-pen is being developed to simplify the *in situ* print procedure [215].

3 MSC-like progenitor cells activated by platelet lysate in human articular cartilage as a tool for future cartilage engineering and reparative strategies

Carluccio S., Martinelli D., Pereira R. C., Palamà M. E., Guijarro A., Benelli R., Cancedda R., Gentili C.

Abstract: Regenerative strategies for human articular cartilage are still challenging despite the presence of a progenitor cell population inside. Platelet derivatives are studied since they can promote tissue healing processes by re-activation of endogenous regenerative mechanisms. While their use in orthopaedics continues, mechanisms of action and efficacy still remain to be elucidated. Primary cultures of human articular chondrocytes (ACs) and cartilage chips were set up from donor biopsies and were treated *in vitro* with platelet lysate (PL). Proliferation, clonogenic potential and phenotype of ACs and chondro-progenitor cells (CPCs) derived from organ culture in PL were characterized. Secretory profile of CPCs were analysed together with their migratory capabilities by mimic osteoarthritis *in vitro*. Tri-lineage differentiation potential were tested *in vitro* and scaffold-assisted chondrogenesis of CPCs were studied in nude mice. PL recruited a CPCs-enriched population from *ex vivo* cartilage culture, that showed high proliferation rate, clonogenicity and nestin expression. CPCs were positive for *in vitro* tri-lineage differentiation, formed hyaline cartilage-like tissue *in vivo* without hypertrophic fate and have migratory phenotype. Some of CPC-feature were found also in ACs-PL compared to ACs-FBS. PL treatment of articular cartilage activates a stem cell subset responsive to injury being therefore promising in cartilage therapeutic applications.

Keywords: articular cartilage, platelet lysate, chondro-progenitors, nestin, chondrocytes

3.1 Introduction

Despite possessing resident progenitors primed for chondrogenesis, articular cartilage has poor intrinsic regenerative capability and cell turnover mainly due to its avascular and alymphatic nature [216]. A dense and abundant extracellular matrix, made of proteoglycans and collagen fibers, surrounds few and no-proliferating chondrocytes, responsible for ensuring tissue mechanical

integrity and functionality by maintaining a dynamic balance between matrix synthesis and degradation [217].

The isolation from the systemic circulation keeps away the inflammatory and reparative mechanisms triggered after injury, precluding damaged cartilage to recover its functional configuration, which leads to tissue degeneration and the subsequent establishment of the osteoarthritis (OA) pathology. Nowadays, OA is one of the major musculoskeletal diseases [64], and affects joints by causing gradual loss of articular cartilage together with osteophyte growth and synovial inflammation [218]. Since articular cartilage works as lubricant and load-bearing surface in healthy joints, symptoms of these disorders are pain and disability, that lead to an impaired patients' quality of life and increased health-care costs for the society.

Currently, several therapeutic approaches for focal chondral defects and OA are used, including bone marrow surgical stimulation aimed at triggering intrinsic reparative mechanisms, cell therapy based on autologous chondrocyte implantation (ACI) and osteoarticular auto/allografts to fill and restore cartilage defects [219]. However, the treatment of extended defects is still challenging, especially for the elderly people, and these techniques are still defective because the neo-tissue is often fibrotic or its integration with neighbouring tissues is not complete [220].

Therefore, research efforts are directed to explore new methods to achieve articular cartilage regeneration and repair. The use of therapies based on stem cells has attracted great interest, since it is widely known that mesenchymal stem cells (MSCs), such as bone marrow-derived MSCs (BM-MSCs), can differentiate into the chondrogenic lineage both *in vitro* and *in vivo* [221,222]. However, stem cell niches are located *in situ*, where they could participate directly in tissue homeostasis and repair processes. In fact, tissues in the joint, such as the synovium, hold MSCs with chondrogenic potential [45] and articular cartilage itself contains a postnatal progenitor cell population [7,223]. Moreover, during OA, pathological joint tissues and synovial fluid become enriched of cells with features of stemness [46,224], probably as an attempt to limit the ongoing damage and restore the integrity of the tissue.

It is reasonable that exploiting local chondro-progenitors (CPCs) for cartilage repair may be a better and more efficient cell-based therapeutic strategy compared to the use of BM-MSCs. CPCs are developmentally primed for differentiation into chondrocytes, while BM-MSCs are more prone to form fibrocartilage with poor bio-mechanical properties and display hypertrophic phenotype [225]. However, the fact that chondrocytes and cartilage-derived CPCs share the same anatomical location, and chondrocytes can dedifferentiate and acquire stemness-like characteristics in culture

makes the distinction between the two populations difficult [226]. Therefore, in this study we tried to find some features that can help to distinguish CPCs from mature chondrocytes.

In the field of regenerative medicine, local transplantation or systemic infusion of stem cells represent an effective cellular therapy in many pathological states, including those that concern musculoskeletal system. Nevertheless, regeneration strategies targeting stem cells *in situ* could be more attractive and more advantageous thanks to the absence of *in vitro* culture steps and loss of injected cells. According to this approach, endogenous stem cells are recruited to the injury site by administration of bioactive factors. Thus, in the last decades, among a wide range of products, platelet rich plasma (PRP) has spread as a clinical treatment tool for musculoskeletal diseases [227]. Since PRP or other platelet derivatives (i.e. platelet lysate, PL) are a mix of growth factors, cytokines, chemokines and microRNAs normally involved in tissue healing, the rationale behind their application is the re-activation of latent endogenous regenerative mechanisms. Several studies have investigated PRP or PL roles both *in vitro* and *in vivo*, highlighting their capacity to exert anti-inflammatory and proliferating effects on cells [128,228,229], as well as to stimulate resident progenitors [230] or to recruit circulating ones (together with immune and endothelial cells) [231].

Regarding cartilage disorders, treatments based on platelet-derived products have shown pain relief and functional improvement in patients, confirming their chondroprotective function in these pathologies [232,233]. From a mechanistic point of view, these beneficial outcomes could be explained by the fact that PRP-derived factors, besides of promoting matrix deposition and downregulating inflammatory signalling in chondrocytes [234,235], induce postnatal maturation of damaged cartilage tissue that during degeneration had come back to an immature stage [236].

However, mechanism of action and efficacy of platelet products in orthopaedics still need to be elucidate, especially due to the wide variety of preparation and standardization methods that can impact the composition of the product [237] thereby affecting the physiological response. A better understanding of the events that lead to cartilage repair induced by PRP or PL may allow to solve these issues.

Here it is reported that *ex vivo* treatment of human articular cartilage with PL induces activation and outgrowth of cells that are endowed with some features of stemness, such as clonogenicity and expression of nestin [238], higher proliferation capacity than resident chondrocytes with concurrent chondrogenic potential maintenance. The stimulation of nestin-positive progenitor cells induced by PL in articular cartilage is of especial interest for the future development of therapeutic strategies given the involvement of these cells in tissue regenerative processes. Moreover, we further

characterize the PL effects on phenotype of mature articular chondrocytes (ACs), by showing that they reverted to an earlier stage similar to that of CPCs.

3.2 Materials and Methods

3.2.1 PL preparation

Buffy coat samples obtained from the whole blood of healthy donors at the Blood Transfusion Center of the IRCCS AOU San Martino-IST Hospital (Genoa, Italy) were used to prepare PL. All the procedures were performed with the approval of the Institutional Ethics Committee. According to Backly *et al*. [126], platelet pellet was obtained after serial centrifugation and resuspended at a concentration of 1×10^7 platelets/µl in plasma to get PRP. Platelet membrane rupture in the PRP suspension was achieved by three cycles of immersion in liquid nitrogen for 1 minute and incubation at 37°C for 6 minutes. The suspension was centrifuged at 900 × *g* for 3 minutes at 4°C and the supernatant was collected to obtain the PL, divided in aliquots and stored at -20°C until use.

3.2.2 Cell primary cultures

- *Chondro-progenitor cells (CPCs)*

Human articular cartilage biopsies were harvested from patients (n = 20, age ranges from 31 to 88 years old, 65-year median age) undergoing hip replacement surgery. All the tissue samples were obtained with written informed patient consent and according to the guidelines of the institutional Ethics Committee of the IRCCS AOU San Martino-IST National Cancer Research Institute (Genoa, Italy). Articular cartilage was separated from subchondral bone and fragmented in slices, which were further cut in disks with a biopsy punch of 8 mm in diameter. Each disk was divided in two halves and each half was then cultured in Dulbecco's Modified Eagle's Medium High Glucose (DMEM HG) containing 1 mM sodium pyruvate, 100 mM HEPES buffer, 1% penicillin/streptomycin and 1% L-glutamine (all from Euroclone) supplemented either with 10% FBS (Gibco) or 5% PL in 6-well plates for 1 month. Putative chondro-progenitor cells (from here on called CPCs), moving from cultured cartilage to the dish, were detached with trypsin/EDTA (Euroclone) and expanded in aforementioned medium supplemented with 5% PL (CPCs-PL). All described cell cultures were maintained in a humidifier incubator at 37°C and with 5% CO_2.

- *Primary articular chondrocytes (ACs)*

Primary articular chondrocytes (ACs) were obtained as described by Pereira *et al*. [128] from the remaining cartilage biopsy. In brief, chondrocytes were released by repeated digestions using an enzymatic solution composed by 1 mg/mL hyaluronidase (Sigma-Aldrich), 400 U/mL collagenase I, 1,000 U/mL collagenase II (both from Worthing Biochemical) and 0.25% trypsin (Thermo Fisher Scientific). The cells obtained were plated in DMEM HG basal medium described above and containing 10% FBS. At ~90% of confluence, cells were trypsinized and split in culture medium supplemented with 10% FBS (ACs-FBS) or 5% PL (ACs-PL). During culture, cells were monitored using a bright field microscope equipped with a digital camera (Leica DMi1; Leica Microsystems).

3.2.3 Growth kinetics

Growth kinetics were determined by plotting cells doublings of ACs-FBS, ACs-PL and CPCs-PL against time in culture. Cell doublings were calculated considering the number of cells plated and recovered at each passage. Briefly, semi-confluent cells were trypsinized, counted and always replated at a density of 1.25×10^4 cells/cm^2 in 60 mm culture dishes. Six primary cultures were tested (n = 6).

3.2.4 Western blot analysis

At passage 2, confluent ACs-FBS, ACs-PL and CPCs-PL were washed with phosphate-buffered saline 1X (PBS), then the monolayer of cells were scraped in cold radioimmunoprecipitation assay (RIPA) buffer containing 50 mM Tris (pH 7.5), 150 mM sodium chloride, 1% deoxycholic acid, 1% triton X-100, 0.1% SDS, 0.2% sodium azide and proteinase inhibitor cocktail (Sigma-Aldrich). Protein extract concentration was quantified by Bradford assay (SERVA) and western blot was performed according to Nguyen *et al.* [135]. Equal amounts of total proteins (10 µg) were loaded on 4%–12% NuPAGE Bis-Tris gel (Thermo Fisher Scientific) and electrophoresis was performed. Gels were blotted onto nitrocellulose membranes (GE Healthcare Life Sciences), immunoprobed overnight at 4°C with primary antibodies raised against cyclin D1 (Abcam) and α-tubulin (Sigma-Aldrich), both at a dilution of 1:10,000. After washing, membranes were exposed to horseradish peroxidase-linked goat anti-rabbit IgG (1:5,000, GE Healthcare Life Sciences) for 1 hour at room temperature (RT) and bands were visualized using enhanced chemiluminescence (ECL, GE Healthcare). Then, X-ray films (Fujifilm GmbH) were exposed to membranes, developed and fixed. Three primary cultures were tested (n = 3).

3.2.5 Evaluation of cell senescence

ACs-FBS, ACs-PL and CPCs-PL were analysed for senescence by detection of the senescence-associated β-galactosidase (SA-βgal) activity in a chromogenic assay, according to previous protocol [239]. In brief, adherent cells in 24-well dishes were fixed in 3% paraformaldehyde (PFA) and stained overnight at 37°C with fresh staining solution containing 40 mM citric acid/sodium phosphate buffer, 5 mM potassium ferrocyanide, 5 mM potassium ferricyanide, 150 mM sodium chloride, 2 mM magnesium chloride and 1 mg/mL 5-bromo-4-chloro-3-indolyl-D-galactoside (X-gal) in distilled water (all reagents from Sigma-Aldrich). Positive cells were observed under microscope Axiovert 200M (Carl Zeiss) and counted from five different fields at 20X magnification for each (five) replicate. Stained cells were calculated as a percentage of the total number of cells on the plate. Cells from 5 donors were subjected to the assay at passage 2 (n = 5).

3.2.6 Assay for *in vitro* and *in vivo* neoplastic transformation of CPCs

To exclude CPCs malignant properties, *in vitro* colony assay formation and *in vivo* tumorigenesis were investigated. For *in vitro* test, anchorage-independent growth assay in methylcellulose media was conducted [240]. Thus, CPCs-PL at passage 3 were plated at a density of 10,000 cells/35 mm petri dishes in the semi-solid culture system provided by StemMACS HSC-CFU Media (Miltenyi Biotec) according to the manufacturer's protocol. After 14 days of incubation, formation of CFU-cells (CFU-C) was assessed under an inverted microscope (Leica DMi1; Leica Microsystems). Three primary cells were tested (n = 3). MDA-MB-231 triple-negative breast cancer cell line was used as positive control. *In vivo* tumorigenesis was assessed with CPCs-PL at passage 2 from two different pools. For each pool, 1×10^6 cells were injected subcutaneously into 12 NOD/SCID mice. The mice were monitored up to 2-3 months.

3.2.7 RNA extraction and real-time quantitative reverse transcription polymerase chain reaction (qRT-PCR)

Total RNA from ACs-FBS, ACs-PL and CPCs-PL at passage 1 until confluence (in 100 mm dishes) was extracted by TRIzol™ Reagent (Thermo Fisher Scientific) according to the manufacturer's protocol. RNA concentrations were measured at 260 nm using Nanodrop TM 1000 (Thermo Fisher Scientific Inc.) and RNA purity was checked considering 260 nm/280 nm ratio with values included in 1.5–2.1 range. Complementary DNA (cDNA) synthesis was performed starting from 1 μg of total RNA and using SuperScript First-Strand synthesis system for reverse transcription polymerase

chain reaction (RT-PCR) (Thermo Fisher Scientific, USA) following the manufacturer's instruction. Transcript levels of target genes were measured by Real Time quantitative PCR (qRT-PCR) using Power SYBR® Green PCR Master Mix on 7500 Fast Real-Time PCR System (Applied Biosystems) under the following conditions: UDG activation at 50°C for 2 minutes, dual-lock DNA polymerase at 95°C for 2 minutes, 40 cycles of amplification at 95°C for 15 seconds (denaturation) and at 60°C for 1 minute (annealing/extension). After amplification, a melt curve was performed at 95°C for 15 seconds, 60°C for 1 minute and 95°C for 15 seconds. The housekeeping gene GAPDH was used as the endogenous control for normalization. The selected human-specific primer sequences were:
type II collagen (COL2A1), forward 5' - GGCAATAGCAGGTTCACGTACA - 3', reverse 5' - CGATAACAGTCTTGCCCCACTT - 3'; type I collagen (COL1A1), forward 5' - CAGCCGCTTCACCTACAGC - 3', reverse 5' - TTTTGTATTCAATCACTGTCTTGCC - 3'; SOX9, forward 5' - CCCGCACTTGCACAACG - 3'; reverse 5' - TCCACGAAGGGCCGCT - 3'; nestin, forward 5' - CAGAGGTGGGAAGATACGGT - 3', reverse 5' - AGCTCTGCCTCATCCTCATT - 3'; GAPDH, forward 5' - CCATCTTCCAGGAGCGAGAT - 3', reverse 5' – CTGCTTCACCACCTTCTTGAT - 3'.
Relative quantification was performed using the $2^{-\Delta\Delta}$Ct method.

3.2.8 Immunofluorescence staining and immunophenotypic characterization by flow cytometry

To perform immunofluorescence staining, ACs-FBS, ACs-PL and CPCs-PL at passage 1 were seeded on coverslips at density of 10.5 cells/cm^2 and fixed with 3.7% PFA after three-four days of culture. Fixed cells were permeabilized with a solution containing 20 mM HEPES (pH 7.4), 300 mM sucrose, 50 mM sodium chloride, 3 mM magnesium chloride and 0.5% triton X-100. After blocking with 20% normal goat serum (NGS, Gibco), samples were incubated overnight at 4°C with primary antibodies raised against SOX9, 1:200 diluted in 10% NGS (Abcam); type II collagen, 1:250 diluted in 10% NGS (CIICI-Developmental Studies Hybridoma Bank, University of Iowa); type I collagen, 1:300 diluted in 10% NGS (SP1.D8-Developmental Studies Hybridoma Bank, University of Iowa) and nestin, 1:2,000 diluted in 10% NGS (Abcam). Positive staining was detected by incubation with Alexa Fluor 488- or Alexa Fluor 594-conjugated anti-mouse or anti-rabbit immunoglobulin IgG secondary antibodies diluted 1:300 in NGS 10% (Life Technologies) for 1 hour at RT, followed by nuclear labeling with DAPI (Sigma-Aldrich). Samples were observed

under epifluorescent illumination using an Axiovert 200M microscope and images were captured with AxiocamHR camera (Carl Zeiss).

Expanded ACs-FBS, ACs-PL and CPCs-PL at passage 2 were phenotypically characterized for a set of surface markers using flow cytometry. After trypsinization, 100,000 cells were incubated separately with 1 µl of one of the following fluorescein isothiocyanate (FITC)- or phycoerythrine (PE)-conjugated antibodies: CD44-FITC, CD166-PE, HLA-ABC-PE, HLA-DR-FITC (all from BD Pharmigen), CD90-PE, CD105-PE, CD73-FITC, CD146-FITC, CD106-PE, CD45-FITC, CD34-PE, CD29-PE and isotype-matched IgG-PE and IgG-FITC control antibodies (all from Biosciences). The staining was performed for 30 minutes at 4°C in the dark to preserve the fluorochromes. Samples were run on a CyAN ADP cytofluorimeter (Beckman-Coulter). Data were analysed using FlowJo V10 software (Tree Star Inc.) and expressed as Log fluorescence intensity *versus* number of cells. Experiments were repeated on three different primary cultures (n = 3).

3.2.9 Colony forming unit fibroblast (CFU-F) assay

Clonogenic potential of ACs-FBS, ACs-PL and CPCs-PL at passage 1 was explored by plating them at low density (10 cells/cm^2) in a 100 mm culture dishes and performing the colony staining after 12 days of culture. At the end of the culture time, cells were washed with PBS, fixed with 3.7% PFA in PBS for 15 minutes at RT and stained with 1% methylene blue in borate buffer (10 nM, pH 8.8) for 45 minutes at RT. CFU-F assay was performed in duplicate for each tested primary cultures. Set of 6-well dishes were prepared for detection of nestin by immunofluorescence.

3.2.10 *In vitro* multilineage differentiation potential

The chondrogenic potential of ACs-FBS, ACs-PL and CPCs-PL was checked at passage 1 by micromass pellet culture *in vitro*. About 2.5×10^5 cells were pelletted in conical tubes and cultured for 3 weeks in chondrogenic medium containing 10 ng/mL human transforming growth factor-β1 (hTGF-β1) (PeproTech), 10^{-7} mol/L dexamethasone and 50 mg/mL ascorbic acid (both from Sigma-Aldrich) according to Johnstone *et al*. [221]. Chondrogenic differentiation was subsequently investigated by histological staining with toluidine blue (see 3.2.12 Histology and immunohistochemistry below).

To test osteogenic differentiation, cells were seeded in 24-well plates at the density of 10.5 cells/cm^2 in presence of osteogenic induction medium containing 5 µg/mL ascorbic acid, 10^{-7}

mol/L dexamethasone and 10 mmol/L β-glycerophosphate (all from Sigma-Aldrich). After 3 weeks of culture, calcium deposits were stained by Alizarin Red S (Sigma-Aldrich) solution.

To induce adipogenesis, cells were seeded as just reported above and grown in cuture medium containing 1 μmol/L dexamethasone, 60 μmol/L indomethacin, 10 μg/mL insulin and 1 mmol/L 3-Isobutyl-1-methylxanthine (IBMX) (all from Sigma-Aldrich). After 3 weeks of culture, intracellular lipid drops were detected with Oil Red O staining (Sigma-Aldrich). Chondrogenic, osteogenic and adipogenic potential of ACs and CPCs were determined, respectively at passage 1 and 2, on three different primary cell cultures (n =3).

3.2.11 *In vivo* cartilage and bone formation

CPCs-PL chondrogenic and osteogenic potential *in vivo* was investigated by implantation of cell pellets and cell-seeded biomaterials in athymic mice (female CD-1 nu/nu; Charles River Laboratories Italia, Italy).

CPC pellets were obtained as already described in previous section (3.2.10 *In vitro* multilineage differentiation potential) and implanted subcutaneously in mice after three days of *in vitro* culture in chondrogenic medium.

Moreover, CPCs-PL at passage 2 were also seeded on absorbable polyglycolic acid-hyaluronan (PGA/HA) scaffolds (BioTissue AG) to detect cartilage formation or on calcium phosphate ceramic scaffolds (MBCP$^{+®}$ Biomatlante SA) for osteogenic induction. Briefly, CPCs-PL were trypsinized at passage 1 and 2×10^6 cells were resuspended in 33% v/v fibrinogen in PBS (Tissucol, Baxter). Constructs with ACs-FBS at passage 1 associated to ceramic granules were also prepared as control. Both types of scaffolds were soaked with CPCs suspension and fibrinogen was polymerized by the addition of 1:10 v/v thrombin in PBS (Tissucol, Baxter). Cell grafts were maintained in chondrogenic or osteogenic medium for 3 days before subcutaneous implantation in mice. A number of at least three primary cells was used for these experiments. Groups of 8 animals were sacrificed 4 and 8 weeks after surgery for chondrogenesis or osteogenesis, respectively, and the harvested implants were processed for the histological analysis to evaluate cartilage and bone formation. All animals were maintained in accordance with standards of the Federation of European Laboratory Animal Science Associations, as required by the Italian Ministry of Health.

3.2.12 Histology and immunohistochemistry

Cartilage fragments, pellets and implants were fixed in 3.7% PFA in PBS, dehydrated in ethanol, and paraffin embedded. Cross sections of 5 µm were cut (by using microtome RM2165, Leica) dewaxed and stained according to the appropriate histological analysis: hematoxylin and eosin staining to observe cell organization and toluidine blue staining to detect sulfated glycosaminoglycans in cartilage.

For immunohistochemical analysis, dewaxed sections were treated with methanol:hydrogen peroxide (49:1) solution for 30 minutes to inhibit endogenous peroxidase activity, then permeabilized with 0.3% triton X-100 in PBS for 10 minutes and finally incubated with hyaluronidase (Sigma-Aldrich) at concentration of 1 mg/mL in PBS (pH 6.0) for 30 minutes at 37°C. After washes in PBS and incubation with 20% NGS for 1 hour to inhibit nonspecific binding, the slices were incubated overnight at 4°C with primary antibodies raised against: type II collagen, 1:250 diluted in 10% NGS (CIICI-Developmental Studies Hybridoma Bank, University of Iowa); type X collagen, 1:1,000 diluted in 10% NGS (Abcam) and proliferating cell nuclear antigen (PCNA), 1:200 diluted in 10% NGS (Abnova). The immunobinding was detected by incubation with biotinylated secondary anti-mouse or anti-rabbit antibodies (Dako) for 30 minutes at RT followed by treatment with streptavidin-peroxidase (Jackson ImmunoResearch). Peroxidase activity was finally visualized by 3-amino-9-ethylcarbazole (Sigma-Aldrich) chromogen substrate. Images were acquired by a microscope Axiovert 200M (Carl Zeiss) at different magnifications.

3.2.13 Production of CPCs and ACs conditioned media

ACs-FBS, ACs-PL and CPCs-PL at passage 1 were grown until 80% of confluence, extensively washed with PBS and incubated with DMEM HG culture medium without any supplements for 24 hours of conditioning. Conditioned media (CM) from each condition (CPCs-PL-CM, ACs 10% FBS-CM and ACs 5% PL-CM) were collected and centrifuged at 300 × g for 10 minutes then at 2,000 × g for 20 minutes and supernatants stored in aliquots at -80°C. In cytokine array experiment, supernatants in each condition were further concentrated by using Amicon™ Ultra Centrifugal Filter Units with 3KDa molecular weight cut-off (Merck Millipore). Amount of proteins in CM from CPCs and ACs was quantified by performing Bradford assay (SERVA).

3.2.14 Cytokine identification in ACs and CPCs secretomes

The release of cytokines and chemokines in CPCs- and ACs-CM (n = 1, from young patient of 31 years old) was analyzed using the Human XL Proteome Profiler™ Array (R&D Systems) according to the user's manual. Briefly, membranes spotted with antibodies were incubated with the same amounts (50 µg/mL) of each CM overnight at 4°C. The following day, detection antibody cocktail was added for 1 h at room temperature, before visualization using enhanced chemiluminescence. Quantitative analysis was performed on scanned (Epson perfection 1260 scanner, Seiko Epson Corporation) X-ray films (Fujifilm GmbH) using the Protein Array Analyser plugin available for ImageJ software (U. S. National Institutes of Health). For each membrane, average spot signal density was determined by densitometry, followed by background subtraction and normalization to the reference spots.

3.2.15 *In vitro* CPCs chemotaxis

CPCs-PL migration was investigated by Boyden chamber assay using serum-free medium as negative control and ACs-CM pre-treated for 24 hours with IL-1β (PeproTech), 5% PL or both stimuli as chemoattractants (see 3.2.13 for CM preparation). Cells were plated at density of 120,000/chamber on the top of the filter inserts and incubated for 4 hours at 37°C, 5% CO_2. Cells migrated to the lower surface of the filters were fixed in ethanol, stained with toluidine blue and quantified by a bright field microscope (Leica DMi1; Leica Microsystems). Each experiments was performed in triplicate and repeated at least three times (n = 3).

3.2.16 *In vitro* scratch assay on ACs and CPCs

ACs at passage 1 were plated in 6-well plates, cultured until confluence and treated with either 10% FBS or 5% PL for 24 hours. In parallel, CPCs-PL were cultured until confluence. Cell monolayers were washed extensively with PBS to remove residual of factors, scratched using 100 µl pipette tips and covered with serum-free DMEM HG culture medium. Scratch closure was monitored from t_0 = 0 h to t_1 = 24 h and t_2 = 48 h with inverted microscope (Leica DMi1, Leica Microsystems). Analysis on acquired images was performed with TScratch software (https://github.com/cselab/TScratch) as reported by Romaldini *et al.* [228]. Experiments were performed in triplicate on three different primary cultures (n = 3).

3.2.17 Statistical analysis

All data are presented as means and standard error of the mean (SEM). Unpaired Student's *t*-test was used to determine statistical significance within ACs-PL *versus* ACs-FBS or ACs-PL *versus* CPCs-PL. Level of significance was set at $p < 0.05$ (* $p < 0.05$, ** $p < 0.01$, *** $p < 0.001$, **** $p < 0.0001$). Two-way ANOVA was used to analyse *in vitro* scratch assay and growth kinetics, one-way ANOVA for *in vitro* chemotaxis assay, both followed by *post-hoc* Sidak's multiple comparisons test. Data were analyzed with GraphPad Prism® 8.0 software (GraphPad Software, Inc.).

3.3 Results

3.3.1 PL induced release of cells with fibroblastic-like phenotype from *ex vivo* cultured cartilage fragments and promoted their proliferation

Articular cartilage biopsies from patients were divided in fragments, some fragments were enzymatic digested to obtain ACs primary cultures and other fragments were directly cultured *in vitro* in petri dishes. Each fragment used for organ culture was divided in two halves. One of them was cultured in 10% FBS and the other one in 5% PL (Figure 3.1). This approach allows to consider the observed tissue reactions as a consequence of the culture conditions and not due to the heterogeneity of the sample.

After 15-20 days of cartilage chip culture in presence of PL, spindle-shaped putative CPCs derived from the tissue could be observed attached to the bottom of the plate (Figure 3.1B) as opposed to FBS-control culture, in which, in most of the cases, no cells exited from the cartilage chips. In the few cases in which cells were derived from tissue cultured in FBS, those cells were unable to proliferate and to be expanded for further analysis. Immunohistochemistry performed on cartilage chips after cell harvesting showed higher positivity to the proliferation marker PCNA in cartilage slices treated with PL compared to FBS ones (Figure 3.1C).

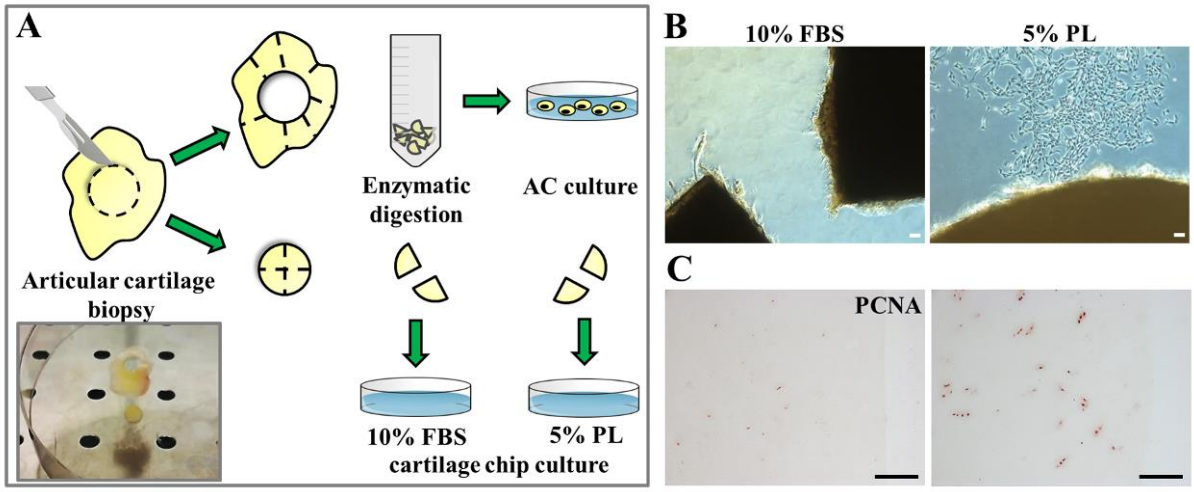

Figure 3.1: Setting up of cell cultures (ACs and CPCs) from human articular cartilage biopsies. (**A**) Representative illustration of biopsy handling to obtain ACs culture and cartilage chips culture. (**B**) Optical images of cartilage chips after 15-20 days in culture with cell coming out in medium supplemented with PL *versus* FBS and (**C**) representative immunohistological distribution of PCNA positive cells inside tissue under both culture conditions (n = 3). All scale bars correspond to 100 μm.

3.3.2 PL increased the proliferation of ACs and reduced their senescence

Growth kinetics analysis (Figure 3.2A) showed similar proliferative rate of CPCs-PL and ACs-PL throughout the culture time, while ACs-PL displayed higher cell doublings than ACs-FBS at all the time points analyzed (9.4 ± 0.6, 10.2 ± 1.3, 1.3 ± 0.3 cell doublings at 23 days in culture respectively). The assessment of cyclin D1 levels, marker of cell cycle progression [241], in confluent cells by western blot confirmed the increased proliferative rate of ACs expanded in PL *versus* almost quiescent ACs grown in FBS as well as the similar growth of CPCs-PL and ACs-PL (Figure 3.2B). These experimental data highlight the drastic potential of platelet-derived products to induce a strong mitogenic response on cells, especially on chondrocytes, which usually have a low turnover.

To confirm the variation observed in the growth kinetics of different cell populations, we analysed also the SA-βgal activity in order to identify senescent cells in culture by a chromogenic assay. This test performed on enzymatically isolated ACs showed that the percentage of βgal-positive cells significantly decreases in PL-treated group compared to control group (20 ± 5 and 39 ± 4, respectively with $p < 0.05$). CPC population recruited from cartilage fragments by PL contains a comparable fraction of labelled cells in respect to ACs grown in PL (12 ± 2 and 20 ± 5, respectively

with no statistically significant difference). Representative images of the three experimental cell groups after staining and the percentage of positive cells are shown in Figure 3.2C. These data, together with the ones described above, suggest that PL have a role in re-activation of quiescent cells, according to which its clinical application in cartilage field could be justified and exploit.

Furthermore, CPCs tumorigenic potential was tested *in vitro* by anchorage-independent growth in methylcellulose media [240]. No CFU-C were detected after CPCs seeding, contrary to positive control metastatic breast cancer cell line MDA-MB-231 as expected (Figure 3.2D). Moreover, CPCs safety was also confirmed *in vivo* by implantation of CPCs in NOD/SCID mice and monitoring of the animals up to 12 weeks. No mouse developed tumors or macroscopic nodules and showed signs of illness. Finally, autopsy did not reveal anatomical abnormalities (data not shown).

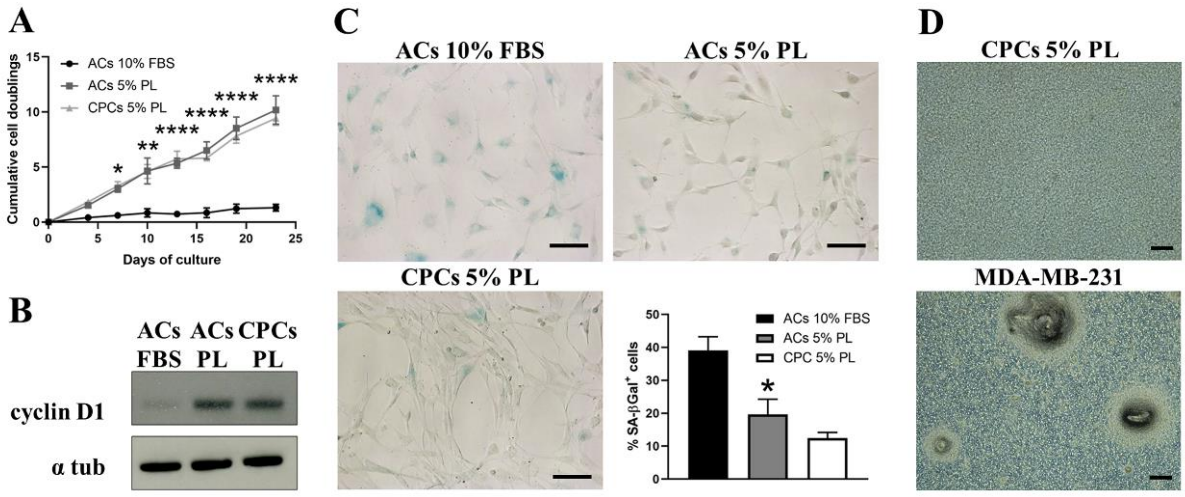

Figure 3.2: Growth rate and senescence profile of ACs and CPCs and *in vitro* tumorigenesis test on CPCs. (**A**) Growth kinetics plotted as number of cell duplications *versus* time of culture: black line indicates ACs expanded in presence of 10% FBS, grey line for ACs in 5% PL and light grey line for CPCs in 5% PL (n = 6, * $p < 0.05$, ** $p < 0.01$, and **** $p < 0.0001$ *versus* ACs 10% FBS at the same time point by two-way ANOVA analysis and Sidak's multiple comparisons test). (**B**) Representative images of the detection of cyclin D1 and α-tubulin as control by western blot in cell lysates from all the examined groups (n = 3). (**C**) Representative images of ACs 10% FBS, ACs 5% PL and CPCs 5% PL stained for senescence associated (SA)-βgal and histogram showing the percentage of positive cells (n = 5, * $p < 0.05$ *versus* ACs 10% FBS by Student's *t*-test analysis). All data are represented as mean ± SEM. (**D**) Anchorage independent growth in methylcellulose for CPCs (upper panel) and human MDA-MB-231 breast cancer cells as positive control (bottom panel) (n = 3). All scale bars correspond to 100 μm.

3.3.3 Effect of PL on gene expression and phenotype in cartilage-derived cells

To characterize and define cells obtained from cartilage chips cultured in PL as real progenitor cells (CPCs), we analysed their phenotype in parallel with that of ACs expanded in PL. Moreover, we also compared ACs-PL *versu*s ACs-FBS cultures. The analysis of typical chondrocyte markers by qRT-PCR (Figure 3.3A) showed a drastic reduction of type II collagen (COL2A1) in ACs-PL compared to ACs-FBS ($p < 0.05$), also found in immunofluorescence staining experiments although in a lesser extent (Figure 3.3B). No statistical differences were observed between ACs-PL and CPCs-PL in this marker. The master regulator of cartilage cells SOX9 and type I collagen (COL1A1) levels were instead not significantly different among all analysed cell types. Flow cytometric analysis performed in all three cell populations reported almost complete positivity for a common set of surface markers such as CD90, CD73, CD105, CD44, CD29 and HLA-ABC (HLA class I), typically expressed by mesenchymal stem/progenitor cells and chondrocytes after *in vitro* expansion [53]. Hematopoietic markers (CD45 and CD34) and HLA-DR (HLA class II) were not expressed, as well as CD146, member of the immunoglobulin (Ig) superfamily of cell adhesion molecules (CAMs), was negative in ACs-FBS and ACs-PL and, although a low positivity in one case, also in CPCs-PL. Differences in the percentages of $CD106^+$ and $CD166^+$ cells were observed among the three populations. The levels of positivity for CD106, constitutively expressed by human articular cartilage [242], did not significantly change between ACs-FBS and ACs-PL cultured *in vitro* ($59 \pm 9\%$ and $41 \pm 8\%$), while the percentage of $CD106^+$ cells was lower in CPCs-PL than ACs-PL ($16 \pm 5\%$ and $41 \pm 8\%$, respectively with $p < 0.05$). Conversely, ACs-PL were enriched of $CD166^+$ cells compared to ACs-FBS (59 ± 10 % and 29 ± 8 % respectively with $p < 0.05$) and CPCs-PL displayed not statistically different levels of CD166 expression *versus* that of ACs-PL (72 ± 8 % and 59 ± 10 % respectively).

Previous work reported a cell population in human adult articular cartilage that coexpresses CD105 and CD166 as multi-potent mesenchymal progenitors with features similar to MSCs [46]. A representative experiment on CPCs-PL and relative percentages of positive cells for all the examined cell groups are reported in Figure 3.3C and D, respectively.

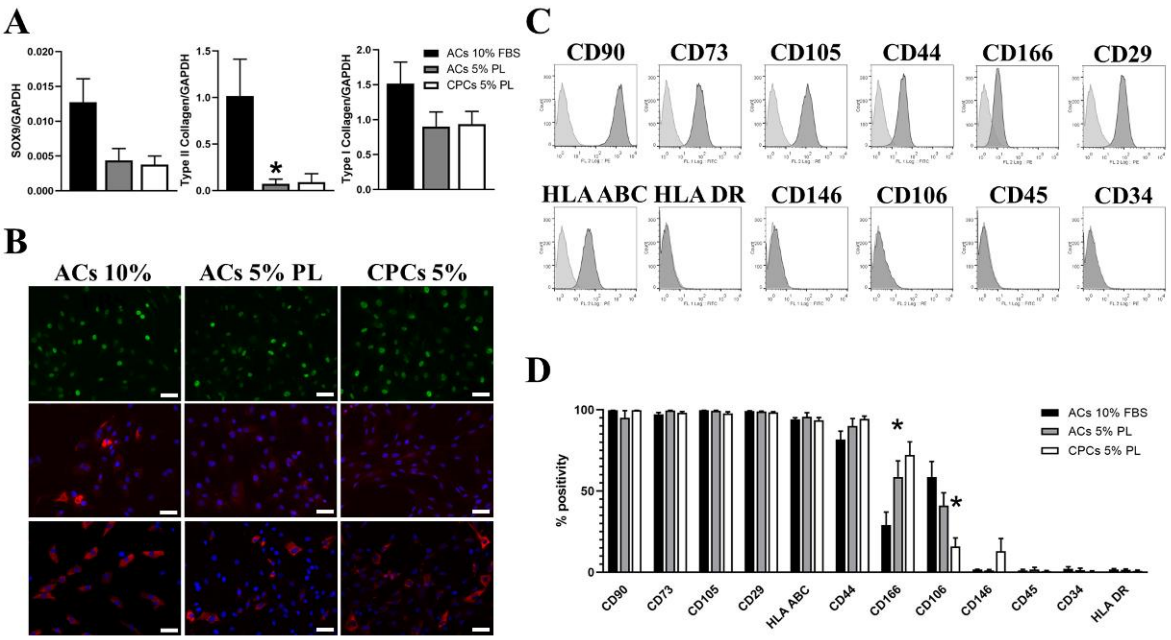

Figure 3.3: Analysis of chondrogenic and cell surface markers in ACs-FBS, ACs-PL and CPCs-PL. (**A**) Expression profile of the chondrogenic markers SOX9, type II collagen and type I collagen in ACs 10% FBS, ACs 5% PL and CPCs 5% PL determined by qRT-PCR; data are represented as mean ± SEM (n = 7, * $p < 0.05$ *versus* ACs 10% FBS by Student's *t*-test analysis). (**B**) Immunofluorescence staining for SOX9 (upper panel) type II collagen (middle panel), and type I collagen (bottom panel) in the three experimental groups. Scale bars correspond to 100 μm. (**C**) Representative flow cytometry characterization of CPCs for a set of typical surface markers: light grey peaks indicate the isotype control staining and dark grey peaks indicate the antibody staining. (**D**) Histogram reporting the percentage of positive ACs 10% FBS, ACs 5% PL and CPCs 5% PL for each tested marker in flow cytometry experiments; data are represented as mean ± SEM (n = 3, * $p < 0.05$ *versus* ACs-FBS for CD166 and *versus* ACs-PL for CD106 by Student's *t*-test analysis).

3.3.4 PL modulated the clonogenic potential and expression of nestin stem marker

Colony forming ability is a recognised trait of stem/ progenitor cells. CPCs obtained from cartilage chips cultured in PL were able to form colonies at low density plating (Figure 3.4A). When we tested the CFU-F potency using mature ACs cultured in FBS and PL conditions, interestingly, we observed that cells exposed to PL (ACs-PL) were able to recover this potential, which was absent in ACs-FBS (sporadic cell spots). Moreover, CPCs and ACs were investigated for nestin expression by qRT-PCR and immunofluorescence experiments. Nestin is an intermediate filament protein involved in cytoskeleton remodelling in several tissues [243]. Nestin has been often considered as a progenitor cell marker and it has been reported that its levels are downregulated during cell

differentiation [244]. This evidence supports the presence of nestin in self-renewing cells that formed colonies in CFU-F assay among CPCs and ACs populations exposed to PL (Figure 3.4B).
As showed in Figure 3.4C, during culture expansion CPCs-PL expressed nestin at higher level than ACs-PL ($p < 0.05$). In mature chondrocytes the level of nestin was low, although there was a slight but not statistically significant increase in ACs-PL compared to ACs-FBS at least on passage 1. These data were confirmed by immunofluorescence staining in Figure 3.4D where we detect no nestin positive cells in ACs-FBS, scant stained cells among ACs-PL and more constant presence of nestin expressing cells in CPC population.

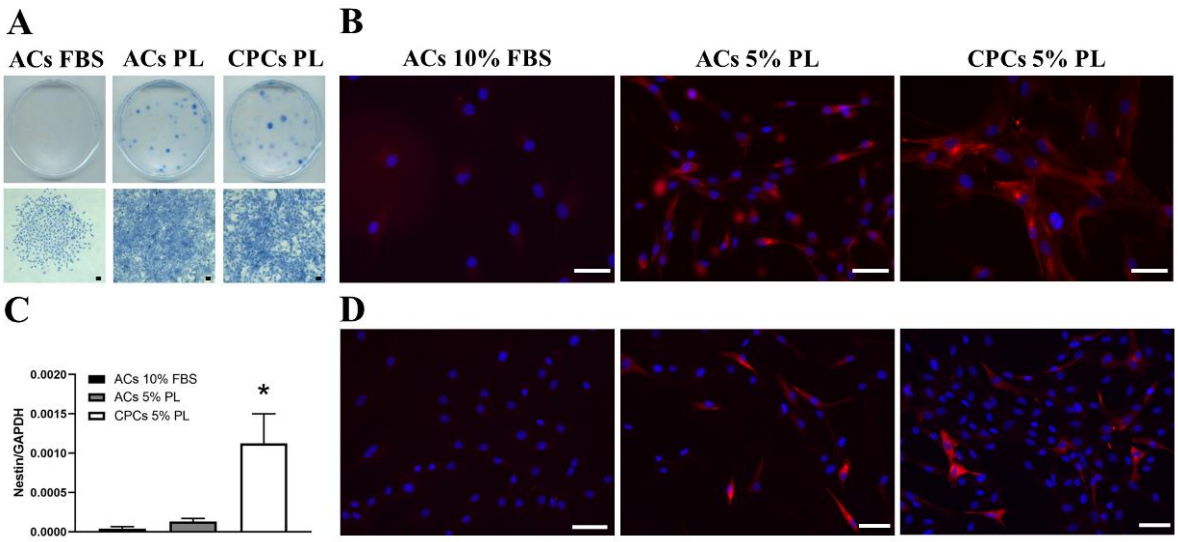

Figure 3.4: Clonogenic potential and detection of nestin expression in ACs-FBS, ACs-PL and CPCs-PL derived from articular cartilage tissue. (**A**) CFU-F assay for ACs isolated in 10% FBS, ACs treated with 5% PL and CPCs recruited by 5% PL from cartilage chips: cell colony staining in culture dish (upper panel) and magnifications of stained colony cells (bottom panel). (**B**) Immunofluorescence staining for nestin in CFU-F cells of the three examined groups. (**C**) Expression level of the stem cell marker nestin in ACs 10% FBS, ACs 5% PL and CPCs 5% PL determined by qRT-PCR; data are represented as mean ± SEM (n = 5, * $p < 0.05$ *versus* ACs 5% PL by Student's *t*-test analysis). (**D**) Immunofluorescence staining for nestin in the three examined experimental groups. All scale bars corresponds to 100 μm.

3.3.5 Comparison of *in vitro* multilineage differentiation potential between CPCs and ACs

CPCs recruited from cartilage in culture by PL were tested *in vitro* for their chondro-, osteo- and adipo-genic potential in parallel with ACs in both culture conditions (PL and FBS) as shown in Figure 3.5. Pellet culture is suitable to investigate chondrogenic differentiation *in vitro* [221]. Thus,

after 21 days of induction in pellet culture, both CPCs and ACs were able to produce metachromatic matrix as shown by toluidine blue staining. The size of the recovered pellets is different among the analysed cell groups, in particular CPCs-PL pellets were bigger than the ACs-PL ones and showed an interesting tissue-like organization. In turn, ACs-PL pellets were bigger than ACs-FBS ones (Figure 3.5A). Osteogenic differentiation was estimated based on calcium deposition in culture after 21 days of induction. CPCs-PL showed positivity to alizarin red staining as well as ACs (Figure 3.5B). Similarly, when cells underwent adipogenesis induction, clusters of lipid vacuoles oil-red positive were observed in all three populations (Figure 3.5C).

Since multilineage potential is a proof to identify stemness properties, this data showed that adult articular cartilage contains cells able to give trilineage differentiation as MSCs. PL treatment may act on cartilage in order to select and mobilize this progenitor cells.

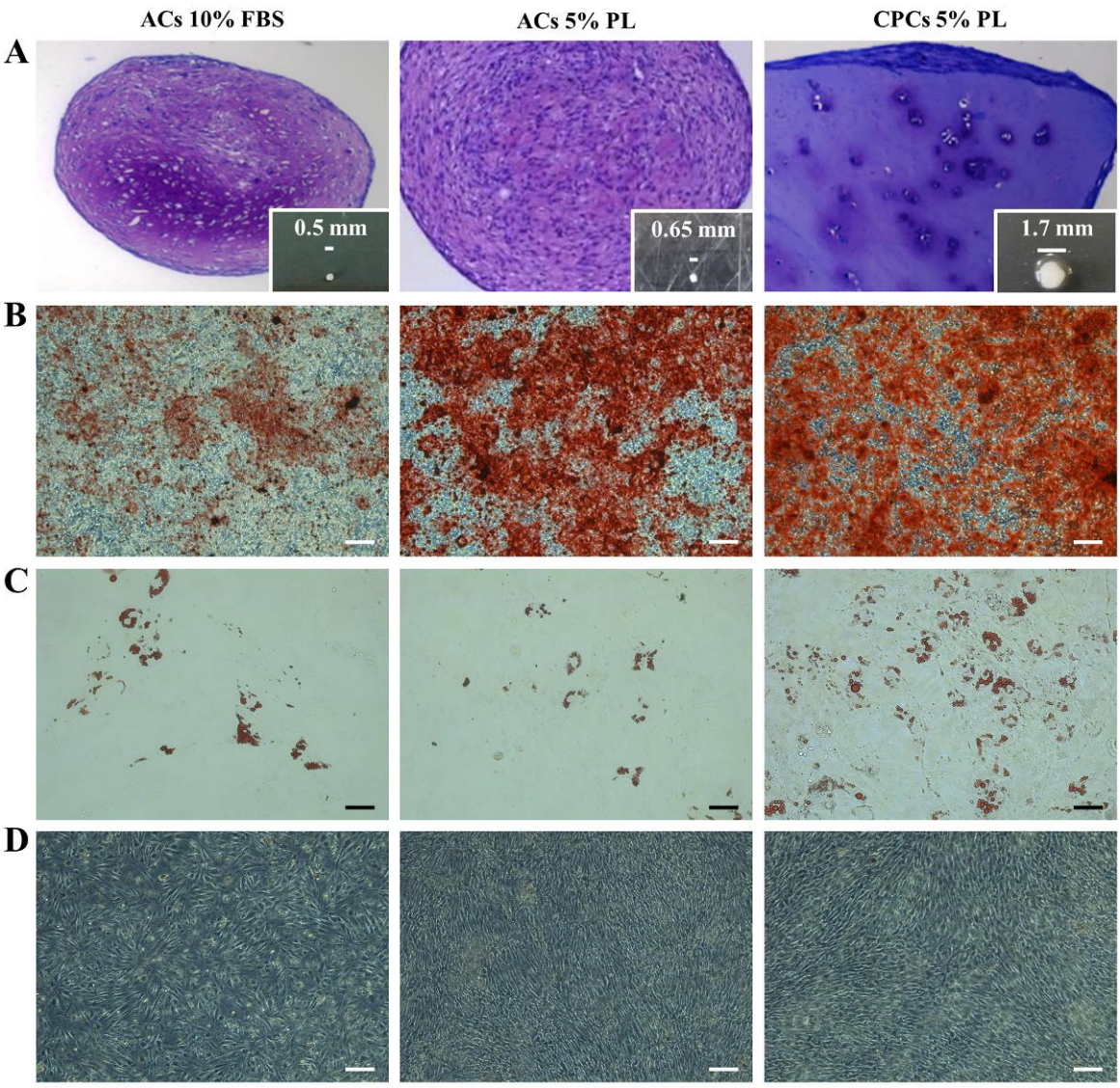

Figure 3.5: Multi-lineage differentiation potential of ACs-FBS, ACs-PL and CPCs *in vitro*. (**A**) Toluidine blue staining of three-dimensional pellets formed by ACs 10% FBS, ACs 5% PL and CPCs 5% PL after 21 days of chondrogenic differentiation *in vitro*; insets show pellet appearance and size. (**B**) Alizarin Red staining for the three experimental groups after 21 days of osteogenic culture *in vitro*. (**C**) Oil Red O staining for the three experimental groups after 21 days of adipogenic culture *in vitro*. (**D**) Uninduced cell controls. Scale bars correspond to 100 µm (n = 3).

3.3.6 CPCs-PL produced hyalin-like cartilage *in vivo* suitable for tissue engineering strategies

Chondrogenic potential of CPCs-PL was investigated by ectopic implantations of pellets and cell-seeded biomaterials in immunodeficient mice. Both types of implants led to a well-defined cartilage tissue-like formation: 1 month after implantation, CPC-pellets (Figure 3.6A) and CPCs-seeded

constructs of PGA-HA biomaterials (Figure 3.6B) showed metachromatic extracellular matrix, therefore rich in proteoglycans, and positivity to type II collagen. Weak or no signs of type X collagen, marker of hypertrophy, were found in the histological analysis. After *in vitro* results, the possible osteogenic potential of CPCs *in vivo* was assessed. CPCs combined to the osteoinductive ceramic granules, as described in [245], 2 months after implantations formed a compact fibrous tissue virtually ascribable to an immature bone-like matrix (Figure 3.6C). Altogether these data demonstrate that CPCs were preferentially committed to a stable chondrogenic fate, evidence that is crucial for cartilage regeneration purposes over traditional MSCs usually predetermined to develop from transient endochondral cartilage to bone [225].

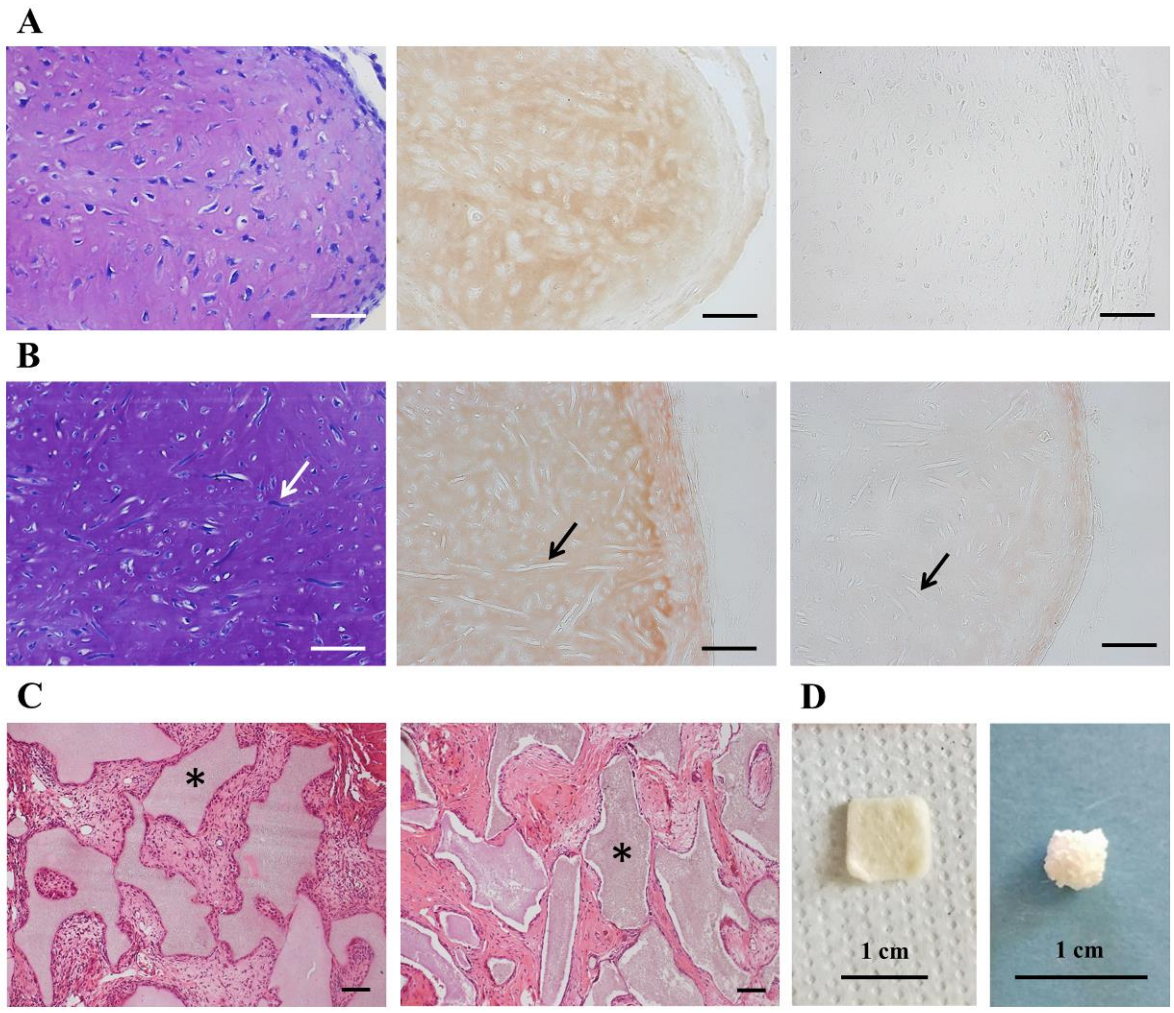

Figure 3.6: *In vivo* ectopic chondrogenesis and osteogenesis assay of CPCs. (**A**, **B**) Histological analysis of ectopic cartilage formed *in vivo* after subcutaneous implantation of CPC-pellets (**A**) and CPCs-seeded biomaterials (**B**) in nude mice; from left to right: toluidine blue staining, type II and

type X collagen stainings. (**C**) Histological analysis by hematoxylin/eosin staining of ectopic tissue formed *in vivo* after subcutaneous implantation of ACs-FBS (left) or CPCs (right)-seeded osteoinductive scaffolds in nude mice. **D**) Representative view of selected scaffolds, PGA-HA (left) and MBCP$^{+®}$ assembled construct (right). Scale bars correspond to 50 µm (upper panel), 100 µm (middle and bottom panel) and 1 cm. Arrows in panel B and asterisks in panel C point out the biomaterials of the scaffolds.

3.3.7 Secretory profile of CPCs revealed an intricate scenario including hypertrophy counteraction, PL-induced pro-inflammatory effects, tissue turnover and chemoattractive capability

CM collected from cultures of ACs-FBS, ACs-PL and CPCs-PL were characterized by using cytokine array (Figure 3.7A). Although examined cell populations were derived from intact and apparently healthy tissue, the biopsies were obtained from patient undergoing hip replacement and probably with ongoing degenerative processes. This assumption may explain the detection of angiogenic molecules (angiogenin and vascular endothelial growth factor, VEGF), molecules expressed in deep and hypertrophic cartilage layers (osteopontin, OPN) and others factors usually related to disorders (B cell activating factor, BAFF/BLys), in all the three experimental groups.

Molecules usually secreted from chondrocytes were identified in CM of ACs grown in FBS, including chitinase-3-like protein 1 (CHI3L1), insulin-like growth factor-binding protein 2 and -3 (IGFBP-2, -3), serpin E1, cystatin C (CST3), apolipoprotein A1 (ApoA1), thrombospondin 1 (THBS1) and pentraxin 3 (PTX3) as previously reported [246]. Moreover, ACs are usually positive, as detected in this analysis, for CD14 [247] and CD147 [248], but not for dipeptidyl peptidase-4 (DPPIV/CD26), whose expression could indicate de-differentiation [53]. Growth differentiation factor 15 (GDF15) is described as a protein expressed in normal chondrocytes and de-regulated in OA disorder [249]. The urokinase receptor (uPAR), a glycoprotein key regulator of the plasmin-mediated pericellular proteolysis, is also present on chondrocyte surface [250].

Among the aforementioned factors, apoliprotein A1 markedly increased in ACs-PL if compared with ACs-FBS, while its amount was similar to that in CM of CPCs-PL, and IGFBP-2 decreased in CM of CPCs-PL in comparison with that of ACs-PL, in turn similar to ACs-FBS.

Dkk-1, an antagonist of the Wnt/β-catenin signalling pathway that prevents hypertrophy and cartilage degradation [251], was not released by ACs-FBS but slightly produced by ACs-PL. CM from CPCs-PL displayed markedly higher levels of this factor in comparison with CM from ACs-PL. On the contrary, in comparison with ACs-PL, CPCs-PL released very low amount of Interleukin 1 receptor-like 1 (ST2/IL1RL1), that has recently been described as RUNX2 target and

it is expressed during hypertrophic differentiation in chondrocytes [252]. Moreover, OPN release from CPCs-PL was much lower than those from ACs-PL.

CPCs-PL also secreted DPPIV, not detected in ACs-PL, and higher amount of the cysteine protease inhibitor cystatin C than ACs-PL. Levels of the factors just reported were comparable between ACs-FBS and ACs-PL. The serine proteinase inhibitor Serpin E1, also known as plasminogen activator inhibitor 1, was instead less released in ACs-PL, similarly as in CPCs-PL, compared to ACs-FBS. Simultaneously, uPAR, urokinase-type plasminogen activator receptor, increased. Thus the catabolic activity changed among the analysed experimental groups.

Other soluble molecules were identified into analysed secretomes, such as leukemia inhibitory factor (LIF) and macrophage migration inhibitory factor (MIF). LIF is actively produced and secreted by articular chondrocytes and its expression is induced after treatment with growth factors [253] as also here confirmed. MIF, whose amount is similar in all three examined CM, usually regulates several biological processes and in cartilage is highly involved in its metabolism [254]. Retinol binding protein 4 (RBP4) is another component that in this analysis decreased in CPCs-PL secretome: its expression has been reported in epiphyseal chondrocytes of secondary ossification regions and a role in OA pathogenesis has been suggested in literature [255,256]. A higher content of vitamin D binding protein (VDB) was detected in CM derived from ACs-PL in comparison with ACs-FBS, while lower levels of this factor were found in CM from CPCs-PL than in CM from ACs-PL: vitamin D is known as immunomodulator and anti-inflammatory agent and its deficiency is associated to OA [257].

Finally, pro-inflammatory cytokines, i.e. interleukin-8 (IL-8), interleukin-6 (IL-6) and lipocalin-2 (LP2/NGAL), and chemokines, i.e. monocyte chemotactic protein 1 (MCP-1/CCL2) and -3 (MCP-3/CCL7), were found as secreted molecules by examined cell groups. In particular, the first three were up-regulated in CM of PL-treated ACs in comparison with ACs-FBS. In fact, it's widely documented the pro-inflammatory effect of PL on cells functional in triggering cascades of pro-resolving events [126,128,228] that could lead to regeneration in injured sites, just like it happens physiologically during wound healing. IL-6 and NGAL release by CPCs-PL was lower than that by ACs-PL, while the release of IL-8 was similar in both types of cells.

Other soluble chemokines, i.e. CXCL1 (GROα), CXCL4, CXCL5, CXCL12 (SDF1), CCL5 (RANTES) and CCL20 were observed in the secretome of ACs-PL but not detected in that of ACs-FBS. Except for CXCL1 and CCL5 levels that are comparable, CXCL5, CXCL4 and CCL20 widely decreased in CPCs-PL, while CXCL12 increased in comparison with ACs-PL. These molecules are usually involved in the regulation of leukocyte trafficking and stem cell

chemoattraction [258,259], but it has also been suggested that chemokines could have a role in cartilage physiological turnover [260].
Finally, metalloproteinase 9 (MMP9) is mainly secreted by ACs-PL compared to control ACs and there are evidence that it is involved in chondrocyte motility [261].

3.3.8 PL-treated ACs acquired migratory capability and exerted chemoattraction on CPCs under inflammatory conditions

Since our final aim was to support biological basis for possible therapeutic application of PL on cartilage defects, migratory capability of ACs and CPCs was tested by an *in vitro* scratch assay (Figure 3.7B). Cell motility was evident for each experimental groups between 24 and 48 hours of monitoring during wound healing assay (ACs-FBS: from 18.9 ± 0.5 % to 29.6 ± 0.8 % with $p < 0.05$; ACs-PL: from 36 ± 1.4 % to 62 ± 1.5 % with $p < 0.0001$; CPCs-PL: from 46.7 ± 0.7 % to 95.1 ± 0.2 % with $p < 0.0001$). Interestingly, PL treatment significantly promoted ACs motility in the migration assay compared to control ACs cultured in FBS. The scratch width in PL-treated ACs was significantly reduced at 24 hours ($p < 0.05$) and further at 48 hours in comparison to ACs-FBS ($p < 0.0001$). As expected also CPCs were able to migrate and close the scratch during the assay, in a similar extent within 24 hours but with a statistically significant increase at 48 hours compared to ACs-PL ($p < 0.0001$). Thus, migratory behaviour of CPCs was further tested by mimicking the inflammatory environment of a pathological state, i.e. by exposition to the CM of ACs underwent treatment with the inflammatory cytokine IL1-β concurrently or not with PL exposition (Figure 3.7C). Under basal conditions, CM of ACs-PL was not enough to act as a chemoattractant for CPCs. However, an enhanced chemotaxis on CPCs occurred in presence of CM from IL1-β-treated ACs ($p < 0.05$) and when CM derived from cells exposed to both stimuli PL + IL1β was tested ($p < 0.01$) compared to control.
These experiments together showed that cartilage cells after PL treatment increase motility, despite they normally have not such a marked behaviour in cartilage. Actually, this effect probably allowed to obtain CPCs from cartilage fragments and furthermore they showed to be reactive to inflammatory stimuli. Thanks to this property, CPCs and also ACs under platelet derivative influence may move towards injured sites *in vivo* and participate in reparative processes.

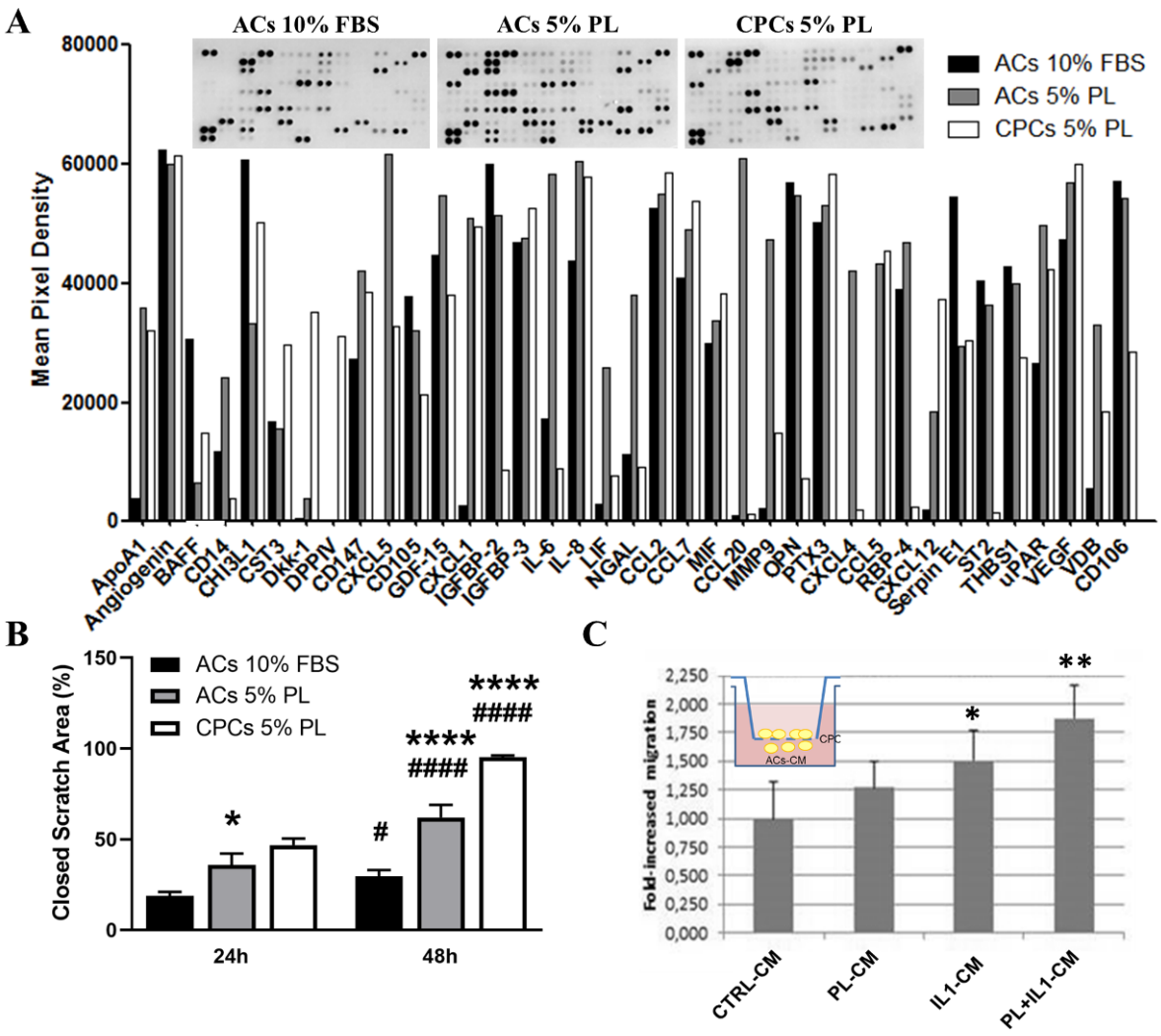

Figure 3.7: *In vitro* analysis of ACs and CPCs secretory profiles, migratory capability and CPC chemotaxis in an OA mimetic system. (**A**) Quantification of the mean pixel density for each identified cytokine in the three experimental groups; inset shows the cytokine array membranes for CM of ACs-FBS, ACs-PL and CPCs-PL respectively. (**B**) "Closed scratch area (%)" calculated by TScratch software at each time points in all three experimental groups. Data are represented as mean ± SEM (n = 3, * $p < 0.05$ and **** $p < 0.0001$ *versus* ACs-FBS or ACs-PL at the same time point; # $p < 0.05$ and #### $p < 0.0001$ *versus* 24 h in the same experimental group by two-way ANOVA analysis and Sidak's multiple comparisons test). (**C**) Relative quantification of CPC migration in presence of ACs-CM obtained in four different conditions: control (CTRL-CM, 10% FBS culture), PL-treatment (PL-CM, 5% PL culture), inflammatory stimulus (IL1-CM, IL1-β culture) and PL-treatment plus inflammatory stimulus (PL+IL1-CM, 5%PL plus IL1-β culture) (n = 3, * $p < 0.05$ and ** $p < 0.01$ *versus* CTRL-CM by one-way ANOVA analysis).

3.4 Discussion

This study sustains that articular cartilage from joints of patients with ongoing OA contains a MSC-like progenitor cell population that could be mobilized and subsequently *ex vivo* recruited from intact tissue by treatment with PL. Several studies have already confirmed the presence of MSC-like cells in articular cartilage able, at least *in vitro*, to migrate from human late-stage OA tissue [49], to repopulate compromised tissue areas after an induced trauma [33], to move from healthy tissue in contact with growth factors or products released following a trauma [48]. Since the outgrowth of the so-called chondro-progenitors needs to be induced, PL showed to be a powerful stimulus in this context. In fact, PL is a cocktail of platelet derived-growth factors, cytokines and chemokines widely studied for its multiple effects in the field of regenerative medicine, including cell chemoattraction during healing processes. In particular, among the factors released from activated platelet granules, PDGF and IGF or SDF-1α (CXCL12) are known to stimulate the migration of human progenitor cells [262–264]. Another effect that has aroused the interest in platelet products concerns the strong proliferative stimulus, due to the high content in mitogenic growth factors, exerted on treated cells as previously reported on different *in vitro* cultured cells including human chondrocytes, keratinocytes, human and murine MSCs [126,128,135,229,265]. Regarding chondrocytes, it has already been described that after PL treatment partially growth-arrested cells show a changed morphology with smaller size and more elongated shape than the native ones, cell cycle re-entry in addition to a strong mitogenic response [128,135].

Given the therapeutic use of platelet derivatives in orthopaedics, the aim of our study was to explore their stimulatory activity on *in vitro* cartilage cell homeostasis, focusing on chondro-progenitor cells. Hence, *in vivo* setting was mimed by performing cartilage explant cultures derived from human biopsy fragments in presence of PL or FBS-supplemented medium. No CPC population could be recruited when cartilage fragments were cultured in medium with FBS. This is the reason why we could not have a direct comparison between CPCs-FBS and CPCs-PL to test the effects of platelet-derived supplement on the biology of this cell type. Therefore, we compared CPCs isolated from cartilage chips cultured in presence of PL with the chondrocyte population enzymatically released from the surrounding tissue and expanded in PL after the first passage in monolayer. In parallel, we considered also the comparison between the latter and the chondrocyte counterpart maintained in culture with FBS.

The proliferative trend, in terms of doubling number and protein levels of cyclin D1, was similar between CPCs-PL and ACs-PL along the time, while markedly higher in ACs-PL compared to

ACs-FBS. The similar replicative potential and clonogenic ability of ACs-PL and CPCs-PL found in our study are in accordance with the absence of differences reported previously between monocultures of ACs and CPCs isolated by fibronectin differential adhesion assay [266]. Moreover, the increase in proliferation was concomitant with a senescence attenuation in ACs-PL, likewise in CPCs-PL. In general, a subset of senescent cells is characterized by cell cycle irreversible arrest, meanwhile quiescent and slowly proliferating cells can restart or increase proliferation after mitogenic stimulation [267,268]. Thus, our results reconfirm that PL is able to induce the re-entry of quiescent ACs into the cell cycle progression with consequent decrease of the senescent cell fraction no longer able to replicate. Therefore, our findings suggest that PL could be suitable for expansion of cells intended to be used in therapeutic applications, especially since senescent cartilage cells are involved in the development of OA in joints and their clearance may attenuate its progression encouraging a pro-regenerative milieu [269].

The immunophenotypical analysis of the three experimental groups showed that ACs-FBS, ACs-PL and CPCs-PL were positive for MSC markers CD105, CD73, CD90, CD106 and CD166, and negative for hematopoietic stem cell markers CD45 and CD34. The presence of these stemness markers in CPCs is in accordance with previous reports [8,47] and further supports their progenitor nature. Although it has been shown that, unlike CPCs, a large percentage of ACs do not express, CD90, CD105 or CD166 [54], it is not surprising that in our study ACs displayed these markers since they undergo phenotypic changes known as dedifferentiation during monolayer culture [53]. No marked differences emerged among analysed cell populations except for vascular cell adhesion molecule 1 (VCAM-1, CD106) and activated leukocyte cell adhesion molecule (ALCAM, CD166) expressions. CD106 is an adhesion molecule belonging to the immunoglobulin superfamily constitutively expressed on human articular chondrocytes and modulated in response to cytokines [270]. Here we found that CPCs-PL exhibited lower expression of this marker than ACs-PL, that is in line with the results reported in a recent study [77] showing that absence of CD106 expression in MSCs-like progenitors isolated from OA cartilage. CD166, also a member of the immunoglobulin superfamily, and CD105 are co-expressed in both bone marrow-derived and cartilage mesenchymal progenitor cells [46,223]. In agreement with these results, we found that CPCs-PL consistently expressed both markers. We also observed that the percentage of $CD166^+$ cells significantly increased in ACs-PL when compared to ACs-FBS. Since this percentage in ACs-PL was similar to that found in CPCs, it suggests that PL is able to bring fully differentiated ACs to an earlier differentiation stage. CD44, hyaluronan receptor highly expressed in chondrocytes, was present at similar levels in ACs-FBS and ACs-PL, as expected. It was also expressed by CPCs as already

demonstrated in migratory chondro-progenitors [49]. CD29, a marker of cells with enhanced chondrogenic potential [49], was similarly expressed in the three experimental groups, in accordance with their ability to undergo chondrogenic differentiation *in vitro,* as well as *in vivo* in the case of CPCs-PL. The absence of CD146 expression in ACs was in agreement with a recent study showing no expression of this surface marker in monolayer cultures of chondrocytes at early passages, instead accompanied by the expression of type II collagen [271]. Despite, *in toto* CPCs-PL population did not show a significant level of CD146 expression in our study, it has been recently reported that small sorted fractions of $CD146^{+}$ cartilage-cells from late OA stage has marked chondro-progenitor features and capabilities [272].

An evident proof of the progenitor nature of cells exposed to PL was the clonogenic potential of CPCs-PL and ACs-PL when tested in CFU-F assay. Interestingly, enzymatically digested ACs, unable to form colonies, acquired this ability when they were switched from FBS- to PL-supplemented medium. Articular cartilage contains a subpopulation of self-renewing cells, mainly concentrated in the superficial layer [7,33], but it was also reported that cells with stem cell phenotype can emerge even from fully differentiated chondrocytes [271]. Despite ACs used in this study were quiescent and mature, PL stimulation seemed to bring out certain features of stemness. Moreover, ACs-PL and CPCs-PL were very similar in terms of proliferation, senescence levels and potential to form colonies. Therefore, our findings suggests that PL retrieved a miscellaneous cell population from cartilage tissue enriched in chondro-progenitors among committed cells. The origin of progenitor cells still needs to be elucidated, since it remains elusive if they derive from below subchondral bone marrow after migration or from reverted chondrocytes or if they are resident progenitors that are involved in cartilage homeostasis. The difficulties for an accurate identification are to date the lack of a well-defined markers and the alteration of cell phenotype upon isolation and monolayer expansion.

Progenitor nature of PL-exposed cells in this study is mainly supported by the expression of the stem cell marker nestin. Initially described in neural stem cells, nestin is a cytoskeletal protein of type VI intermediate filaments known to be expressed in proliferating and migrating stem/progenitor cell subsets in several human tissues [243], both during embryonic development [273] and after injuries in adulthood [238]. Our results are in line with the study of Fellows *et al.* [274], which demonstrated the presence of nestin-labelled cells in human articular cartilage. Data from qRT-PCR and immunostaining experiments for nestin showed an up-regulation of this marker in CPCs-PL compared to the weak expression observed in ACs-PL. Furthermore, no nestin-positive cells were observed in ACs-FBS but some could be detected when PL was used as a supplement

instead of FBS in culture at first passage. Nevertheless, as expected, self-renewing cells in colony units of CPCs-PL and ACs-PL were positive to Nestin.

Nestin expressing cells compose a quiescent reserve in adults that, if properly re-activated, is able to proliferate, differentiate and migrate. These events are triggered after injury, implying the involvement of these cells in processes of tissue regeneration [238], although the precise mechanisms have not been understood yet. Therefore, given the involvement of PL in such events, including the transient activation of the inflammatory cascade during tissue regeneration, some of its effects on cell self-renewal, proliferation, differentiation and migration could be due to activation and expansion of a subset of nestin-positive cells within the cartilage.

Considering the status of the PL-recruited cells, that showed high proliferation capacity and stem/ progenitor behaviour, we analysed their chondrogenic potential in view of a future therapeutic applications. Generally, adult chondrocytes are characterized by a finite capability to form stable cartilage *in vivo*, that is gradually lost during *in vitro* monolayer culture [275]. Chondrocytes express mainly type II collagen, with a switch to type I collagen during culture due to dedifferentiation [226]. We found a slightly higher expression of type I collagen than type II collagen in *in vitro* expanded ACs-FBS, while ACs-PL displayed very low expression of type II collagen in comparison to ACs-FBS and maintain a similar level of type I collagen, as previously reported [128]. CPCs-PL showed similar collagens expression to ACs-PL, a trend that is also confirmed by previous works [49,77]. Despite this change in collagens, no statistically significant difference were found in the expression of the master regulator of chondrogenesis SOX9 [61] among the three experimental groups, just a slight decrease in ACs-PL compared to ACs-FBS that occurs also in CPCs-PL. Indeed, it has been previously reported that chondro-progenitors show decreased SOX9 expression compared to fully differentiated chondrocytes, but it is maintained over extended monolayer culture passages together with chondrogenic potential [56]. Moreover, SOX9 is even not highly expressed in MSCs, which are the precursors to CPCs, since they are not yet fully committed to the chondrogenic lineage [216]. Finally, Pereira *et al*. [128] have already demonstrated that PL, contrary to animal supplement, supports chondrocyte expansion preserving their chondrogenic phenotype both *in vitro* and *in vivo*. The lack of differences in mRNA levels of SOX9, type I collagen and type II collagen between ACs-PL and CPCs-PL found in our study is in agreement with the results obtained by Vinod *et al.*, who showed similar levels of these markers between monocultures of ACs and CPCs isolated by fibronectin differential adhesion assay [266].

Consistently with these data, we show here that, in a permissive 3D pellet culture *in vitro*, CPCs-PL regained chondrogenic phenotype with cartilage tissue-like formation and form larger aggregates

compared to ACs-PL, that in turn were bigger than those of ACs-FBS. In agreement with previous reports [8,49] these cells also underwent osteogenic and adipogenic differentiation, capabilities usually not present in articular cartilage. Such a trilineage differentiation potency is a typical property of adult MSCs, although adipogenesis in chondro-progenitors is controversial and sometimes reported as limited or not inducible [33,41,77]. Indeed, the potential for chondrogenic, osteogenic and adipogenic differentiation has become a defining trait of CPCs that distinguish them from mature chondrocytes [76]. However, ACs-FBS and ACs-PL, derived from enzymatically digested tissue *in toto*, showed trilineage differentiation potency in our hands, probably because these two populations contain a subset of progenitor/stem cells, as also reported by Alsalameh *et al.* [46]. Moreover, given the nature of the available donor biopsies, the latter evidence could even be in accordance with previous reports showing that ACs isolated from OA cartilage are able to differentiate into osteogenic, adipogenic and chondrogenic lineages [276].

In orthopaedics, several trials have been conducted to test the potential application of platelet derivatives, although their contributions still need to be clarified. The strategies for progenitor cell recruitment/enrichment could be exploited for *in situ* reparative therapies based on platelet products, as previously demonstrated by Siclari *et al*. [233] or in a conventional tissue engineering approach since the CPCs have shown multiple advantages compared to ACs and even to BM-MSCs for scaffold-assisted cartilage regeneration, as recently reported by [277].

Indeed, ectopic cartilage formation was obtained in this work when expanded PL-recruited progenitors (CPCs-PL) were implanted in nude mice as high density pellets or after seeding on a hyaluronan-based resorbable scaffold. Neo-formed tissue showed a typical metachromatic staining, it was type II collagen positive and type X collagen negative, thus ascribable to a hyaline-like cartilage without hypertrophy signs. Therefore, migrating cells from articular cartilage under PL treatment (CPCs-PL) can be properly considered a population consisting of chondro-progenitors since they showed to be committed towards chondrocytic lineage, but were not able to form a mature bone tissue *in vivo*, despite their *in vitro* multipotency. From a translational point of view, a high safety profile may be achieved following this approach for cartilage tissue engineering, since progenitor cells from patient may be harvested and expanded in autologous platelet derivatives without any tumorigenic risk and then delivered by a clinical-approved biomaterial to the lesion site. Recent findings have demonstrated that cartilage-derived progenitor cells have also a strong immunomodulatory capacity similarly to MSCs [278] that may be crucial in counteracting tissue inflammatory/pathological processes that usually accompany cartilage injury.

Characterization of the CM from ACs-FBS, ACs-PL and CPCs-PL could help in understanding the effects of PL on cartilage-derived cells and their involvement in tissue dynamics. Indeed, human chondrocytes, both normal and osteoarthritic, produce chemokines and express a variety of chemokine receptors, suggesting that their autocrine/paracrine pathway within cartilage may be involved in its homeostasis and matrix remodelling [260].

Secretome derived from digested ACs in this study contained a plethora of molecules, including not only chondrocyte factors, but also angiogenic proteins, pro-inflammatory cytokines, hypertrophic differentiation markers and chemokines with chemoattractant activity on immune system cells. Since cells used in the present study derived from articular cartilage biopsies with ongoing inflammatory processes, the described secretory profile could reflect the long-lasting exposure to a pathological joint environment.

PL treatment induced increased release or *de novo* secretion of some pro-inflammatory cytokines by ACs. In line with this evidence, PL elicited an elevation of the release of ApoA1, which has pro-inflammatory properties *in vitro* [279]. In addition, PL was also able to induce an increase in the secretion of neutrophil gelatinase-associated lipocalin (NGAL), another pro-inflammatory cytokine that has been implicated in inflammatory degenerative articular diseases [280]. Indeed, it is well known from previous works that PL exerts an initial strong pro-inflammatory activity resulting in NF-κB activation and secretion of pro-inflammatory cytokines, events that are transient in order to prime certain defensive and reparative tissue mechanisms, then it inhibits and promotes resolution of the inflammatory phase [128,228].

Apart from pro-inflammatory cytokines, PL was able to modulate the secretion of other factors. Thus, compared to ACs-FBS, ACs-PL released higher amounts of uPAR that regulates MSCs mobilization and their engraftment at injury site [281]. Culture of ACs with PL also elevated the secretion of Dkk-1, an antagonist of the Wnt signalling, which activation is correlated with OA and osteoporosis [282,283]. Growth differentiation factor 15 (GDF15) [284], which has been involved in initiation of cartilage formation, was higher in ACs-PL CM than in ACs-FBS CM. Leukemia inhibitory factor (LIF) inhibits chondrocyte maturation and hypertrophy [32] and it was more contained in ACs-PL CM than in ACs-FBS CM. The AC secretion of Serpine1, that together with the relevant components of plasminogen/plasmin system are involved in the degradation of extracellular matrix [285], was markedly reduced by PL. Moreover, PL markedly increased the release of CCL5 (RANTES) by ACs, suggesting that PL exposure may promote the migration of joint resident cells towards damaged areas where they could engraft and take part in regenerative processes, as previous observed for annulus fibrosus cells mobilized in response to this secreted

chemokine in degenerated intervertebral disk [286]. CCL5 has been reported to be involved also in MSCs recruitment [259] and thus it is considered attractive for regenerative therapies. Moreover, PL enhanced the release of CXCL12, known to stimulate the migration of human stem/progenitor cells [287].

Interestingly, secretory profile of CPCs-PL differed from that of ACs-PL for soluble components involved in bone and cartilage biology or correlated with hypertrophic phenotype. Among them, the Wnt pathway antagonist Dkk-1 was highly up-regulated in CPCs-PL. Dkk-1 is highly expressed in cartilage and its expression is required for chondrogenic differentiation of MSCs, redifferentiation and preventing hypertrophy of chondrocytes [288]. Furthermore, a low amount of ST2 was also detected in CPCs-PL compared to ACs-PL. It has been recently described ST2 as chondrocyte differentiation regulator that promotes expression of hypertrophic markers after RUNX2 induction [252]. Finally, osteopontin (OPN), a protein that contributes to hypertrophic phenotype in chondrocytes [289] was lower in the CM of CPCs-PL compared to the CM of ACs-PL.

Another advantage of CPCs-PL over ACs-PL is that the former cell type secreted higher amounts of CST3, an inhibitor of cathepsins. In OA cartilage with severe lesions, a reduced inhibitory activity of CST3 has been reported, suggesting that down regulation of CST3 contributes to articular cartilage damage [290]. DPPIV release was significantly higher in CPCs-PL than in ACs-PL. In a murine model of collagen-induced arthritis (CIA), it has been demonstrated that DPPIV injection decreases the overall extent of inflammation and articular damage around the arthritic joint and periarticular tissue [291]. Overall, CPCs-PL secreted less amount of pro-inflammatory cytokines than ACs-PL, thus representing a better candidate to be effective in clinic setting for treatment of cartilage degenerative pathologies that are characterized by some degree of inflammation.

As already reported [44], high levels of CXCL12/SDF-1α in chondro-progenitor secretome may indicate their ability to mobilize other endogenous progenitor cells within injured articular joint and recruit immune cells in order to help in mediating tissue repair.

A recent study has confirmed that chondro-progenitors are more suitable candidates for therapeutical treatment of meniscus injury than BM-MSCs since they resist to hypertrophic differentiation during tissue repair [292]. Similarly, and according with our findings, we can suggest that PL-induced activation of such CPC population able to counteract cell hypertrophy within articular cartilage could be considered beneficial in therapeutic treatments for OA.

Although their role in cartilage disorder (OA) progression has not yet been clarified, chondro-progenitor cells are responsive to injury. In this study we demonstrated that they are able not only to release into the surrounding environment chemoattractant factors, but also to actively migrate in

response to signals coming from inflamed chondrocytes. This is in accordance with the demonstrated capability of CPCs to migrate across the articular surface to sites that have suffered trauma and therefore display an ongoing inflammation [33]. These findings suggest that these mobilized cells may organize a kind of regenerative response in an attempt to restore the perturbed cartilage homeostasis in a damaged joint. Finally, PL exerts a general strong chemotactic action on the entire cartilage cell population, including mature chondrocytes (ACs) that usually are considered not provided with a mobile phenotype. Conversely to culture with FBS supplemented medium, ACs exposed to PL, probably as a result of changes in cell morphology and cytoskeletal rearrangements, acquired enhanced motility and were able to close a wound scratch *in vitro*, suggesting the possibility of using PL to promote their involvement in the overall tissue reparative process.

3.5 Conclusions

In conclusion, as reported previously, articular cartilage contains a reserve of progenitors, but since the tissue shows a limited regenerative potential, they seem to be not suitable to organize a proper resolving response after injury. Platelet products attract much interest for their intrinsic capacity to induce endogenous reparative and regenerative mechanisms when administered both *in vitro* and *in vivo*. In this study, it has been demonstrated that PL exerts stimulant effects on articular cartilage, such as promotion of chondrocyte proliferation, cell mobilization and activation of nestin expressing progenitors. In particular, these PL-recruited progenitor cells (CPCs-PL) are able to migrate in response to inflammatory stimulus, show paracrine activity in attracting other cells (ideally toward injured sites), high chondrogenic potential and resistance to hypertrophy. Thus, they potentially may replace damaged chondrocytes in a compromised cartilage environment and represent a promising target for future therapeutic approach for cartilage disorders.

4 Primary human articular chondrocyte re-differentiation in 3D-printed Platelet Rich Plasma (PRP) and alginate-based bioink

Carluccio S., Palamà M. E., Pitto M., Ghelardoni M., Guijarro A., Gentili C.

Abstract: Tissue engineering strategies in current clinic treatments of cartilage defects are mainly based on *in vitro* expansion of autologous chondrocyte monolayer and subsequent *in vivo* transplantation in patient tissue damaged areas. However, chondrocyte de-differentiation occurs during *in vitro* expansion often leading to sub-optimal outcomes of the therapeutic intervention. Three-dimensional (3D) culture systems are able to revert chondrocyte de-differentiated state and re-establish chondrogenic phenotype. In this context, 3D-bioprinting, that consists in layer-by-layer fabrication of patient-shaped grafts starting from cell-laden bioink, is a suitable technology to create a more physiological environment for transplanted cells favouring tissue regeneration and repair. Thus, human articular chondrocytes (hACs) were isolated from patient tissue biopsies and *in vitro* expanded in monolayer (2D culture). 3D-bioprinting was performed by embedding expanded hACs in alginate or alginate-Platelet Rich Plasma (PRP)-mixed bioinks. Cell morphology, viability, growth and chondrogenic differentiation in both types of printed constructs were studied *in vitro* before implantation in nude mice. PRP addition to alginate bioink did not interfere with the printing process, rather obtained constructs released PRP-derived factors to the surrounding environment within 120 hours from the fabrication. In alginate/PRP constructs, hAC viability and growth were enhanced compared to alginate ones. 3D-culture in bioink significantly increased the expression of chondrogenic markers in hACs compared to 2D condition. Furthermore, the addition of PRP to alginate up-regulated the expression of these markers. The analysis of the constructs implanted for two months in mice showed a slight cartilage tissue-like organization, but did not reveal any evident difference between the two typologies of bioinks. Finally, 3D-bioprinting of de-differentiated hACs allowed them to regain chondrogenic phenotype and the embedding in PRP-supplemented bioink supported chondrogenic culture inside the printed constructs. In view of future clinic translation, the choice of cell source for 3D-bioprinting of patient-specific grafts will have to be oriented towards cell types with higher potential, such as chondro-progenitors, than mature hACs in order to ensure a successful cartilage regeneration and repair.

Keywords: 3D-bioprinting, articular chondrocytes, platelet rich plasma, alginate, re-differentiation

4.1 Introduction

Hyaline articular cartilage covers the bone extremities and bears the load in the joint. Cartilage extracellular matrix (ECM) is a dense and hydrated network of type II collagen, proteoglycans and other non-collagenous proteins that confers unique mechanical properties to the tissue, such as tensile and compressive strength [293,294]. ECM components are synthetized by chondrocytes, a specialized cells that are surrounded and isolated by their own products within the tissue. Damages are particularly critical for articular cartilage because of its avascular, alymphatic and aneural nature that impairs healing process [295]. Thus, cartilage injuries, if not properly treated, may worsen and progress to pathologic states such as osteoarthritis [296]. Current therapeutic strategies for cartilage defects, including microfracture surgery [297] or autologous chondrocyte implantation (ACI) [298], provide neo-tissue formation to fill and restore the damaged area, but often it results in fibrocartilage [299] that fails mechanically on the long term, or in symptom recurrence with consequent need to repeat surgery [300]. ACI and its advanced generation, i.e. matrix associated chondrocytes implantation (MACI) [99], are tissue engineering methods in which autologous articular chondrocytes are mainly enrolled in regenerative events. Generally, after enzymatic isolation from patient biopsy, long expansion time and multiple passaging *in vitro* are required in order to obtain sufficient amount of cells prior implantation. Unfortunately, during *in vitro* two dimensional (2D) expansion, harvested chondrocytes undergo de-differentiation, losing their chondrogenic phenotype [301,302]. In particular, expression of typical differentiated chondrocyte markers, such as ECM molecules, including glycosaminoglycans (GAGs), type II collagen (COL2A1) and aggrecan (ACAN) are downregulated [24,303]. At the same time, the cells acquire a fibroblastic morphology and shift towards fibrochondrogenic phenotype, characterized by type I collagen (COL1A1), which expression increases over time in culture [304]. Thus, the subsequent use of these non-performing cells in cartilage therapy results in poor outcomes, including the formation of low quality tissue (fibrocartilage).

The de-differentiation process can be decelerated by adopting several strategies during cell culture step, including supplementation with several growth factors [305,306] or variations in cell density [307] or in oxygen tension [308,309]. Furthermore, re-differentiation of de-differentiated chondrocytes with the recovery of the expression of cartilage markers can be achieved by specific culture condition, such as three-dimensional (3D) culture systems [310,311]. The 3D environment

influences cellular morphology and the cytoskeletal organization that play an important role in modulating chondrogenic features [312]. It was first shown that expanded chondrocytes can re-differentiate when embedded in agarose gel [313,314], but also in other biomaterials such as fibrin glue [315,316], alginate beads [317,318] and synthetic polymer [110,319] or by forming pellets after centrifugation [320,321]. In particular, chondrocyte encapsulation in hydrogels attracts particular interest for regenerative strategies since they also provide a highly hydrated environment similar to that of native cartilage tissue [322]. In this context, advances in tissue engineering and regenerative medicine are expected thanks to the application of the 3D-bioprinting. This technology allows to deposit biomaterials, such as hydrogels, and cells in a layer-by-layer fashion with high control in 3D pattern, architecture and cell distribution [152]. Bioprinted constructs may represent a new generation tool suitable for regenerative therapies since they are fabricated to be a 3D patient-specific and anatomically-shaped grafts [323]. Furthermore, these constructs provide the native 3D arrangement to embedded cells that finally drive the regeneration. The crucial step in bioprinting is the bioink choice, that has to be provided not only with certain rheological properties needed for good printability, but also with biological cues [164]. However, the field of biofabrication often strongly focuses on the first feature to allow for bioink controlled extrusion, taking less care of its inherent impact on cellular phenotype. The combination of both aspects can be achieved by incorporation of biological components in printable hydrogels that often lack of bioactivity. Thus, these biological components can act improving cell adjustment within the construct and also promote its host integration if released to the surrounding environment. In this context, the use of platelet rich plasma (PRP), a cocktail of platelet-derived growth factors involved in tissue healing and regeneration processes, is very appealing given that several studies have described its anti-inflammatory properties and beneficial effects on proliferation and differentiation of many cell types including chondrocytes [231].

In this work, we bioprinted primary human articular chondrocytes (hACs) derived from previous monolayer culture expansion by embedding them in a commercial available alginate-based ink and evaluated their ability to regain the chondrogenic potential both *in vitro* and *in vivo*. Furthermore, we hypothesized that by adding PRP, as a source of biological agents, the ability of the alginate-based ink to sustain cell viability inside the construct will increase. In fact, after mixing the pristine hydrogel with PRP we found an increase in cell proliferation and viability as well as a certain degree of re-differentiation and rescue of the chondrogenic phenotype.

4.2 Materials and methods

4.2.1 PRP preparation

Buffy coat samples from the expired whole blood of healthy donors were used to produce PRP at the Blood Transfusion Center of the IRCCS AOU San Martino-IST Hospital (Genoa, Italy), according to protocol reported by [324]. Briefly, pooled buffy coats were centrifuged at 400 × g for 10 min at 4°C and the plasma fraction - representing the PRP - was transferred to a new blood bag. After a complete blood count (CBC), the PRP preparation was centrifuged at 2,200 × g for 20 min at 4°C to sediment the platelets, that were subsequently re-suspended in an appropriate volume of platelet-poor-plasma in order to have a platelet count of 10×10^6 plt/μL. These preparations were divided into aliquots and stored at -20°C.

4.2.2 Primary human articular chondrocyte (hACs) isolation and 2D-expansion in culture

Femoral heads were collected from patients undergoing hip arthroplasty, with their informed consent and the approval of the institutional Ethics Committee of the IRCCS AOU San Martino-IST National Cancer Research Institute (Genoa, Italy). The patients' age ranged from 65 to 80 years (n = 6). After surgery, samples were washed with sterile PBS, minced into small pieces and digested repeatedly at 37°C in serum free Dulbecco's modified Eagle's medium High Glucose (DMEM HG, Euroclone) containing 0.25% (v/v) trypsin (Gibco), 1 mg/ml hyaluronidase (Sigma-Aldrich), 400 U/ml collagenase type I and 1000 U/ml collagenase type II (both from Worthington Biochemical, USA). Isolated cells were plated in 6-well plates and expanded for one passage in complete medium DMEM HG supplemented with 1 mM sodium pyruvate, 100 mM HEPES buffer, 1% (v/v) penicillin/streptomycin, 1% L-glutamine (all from Euroclone, Italy) and 10% (v/v) Fetal Bovine Serum (FBS) (Gibco). Cells were maintained in a humidifier incubator with 5% CO_2 at 37°C and monitored using a bright field microscope equipped with a digital camera (Leica DMi1; Leica Microsystems). When reaching 80–90% confluence, cells from different primary cultures were detached, pooled and counted before mixing with the bioinks.

4.2.3 Alginate/PRP-based bioink preparation and protein release assessment from 3D-printed constructs

CELLINK® bioink (CELLINK AB) was used as basic bioink in this study. It contains 2% (w/w) of plant-derived nanofibrillated cellulose (NFC) and 0.5% (w/w) sodium alginate. In order to obtain an

alginate/PRP bioink, 200 µL of PRP were mixed with 1 mL of CELLINK® bioink to reach a final concentration of 2×10^6 plt/µL, previously reported as physiologically effective in tissue healing process [324]. To generate alginate and alginate plus PRP (alginate/PRP) constructs, each ink was respectively loaded into a printer-compatible syringe cartridge with a 25G nozzle. A series of (5 × 5 × 1) mm grids was printed using an extrusion 3D-bioprinter (BioX, Cellink AB, Sweden) equipped with a laminar flow cabinet that allows to perform the printing process under sterile conditions. The printing parameters of pressure and velocity were set in the following range: 9-18 kPa and 9-11 mm/s. After bioprinting, the alginate and alginate/PRP constructs were immediately cross-linked with 50 mM acqueous $CaCl_2$ solution for 10 min. The total protein release from bioinks was evaluated as follows. Each tested grid was immersed in 400 µL of phosphate-buffered saline 1X (PBS) at 37°C and at selected time points (0.5, 3.5, 6, 24, 48, 120 and 144 hours) a volume of 350 µL was removed and replaced with fresh one. The supernatants recovered at each medium change were used to determine protein release kinetics (supernatants from alginate grids were used as negative control). Protein concentration in each sample was quantified by Pierce™ BCA Protein Assay Kit (Thermo Fisher Scientific) and the results are presented as percentage (%) of PRP-derived proteins released by printed grids as a function of time. Curve fittings of the experimental data were performed by using OriginPro 8.5 software (Originlab Corporation). Measurements were performed on five 3D-printed grids for both groups (n = 5).

4.2.4 Preparation of cell-laden bioinks and 3D-bioprinting

Trypsinized 2D-expanded hACs were pooled and resuspended in 200 µL of culture medium or PRP and mixed with CELLINK® bioink to obtain a final concentration of 10×10^6 cells/mL. Cell-laden bioinks were used to generate grids as described above. After bioprinting, cell-laden alginate and alginate/PRP constructs were immediately cross-linked with 50 mM aqueous $CaCl_2$ solution for 10 min and then incubated in culture medium in standard conditions (37°C, 5% CO_2). Each printed grid contains approximately 2×10^5 cells. Cell-laden 3D-constructs were monitored during culture time by using a bright field microscope equipped with a digital camera (Leica DMi1; Leica Microsystems).

4.2.5 Chondrogenic re-differentiation in 3D-culture

Both groups of 3D-printed constructs (alginate and alginate/PRP) embedding hACs were incubated in culture medium supplemented with inductive factors of chondrogenic differentiation for 3 weeks.

Chondrogenic culture medium contains 10 ng/mL human transforming growth factor-β1 (hTGF-β1) (PeproTech), 10^{-7} mol/L dexamethasone and 50 mg/mL ascorbic acid (both from Sigma-Aldrich) according to [18]. In parallel, some hAC-laden constructs of both groups were maintained in basal medium without chondrogenic factor supplementation for the same period as control.

4.2.6 Cell viability tests

- *Live/dead® assay*

Cell viability was assessed within 3D-constructs after printing process using LIVE/DEAD® assay (Thermo Fisher Scientific) in order to distinguish between live and dead cells printed inside. Both alginate and alginate/PRP constructs were washed in PBS 1X and incubated in the staining solution for 45 minutes at room temperature (RT) according to manufacturer's instructions. Samples were observed under epifluorescent illumination using an Axiovert 200M microscope and images were captured with Axiocam HR camera (Carl Zeiss).

- *Alamar Blue™ assay*

Cell-laden constructs (alginate and alginate/PRP) were placed in separate wells of a 24-well plate. Then 0.4 mL of 10% Alamar Blue™ (Thermo Fisher Scientific) solution were added to each well and reactions were then incubated (37°C, 5% CO_2) in darkness for 4 h. After incubation, 200 µl from each replicate well (n = 5) were taken and transferred to a 96-well plate for absorbance reading at two wave lengths of 570 nm and 600 nm respectively. Viability assay was repeated on the same constructs at consecutive time points of 1, 7, 14 and 21 days after 3D-printing process. Cell viability was reported as percentage (%) of reduced dye along culture time.

4.2.7 Cytoskeleton-imaging

To visualize cell cytoskeleton within the 3D-constructs, Phalloidin-Alexa Fluor 594 (Thermo Fisher Scientific) was used for the staining of F-actin. AC-laden constructs (alginate and alginate/PRP) were fixed in 3.7% paraformaldehyde (PFA) for 30 minutes at RT. After rinsing the samples with PBS 1X, the cells were permeabilized with 0.1% triton X-100 for 15 minutes. The 3D-constructs were rinsed twice and then stained with the reagent for 30 minutes at RT, using the manufacturer's recommended concentration. Cell nuclei were stained by DAPI (Sigma-Aldrich) for 15 minutes. Following the staining, 3D-constructs were washed twice and observed by fluorescence microscopy (Axiovert 200M, Carl Zeiss).

4.2.8 DNA content

Quantification of DNA and cell number in cell-laden constructs at 7 and 21 days of culture was performed using the fluorimetric CyQUANT™ Cell Proliferation Assay (Thermo Fisher Scientific), according to the manufacturer's instructions. Briefly, culture medium was removed from printed constructs and samples were stored at -80°C. After thawing just before the assay, cells were lysed by adding 200 µl of CyQUANT™ reagent to each sample for 5 minutes at RT in darkness. Fluorescence was measured at excitation/emission wavelengths of 480/520 nm in a microplate reader (VICTOR X Multilabeled Plate Reader, Perkin Elmer) coupled to a Perkin Elmer 2030 Workstation. Cell number and DNA content were determined by comparing the average fluorescence of each sample (n = 3) to a cell standard curve and a DNA standard curve, respectively.

4.2.9 Glycosaminoglycan (GAGs) content

Neo-synthesis of GAGs was assessed by the spectrophotometric 1,9-dimethylmethylene blue (DMMB) assay as described by [325]. 3D-printed constructs were collected at 7 and 21 days of chondrogenic culture and digested in papain buffer (Sigma-Aldrich) at 60°C overnight. Following centrifugation at 10,000 × g for 10 minutes, 100 µl of the digested samples were added to 200 µl DMMB solution (pH 1.5) and the absorbance was measured spectrophotometrically at 595 nm. The GAG content was calculated against a standard curve of chondroitin sulphate C derived from Shark (Sigma-Aldrich). For each sample, the amount of GAGs (µg) was corrected for the mean dsDNA (µg) content as determined by the CyQUANT™ Cell Proliferation Assay (n = 3) (see section 4.2.8 above).

4.2.10 Gene expression analysis by qRT-PCR

Expression of aggrecan (ACAN), collagen type II (COL2A1), collagen type I (COL1A1) and transcription factor SOX9 were investigated after monolayer expansion of hACs and 3D-culture of cell-laden constructs by analysing mRNA levels. Samples were resuspended in TRIzol™ Reagent (Thermo Fisher Scientific) and total RNA was extracted according to the manufacturer's protocol. RNA concentrations were measured at 260 nm using Nanodrop TM 1000 (Thermo Fisher Scientific) and its purity was checked considering 260 nm/280 nm ratio with values included in 1.5–2.1 range. Complementary DNA (cDNA) synthesis was performed starting from 2 µg of total RNA and using SuperScript™ VILO™ Master Mix (Thermo Fisher Scientific) following the

manufacturer's instructions. Transcript levels of target genes were measured by Real Time quantitative PCR using Power SYBR® Green PCR Master Mix on 7500 Fast Real-Time PCR System (Applied Biosystems). The housekeeping gene GAPDH was used as the endogenous control for normalization. The selected human-specific primer sequences were:
COL2A1, forward 5' - GGCAATAGCAGGTTCACGTACA - 3', reverse 5' - CGATAACAGTCTTGCCCCACTT - 3'; COL1A1, forward 5' - CAGCCGCTTCACCTACAGC - 3', reverse 5' - TTTTGTATTCAATCACTGTCTTGCC - 3'; SOX9, forward 5' - CCCGCACTTGCACAACG - 3'; reverse 5' - TCCACGAAGGGCCGCT - 3'; ACAN, forward 5' - ACCAGACGGGCCTCCCAGAC - 3', reverse 5' - ACAGCAGCCACACCAGGAAC - 3'; GAPDH, forward 5' - CCATCTTCCAGGAGCGAGAT - 3', reverse 5' - CTGCTTCACCACCTTCTTGAT - 3'. Relative quantification was performed using the $2^{-\Delta\Delta Ct}$ method.

4.2.11 Subcutaneous implantation of 3D-constructs in nude mice

AC-laden 3D-constructs of both groups (alginate and alginate/PRP) were maintained in chondrogenic medium for 3 days before implantation in athymic mice (female CD-1 nu/nu; Charles River Laboratories Italia). The constructs were surgically implanted in subcutaneous pockets on the back of mice. 3D-printed constructs without embedded cells were implanted as control. Six animals were used for each group. After 60 days the mice were euthanized and the constructs retrieved and processed for histological analysis. All animals were maintained in accordance with standards of the Federation of European Laboratory Animal Science Associations, as required by the Italian Ministry of Health.

4.2.12 Histological and immunohistochemical analysis

Explanted and *in vitro* cultured 3D-constructs (alginate and alginate/PRP) were fixated in 3.7% buffered paraformaldehyde overnight and 20 minutes respectively at 4°C, then embedded in paraffin and sectioned at 5 µm by using microtome RM2165 (Leica). Prior to histological and immunohistochemical staining, all sections were deparaffinized and rehydrated. To visualize cell morphology, cell distribution and deposition of sulphated-GAGs within the 3D-constructs, the sections were stained with haematoxylin/eosin and alcian blue (pH 2.5), respectively.
For immunohistochemical analysis, dewaxed sections were treated with methanol:hydrogen peroxide (49:1) solution for 30 minutes to inhibit endogenous peroxidase activity, then

permeabilized with 0.3% triton X-100 in PBS for 10 minutes and finally incubated with hyaluronidase (Sigma-Aldrich) at concentration of 1 mg/ml in PBS (pH 6) for 30 minutes at 37°C. After washing in PBS and incubation with 20% normal goat serum (NGS) for 1 hour to inhibit nonspecific binding, the slices were incubated overnight at 4°C with primary antibodies raised against: type II collagen, 1:250 diluted in 10% NGS (CIICI-Developmental Studies Hybridoma Bank, University of Iowa); type I collagen, 1:300 diluted in 10% NGS (SP1.D8-Developmental Studies Hybridoma Bank, University of Iowa); SOX9, 1:200 diluted in 10% NGS, and aggrecan, 1:100 diluted in 10% NGS (both from Abcam). The immunobinding was detected by incubation with biotinylated secondary anti-muose or anti-rabbit antibodies (Dako) for 30 minutes at RT followed by treatment with streptavidin-peroxidase (Jackson ImmunoResearch). Peroxidase activity was finally visualized by 3-amino-9-ethylcarbazole (Sigma-Aldrich) chromogen substrate. Images were acquired by a microscope Axiovert 200M (Carl Zeiss) at different magnifications.

4.2.13 Statistical analysis

All values are reported as mean and standard error of the mean (SEM). Statistical tests were performed to compare group data sets as follows: two-way ANOVA followed by Bonferroni's *post-hoc* test in cell viability assay, cell quantification, DMMB assay and gene expression in 3D-bioprinted constructs; Student's *t*-test in gene expression 2D *versus* 3D comparison. Values of $p < 0.05$ were considered statistically significant (* $p < 0.05$, ** $p < 0.01$, *** $p < 0.001$). Data were analyzed with GraphPad Prism® 8.0 software (GraphPad Software, Inc.).

4.3 Results

4.3.1 Feasibility in 3D-bioprinting of hACs embedded in alginate alone or supplemented with PRP

Primary hACs were isolated from hip cartilage biopsy of patients underwent arthroplasty by serial digestions with enzymes degrading ECM components (i.e. mix of collagenases and hyaluronidase) (Figure 4.1A). The tissue portions selected for the primary cell culture preparation were apparently healthy, free of visible defects and quite white in colour. As illustrated in Figure 4.1A, harvested hACs were expanded in monolayer (2D) culture in order to obtain an amount enough to be printed through a bioprinter and not beyond passage 2 to avoid irreversible dedifferentiation process. Expanded hACs were mixed with hydrogel just before the printing process (Figure 4.1B) with the

help of a spatula. The resulting mix of biomaterial and embedded cells are defined bioink. The printability of the bioink depends on some rheological parameters specific for the adopted biomaterial, that in this study is composed of alginate and nanocellulose (nanofibrillated cellulose, NFC) as the one reported in [153]. Besides offering a biocompatible 3D environment for cells, this NFC-based bioink is highly viscous and shows shear thinning behaviour, two properties that make possible to bioprint even complex anatomically-shaped constructs without the need of sacrificial support structures. In parallel with the basic aforementioned hydrogel, another bioink formulation was proposed in this work based on the addition of PRP in order to provide a supply of biological factors able to better support cell growth and differentiation. As shown in Figure 4.1C, the two typologies of final bioinks (alginate and alginate/PRP) retained their correct printing behaviour despite the dilution with cell suspension and grids were printed with a resolution not really high, but typical of soft materials such as hydrogels. Alginate in the bioinks could be cross-linked after printing process with a cell-friendly calcium solution and a free-standing constructs could be obtained at the end of the 3D-printing procedure (Figure 4.1C).

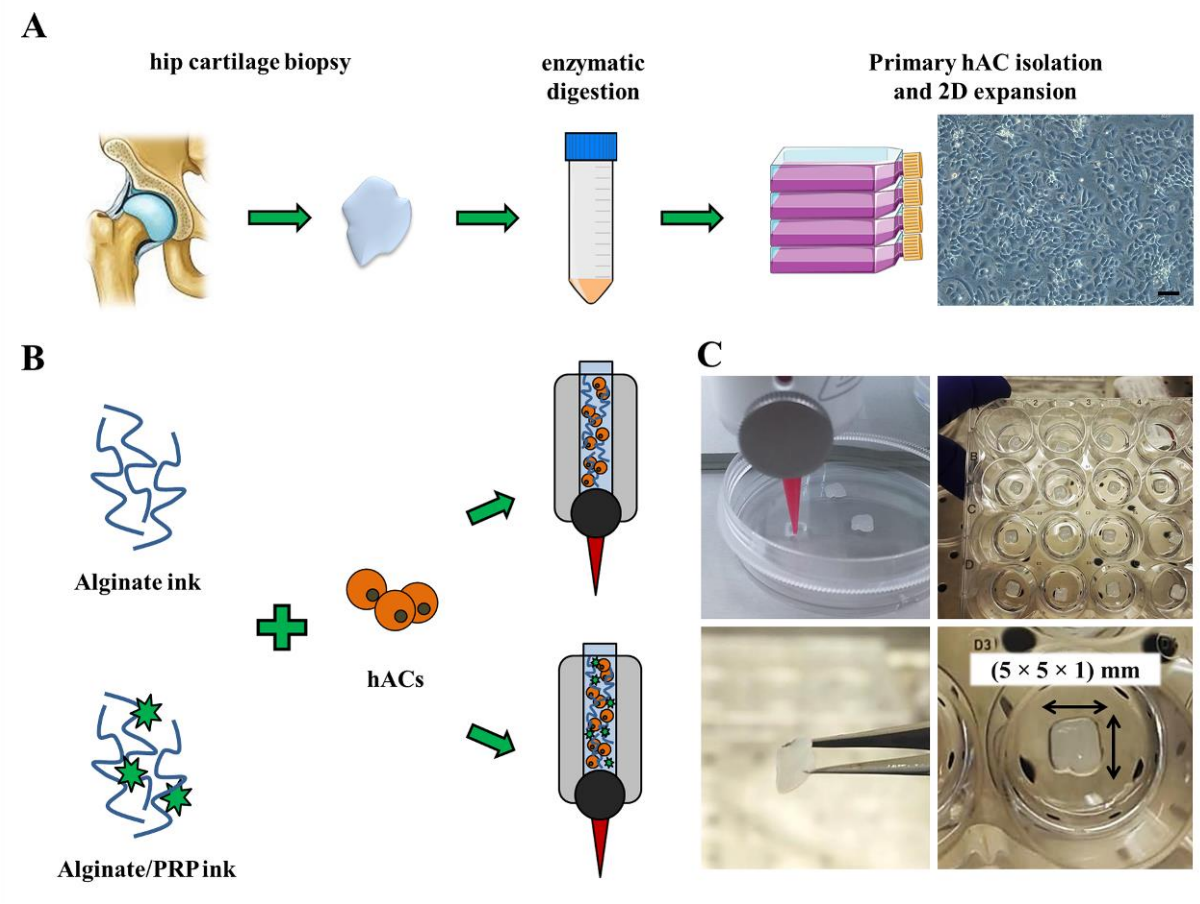

Figure 4.1: Primary culture of hACs and bioprinting of 3D cell-laden grids. (**A**) Isolation of hACs from hip cartilage biopsy by enzymatic digestion and monolayer (2D) expansion *in vitro*. (**B**) Preparation of bionks suitable for 3D-bioprinting process by mixing biomaterials (alginate or alginate plus 2 × 10^6 plt/μL PRP) with expanded hACs. (**C**) 3D-bioprinting process of the bioink directly deposited in a 24-well dish (upper left and right panels) in (5 × 5 × 1) mm grids (bottom right panel) derived from a computer-aided design (CAD) models; cross-linked construct immediately after printing are compact and free-standing (bottom left panel).

4.3.2 Cell morphology, viability and growth in 3D-bioprinted constructs and PRP-based bioink contribution in embedded cell responses

Alginate/PRP bioink was obtained by simply blending the platelet concentrate (the amount is reported in Materials and methods section) with the commercial alginate-NCF hydrogel and not by chemical linking. Thus, the PRP derived factors embedded in the printed constructs were released in the surrounded medium following a kinetics affected by the type of non-covalent interaction with the hydrogel molecular structures. The cumulative release of PRP-derived proteins from the printed grids (before cell embedding) was evaluated for 6 days (144 hours) and the analysis revealed a burst

in the first 24 hours from the biofrabrication followed by a minor train in the subsequent time points (mostly 48 hours) (Figure 4.2A). As shown in Figure 4.2A, among three different models of drug kinetics release from a matrix, Korsmeyer-Peppas, single stage desorption and double stage desorption models, our data of protein release by alginate/PRP bioink fitted to the latter one. Alginate bioink without PRP supplementation was used as negative control in the protein release quantification assay.

Morphology and distribution of the cells embedded in both types of printed constructs were evaluated by observations under optical microscope and fluorescent staining of actin cytoskeleton (Figure 4.2B). Overall, the cell density within the hydrogel appeared homogeneous and their shape was rounded as induced by 3D-environment. Moreover, cells were small in size, they showed low surface/volume ratio and their actin cytoskeleton assumed a cortical arrangement with no apparent monolayer typical features (stress fibers, focal adhesions, lamellipodia and filopodia). Interestingly, at the end of the chondrogenic re-differentiation *in vitro* (3 weeks) cells in alginate/PRP group formed spherical and dense aggregates mainly concentrated on the surface of the constructs (Figure 4.2B).

Since the printing process could subject cells to stress, mainly due to the extrusion pressure through the syringe nozzle, a qualitative assessment of hAC viability post-fabrication in both experimental groups was performed by a fluorescent LIVE/DEAD assay (Figure 4.2C). The observations did not reveal an evident difference between the two bioink groups, and most of the stained cells were alive, while the dead ones were damaged because of the manual mixing with hydrogels or the time duration of the whole printing process (2/3 hours from the cell monolayer detachment to the cell-laden bioink cross-linking). Cell viability monitoring along the whole culture time *in vitro* (3 weeks) revealed that it was higher in alginate/PRP constructs at 7 ($p < 0.001$), 14 ($p < 0.001$) and 21 days ($p < 0.01$) compared to alginate constructs. Moreover, PRP enhanced cell viability at day 7 compared to day 1 ($p < 0.01$), an increase that was not observed in alginate constructs. However, PRP was unable to revert the decrease in cell viability observed with time (Figure 4.2C). This finding could be explained both by the not optimal perfusion of nutrients in the inner construct layers, with subsequent cell necrosis, and the weakening of the cross-linking strength (due to the diffusion of calcium ions in the medium) with consequent loss of cells from the hydrogels along culture period. Finally, despite the cell density at the starting point was the same for both types of bioinks, a higher number of cells in alginate/PRP group compared to alginate constructs was observed at both 7 and 21 days ($p < 0.001$ and $p < 0.01$, respectively), as demonstrated by the quantification of the DNA amount *per* construct. However, it was not observed a statistically

significant change in cell number over time during differentiation culture period within the same experimental group (Figure 4.2D).

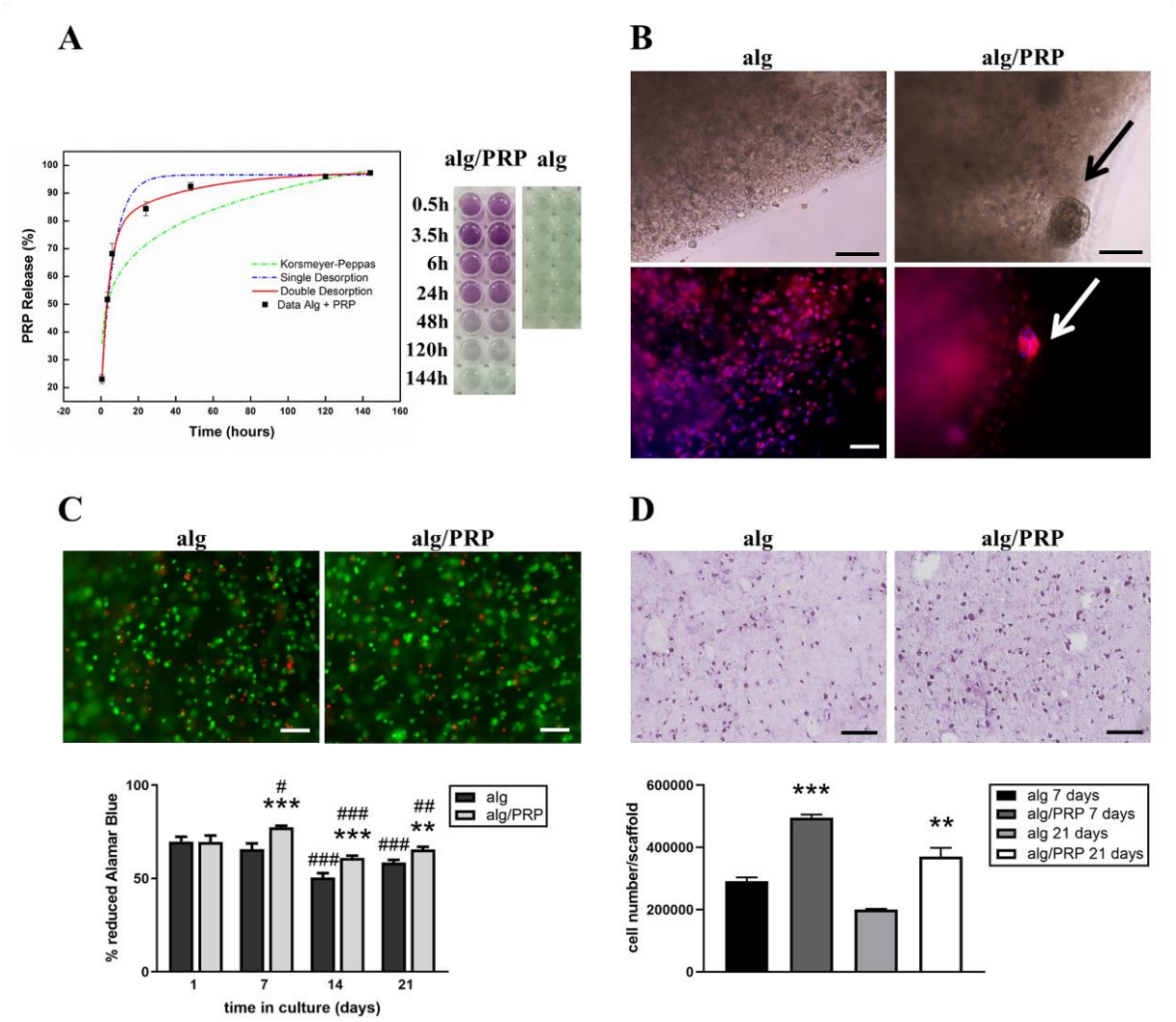

Figure 4.2: Analysis of PRP-derived protein release from bioink and evaluation of cell morphology, viability and growth in alginate and alginate/PRP-printed constructs. (**A**) PRP-derived protein release (%) from printed alginate/PRP grids plotted *versus* time (hours) and data curve fitting with Korsmeyer-Peppas (green), single- (blue) and double- (red) stage desorption kinetic models (left panel) (n = 5); representative image of media withdrawals from alginate and alginate/PRP constructs assayed during protein quantification (BCA assay). (**B**) Optical microscope images (upper panel) of both alginate and alginate/PRP constructs; immunofluorescent staining for cellular F-actin cytoskeleton (red) and nuclei (blue) inside the constructs during *in vitro* chondrogenic culture (bottom panel). (**C**) Fluorescent staining (LIVE/DEAD® assay) for alive (green) and dead (red) cells inside the bioinks after printing process (upper panel) and cell viability quantification (Alamar Blue™ assay) during 3 weeks of chondrogenic culture *in vitro* (bottom panel) for both the experimental groups (** $p < 0.01$ and *** $p < 0.001$ *versus* alginate within the

same day; # $p < 0.05$, ## $p < 0.01$ and ### $p < 0.001$ *versus* t = 1 day within the same group by two-way ANOVA analysis and Bonferroni's multiple comparisons test) (n = 5). (**D**) Hematoxylin/eosin staining of histological section of both types of constructs at 21 days of chondrogenic culture *in vitro* (upper panel) and determination of cell number (CyQUANT™ assay) in each group at 7 and 21 days of culture period (** $p < 0.01$ and *** $p < 0.001$ *versus* alginate within the same day by two-way ANOVA analysis and Bonferroni's multiple comparisons test) (n = 3). All data are represented as mean ± SEM. All scale bars correspond to 100 μm.

4.3.3 *In vitro* chondrogenic differentiation of hACs in 3D-bioprinted constructs

GAGs deposition by hACs within both types of scaffold was evaluated with DMMB assay during *in vitro* chondrogenic culture (Figure 4.3A). GAGs secretion increased during the re-differentiation period in both experimental groups (alginate, $p < 0.01$ and alginate/PRP $p < 0.001$ *versus* 7 days of culture). However, no statistically significant differences were found between the two typologies of constructs at any time.

The hAC expression of chondrogenic markers such as type II and type I collagens, aggrecan and SOX9 were investigated at the end of the chondrogenic culture by immunohistochemistry on paraffin-embedded sections of the two types of constructs (Figure 4.3B). The cellular staining was found similar in both conditions for all chondrogenic molecules.

From the comparison of gene expression levels by qRT-PCR (Figure 4.3C), it emerged a clear difference of hAC differentiation state between 2D (monolayer) culture and 3D-culture (printed constructs), even in absence of chondrogenic induction. Expanded hACs in monolayer before 3D-bioprinting were de-differentiated and after the change of spatial arrangement they increased the expression of the chondrogenic markers COL2A1 ($p < 0.05$), SOX9 ($p < 0.01$), and ACAN ($p < 0.01$) without chondrogenic factor supplementation. Conversely, the expression level of COL1A1, a fibrocartilage marker, decreased in 3D-arranged cells compared to 2D ones ($p < 0.001$). The analysis of gene levels in the 3D-printed constructs incubated in chondrogenic conditions confirmed the aforementioned immunohistochemistry results. Two additional groups represented by alginate and alginate/PRP constructs cultured for 21 days without chondrogenic factors were added to the previous investigation. The expression levels of COL2A1 ($p < 0.01$) and ACAN ($p < 0.001$) were higher in differentiation culture conditions in both types of constructs than in non-differentiation ones, while SOX9 increased under chondrogenic conditions only in alginate constructs ($p < 0.05$). COL1A1 did not change in any of the 3D-constructs after chondrogenic conditions compared to non-chondrogenic conditions. Interestingly, an up-regulation of ACAN and SOX9 expression levels

was detected in alginate/PRP constructs compared to alginate ones cultured in absence of chondrogenic factors ($p < 0.05$).

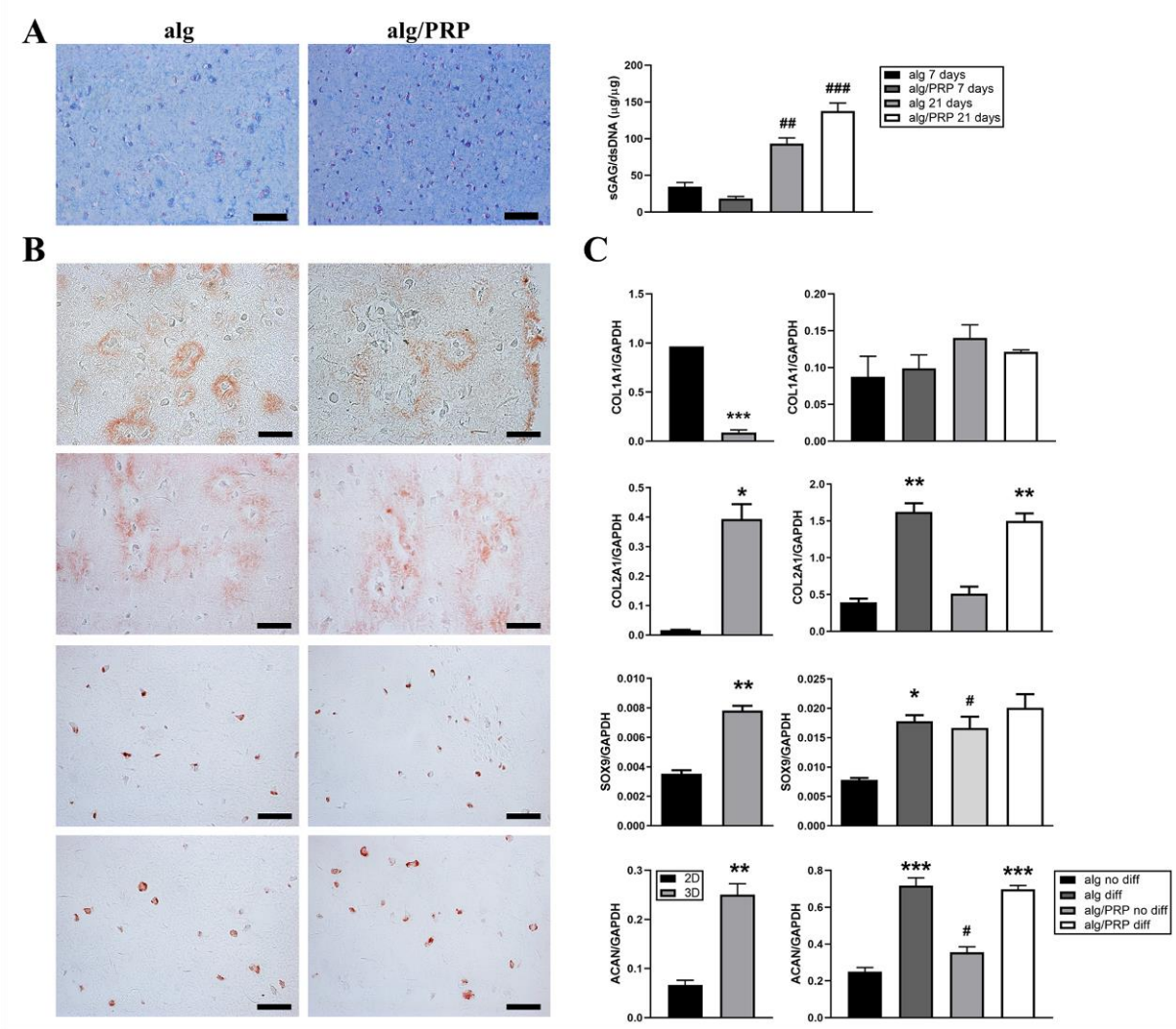

Figure 4.3: GAG deposition and chondrogenic marker expression by hACs embedded in alginate and alginate/PRP printed constructs. (**A**) Alcian blue staining on paraffin-embedded sections of alginate and alginate/PRP constructs at 21 days of chondrogenic culture (left panel); GAG quantitative levels (DMMB assay) normalized to DNA content in both experimental groups at 7 and 21 days of chondrogenic culture (## $p < 0.01$ and ### $p < 0.01$ *versus* 7 days of culture within the same group by two-way ANOVA analysis and Bonferroni's multiple comparisons test) (right panel). (**B**) From top to bottom: immunohistochemical staining for type I and II collagens, SOX9 and aggrecan on paraffin-embedded sections of both experimental groups after 21 days of chondrogenic culture; all scale bars correspond to 100 µm. (**C**) Gene expression analysis by qRT-PCR of COL1A1, COL2A1, ACAN and SOX9 in hACs monolayer (2D) culture *versus* 3D-printed constructs (left panels) and in both types of constructs after 21 days of culture with or without differentiation factors (right panels) (* $p < 0.05$, ** $p < 0.01$, *** $p < 0.001$ *versus* 2D condition or non-differentiation culture by Student's t-test analysis; # $p < 0.05$ *versus* alginate within the same

culture condition by two-way ANOVA analysis and Bonferroni's multiple comparisons test) (n = 3). All data are represented as mean ± SEM. All scale bars correspond to 100 µm.

4.3.4 *In vivo* chondrogenic differentiation of hACs in 3D-bioprinted constructs

Printed constructs implanted for 2 months in mice were well integrated subcutaneously and, when explanted after animal sacrifice, were intact, not reabsorbed, glossy in appearance and white in color (Figure 4.4A). Printed constructs without embedding of cells (empty) were implanted as control to detect and define murine cell colonization. Host cells were mailnly concentrated at the edges and sometimes in internal fissures of the implanted constructs (Figure 4.4A). Most of the scaffold area in cell-free constructs was empty, evidence that should allow to consider cells in samples as hACs previously encapsulated. The histological analysis showed that hACs in the constructs divided, began to form clusters and to be surrounded by pericellular matrix. However, no evident differences were noted between the two types of constructs in terms of morphology or GAG deposition (Figure 4.4B). Immuhistochemistry for human ECM molecules, type II collagens and aggrecan, and the human transcriptional factor SOX9 showed a diffused staining with a similar distribution between the two experimental groups (Figure 4.4C).

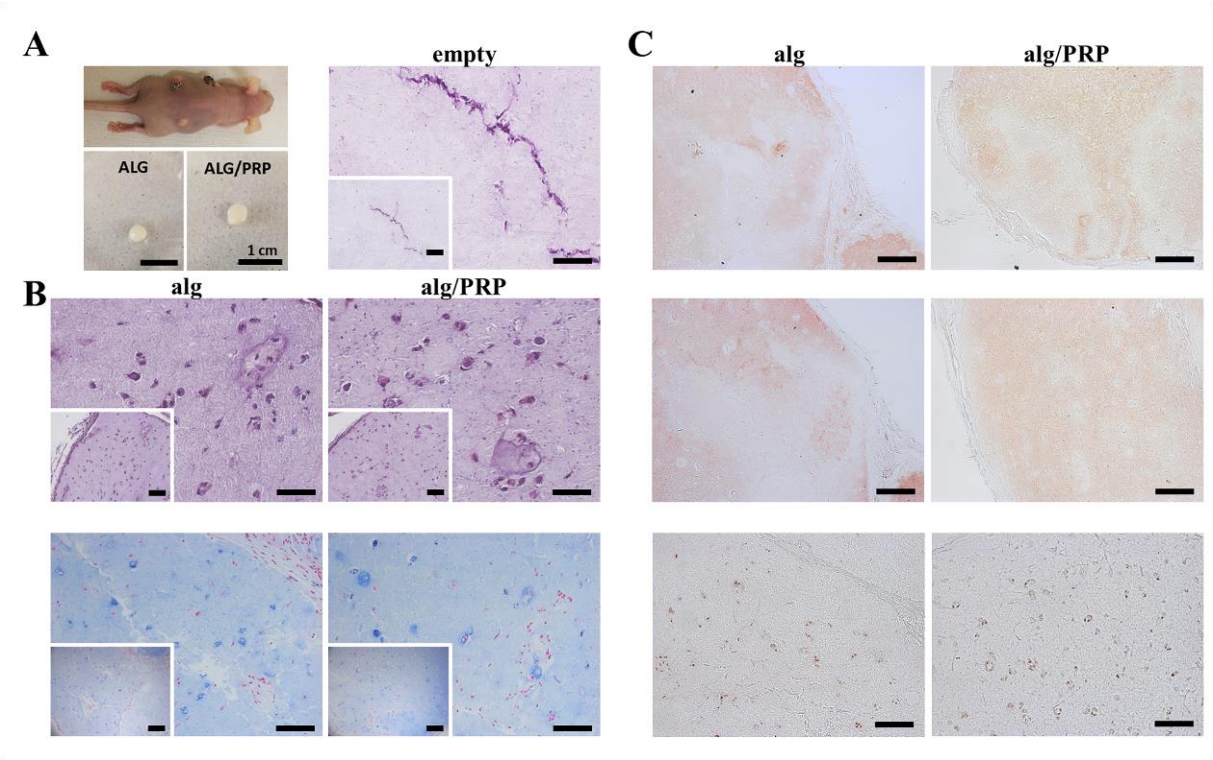

Figure 4.4: Implantation of hAC-laden alginate and alginate/PRP constructs in nude mice and histological analyses on explanted grafts. (**A**) Representative images of an euthanized nude mouse just before the recovery of the implanted constructs (upper left panel) and of the explanted alginate and alginate/PRP constructs after two months from the surgery (below left panel); hematoxylin/eosin staining on paraffin-embedded sections of explanted constructs without hAC embedding (empty). (**B**) Hematoxylin/eosin (upper panel) and alcian blue (lower panel) stainings on paraffin-embedded sections of explanted alginate and alginate/PRP constructs after two months from *in vivo* implantation; insets show minor magnifications. (**C**) Immunohistochemistry for type II collagen (upper panel), aggrecan (middle panel) and SOX9 (bottom panel) on paraffin-embedded sections of alginate and alginate/PRP explanted constructs. Scale bar correspond to 50 µm and 100 µm (insets) (n = 6).

4.4 Discussion

Natural hydrogels, such as alginate, are common biomaterials exploited in the field of cartilage tissue engineering thanks to their biocompatibility and since the high water content makes them structurally similar to native tissue ECM. Alginate is extracted from brown algae and it gels when in contact with divalent cations such as calcium chloride ($CaCl_2$) [326]. The latter property, i. e. the cross-linking ability, makes a hydrogel especially suitable for 3D-bioprinting as a component of bioinks, given that it allows to maintain the printed structure after the fabrication. Furthermore, shape fidelity has to be ensured also during the printing process by high solution viscosity. Since

alginate is not viscous enough to keep the shape and an acceptable printing resolution, even at high concentration and high molecular weight, it has been proposed to reinforce the solution formulation with NFC for an optimal printing process [153]. Cellulose nanofibres are biocompatible and their similarity in size (~ 100 nm) with collagen fibers makes them interesting in biomaterial design for cartilage tissue engineering purposes. NFC, as bioink for bioprinting, has optimal viscosity and shear thinning, however printed constructs cannot be gelled and thus their shape is easily lost after fabrication. Indeed, combining the two components together in an unique solution allows to merge the gelation properties of alginate with the rheological ones of the NFC and to obtain a high performing ink [153].

In this work two types of hAC-laden constructs were bioprinted based on alginate alone or mixed with PRP exploiting the aforementioned properties of NFC supplementation to the hydrogel. Such experimental conditions allowed to dispense the cell-laden bioink at low ("cell-friendly") pressure (< 40 kPa) and to provide embedded cells with a stable 3D environment at the end of the process.

PRP formulations contain a high concentration of blood-derived platelets and are widely use in regenerative medicine because they are able to mimic the events that take place during the physiological reaction to injury, in particular the phase in which platelet-released growth factors and cytokines trigger tissue healing [327]. Among these platelet-released factors are included platelet-derived growth factor (PDGF), vascular endothelial growth factor (VEGF), epidermal growth factor (EGF), fibroblast growth factor (FGF), transforming growth factor-β (TGF-β) and interleukin 8 (IL8), all with relevant roles in several biological events such as cell proliferation, differentiation, migration and inflammatory response [231,328,329].

The local delivery of PRP for the treatment of musculoskeletal disorders has led to promising outcomes [330]. Moreover, platelet-derived products (i.e. platelet lysate) exert several stimulating effects on different types of cells *in vitro*, including chondrocytes [128,135]. PRP supplementation to bioinks for bioprinting has been recently developed by Faramarzy *et al*. [331], with the aim to introduce a new tool for the embedding and controlled-release of autologous biological factors in the field of personalized therapies.

In this study PRP was added to NFC/alginate-based bioink in order to provide biological stimuli to hACs encapsulated within an inert environment and, given the release of platelet-derived factors to the surrounding environment, to further promote the integration of the printed cell-laden graft in the host, especially required for its successful transplantation in regenerative medicine applications. The chosen PRP concentration to be added to the bioink was that already tested by Spanò *et al.*

[324] and proved to be effective in the generation of an activated membrane intended for wound care.

PRP biological effects are physiologically achieved after platelet activation that generally involves the polymerization of plasma fibrinogen and the formation of a protein-based 3D-mesh with entrapped platelets that release their cargo out [332]. Calcium ions have a role in events that lead to platelet activation [333] and, in the context of the aforementioned bioprinting process with alginate-based bioinks, they are also necessary for the cross-linking of the printed constructs. In our hands, alginate/PRP-based bioink resulted more compact after cross-linking than the alginate alone one, however this merely qualitative observation was validated by Faramarzi *et al*. [331], who reported an increased mechanical stiffness of the cross-linked constructs explained by the network formation of activated platelets. However, the addition of PRP did not modify the rheological properties of the pristine bioink and it did not interfere with the printing process.

The total release rate of proteins from alginate/PRP bioink was similar to the one reported for other hydrogel systems [334] and it was characterized by an initial burst followed by a slower and more gradual release phase over 144 hours. This biphasic release process followed the desorption model described by Khansari *et al.* [335] for nanostructured scaffolds. Furthermore, as reported by Faramarzi *et al*. [331], protein release from PRP-containing bioinks showed the same trend seen for PRP gels, that are commonly produced but with the drawback of poor mechanical integrity.

Regarding the fate of hACs embedded in bioinks and bioprinted, cell distribution and morphology were investigated. An homogeneous cell distribution was observed within the printed constructs as a result of an optimal mixing process and a biomaterial ability to keep cells in suspension. Furthermore, embedded hACs, as also reported by Martínez Ávila *et al.* [336] using nasoseptal chondrocytes in the same typology of bioink, showed a spherical morphology, that is typical of their native phenotype, with a diffuse actin organization. Some spheroids of aggregated cells were found in alginate/PRP-based constructs and sometimes flattened cells on the edge surface of both construct types were observed. This morphological difference between the hACs cultured in 2D and those grown in 3D could have been crucial in influencing the differentiation state of chondrocytes, as already demonstrated after 3D chondrocyte encapsulation in several biomaterials [337,338].

A challenging aspect of the mixing process of cells with biomaterials and their subsequent culture is to preserve cell viability during and after encapsulation over time. Martínez Ávila *et al.* [336] have already evaluated cell viability at each bioprinting step until construct fabrication, i.e. embedding, bioprinting and cross-linking. As expected, they reported that cell handling before embedding significantly decreased cell viability compared to their previous condition, but no further adverse

effects occurred after bioprinting and cross-linking of the bioink. Furthermore, they observed an increment in cell viability and cell number in the printed constructs as *in vitro* culture progressed along 28 days. Here, we did not find the same phenomenon, likely due to the different source of the cells used or to the tight meshes adopted in the grid design of the construct. In our study, hACs were obtained from elderly patients and therefore they were mostly resting cells expected to hardly proliferate *in vitro*, according to the low doubling rate of these cell type previously reported by Pereira *et al.* (about two doublings in 25 days of culture in monolayer) [128]. It has already been demonstrated that switch from 2D to 3D-culture conditions slowed down the proliferation of hACs [311]. In addition, chondrocytes derived from different cartilaginous sites of the same individual showed different behaviour, including that concerning growth rate [339]. Furthermore, the detected decrease in cell viability after the first week in 3D-culture could be due to the low nutrient diffusion from the medium to the inside of the constructs caused by the geometrical pattern of the grids with small pores. Finally, we cannot rule out the occurrence of an impairment of the grid structure due to low supply of calcium ions. This putative loss of the original construct structure could have caused cell spillage from the scaffolds. To avoid this issue probably a multiple cross-linking repetitions during the culture time will be required. Cell viability was higher in PRP supplemented bioink at day 7 compared to day 1 of culture, while it was lower at day 14 and day 21 compared to day 1 in both types of constructs. After 7, 14 and 21 days of 3D-culture, cell viability was higher in alginate/PRP than in alginate constructs. Furthermore, the number of cells *per* construct increased after 7 and 21 days of 3D-culture in presence of PRP compared to the pristine bioink, although hACs did not proliferate further between these two time points. In this regard, it is necessary to keep in mind that during an inductive culture with specific factors, differentiation is generally favored over proliferation. Data concerning cell viability and number *per* constructs were quite concordant each other. This mitogenic effect of platelet derivatives on chondrocytes both in 2D and 3D-culture conditions was already reported in literature [133,340], but in our study, PRP was not used as a medium supplements but as a supporting component of the scaffolds.

Re-differentiation potential of hACs in both 3D-printed constructs was evaluated on the basis of their capability of regaining ECM molecules production by the analysis of GAG deposition and gene expression profile. Compared to the first week of culture *in vitro* under chondrogenic conditions, encapsulated chondrocytes in both alginate and alginate/PRP constructs increased markedly the production of GAGs after 3 weeks.

As previously anticipated, 3D environment affected hAC chondrogenic phenotype. Upon expansion in monolayer culture, hACs underwent de-differentiation, as indicated by high levels of COL1A1

and low expression of COL2A1, but after embedded in bioinks and bioprinting their gene expression pattern reverted to a more differentiated state. Indeed, this phenotypic change was confirmed by the up-regulation of cartilage-related genes, including those coding for SOX9, COL2A1 and ACAN in 3D-printed constructs *versus* cell monolayer in basal culture condition without chondrogenic factors. Simultaneously, the expression of COL1A1, a marker of fibrocartilage, up-regulated during *in vitro* expansion, was significantly reduced upon 3D-culture. This finding indicated that the switch in type II/I collagen ratio typical of chondrogenic phenotype loss *in vitro* was reverted. Although this reversion was already known in literature in the context of 3D biomaterials, it is particularly interesting the up-regulation in gene expression of the chondrogenic markers SOX9 and ACAN in cells embedded in alginate/PRP constructs cultured without differentiation factors. This effect of PRP may be elicited by the platelet-derived TGF-β, a factor known to be critical for maintenance of cartilage [341] and a regulator of SOX9 [342] and other cartilage proteins. All the discussed findings make the hAC-laden constructs with PRP embedding a promising and suitable 3D-model for studies on cartilage homeostasis and pathology-related mechanisms, at least *in vitro*.

The analysis of the constructs implanted in nude mice revealed a moderate cartilage-like organization of cells within the printed grids after 2 months, but there was not an evident effect of PRP in that organization. Probably the PRP dose used in this work is not strong enough to be effective in driving *in vivo* cartilage regeneration, mostly when it is expected to start from adult hACs. Although they recovered the ability to deposit cartilage-like matrix when embedded in 3D-environment, they are mature cells destined to exhaust its potential faster than cells with stemness features such as multipotent progenitor cells. Recently, the identification and characterization of such a cartilage-resident population has opened new avenues for cartilage repair [8,46]. Despite their promising features, the use of cartilage stem/progenitor cells are almost unexplored in tissue engineering and bioprinting, with some exceptions recently published [343]. This absence of studies may be likely due to the low frequency of these cells in the tissue and a lack of definitive and proper identification markers for this particular population [34]. So far, advanced biofabrication strategies for clinical applications in cartilage regeneration still use patient-derived mature chondrocytes expanded *in vitro* prior to the shape-specific 3D-construct assembly [344]. PRP contribution in this field could be exploited given its well-known role in tissue regeneration mechanisms.

4.5 Conclusions

Based on the results reported in this study, we conclude that alginate/PRP bioink provides a biologically relevant environment that supports re-differentiation of hACs, re-establishing and maintaining their chondrogenic phenotype. This bioactive property combined with a proper printability make it a promising bioink to be exploited for articular cartilage tissue engineering and other biomedical applications.

Conclusions

In this PhD thesis, contributions and applications of platelet-derived products have been investigated on articular cartilage cells, targeting tissue regeneration. Given the wide and varied molecular content of platelet derivatives, they induce multiple cellular reactions. Treatment with platelet products promotes proliferation in low turnover chondrocytes, as well as cell phenotypic changes towards an earlier stage (self-renewal capability), enhanced migratory activity and modulated secretion of inflammatory and chemotactic molecules. All these events together could summarise tissue regeneration mechanisms, that in cartilage rarely occur because its poor intrinsic self-healing capacity. PRP or PL-induced effects support their use in biomedical applications concerning cartilage repair, from direct injections in injured joints to culture media supplementation for expansion of transplantable chondrocytes or embedding in scaffold assembly for tissue engineering and *in vitro* model generation. Hence, study of cartilage cell behaviour exposed to platelet products could be useful to improve current therapeutic strategies (that sometimes appear controversial because of the lack of consensus in adopted methods and protocols) and design of innovative ones consistent with tissue engineering and regenerative medicine advances.
Main outcomes and conclusions of this thesis are presented below.

1) PL exerted stimulant effects on articular cartilage, such as promotion of chondrocyte proliferation, cell mobilization and activation of nestin expressing progenitors. These PL-recruited progenitor cells were able to migrate in response to inflammatory stimuli, showed paracrine activity in attracting other cells (ideally toward injured sites), high chondrogenic potential and resistance to hypertrophy. The findings are remarkable in terms of a local chondro-progenitor cell subset, not previously identified, that may replace damaged chondrocytes in a compromised cartilage environment and represent a promising target in future therapeutic approach for cartilage disorders.

2) 3D-bioprinting of de-differentiated human articular chondrocytes allowed them to regain chondrogenic phenotype and the embedding in PRP-supplemented bioink supported chondrogenic culture as well as cell growth inside the 3D-printed constructs. In view of future clinic translation, the choice of cell source for 3D-bioprinting of patient-specific grafts will have to be oriented towards high performing cell types, such as chondro-progenitors, in order to ensure a successful cartilage regeneration and repair. Nevertheless, the bioactive property combined with a proper printability of the PRP-based hydrogel analysed in this preliminary study, make it a promising bioink to be exploited for articular cartilage tissue engineering and other biomedical applications.

5 References

1. Horvai, A. Anatomy and Histology of Cartilage. *In Cartilage Imaging*; Springer New York, **2011**; pp. 1–10.

2. Correa, D.; Lietman, S.A. Articular cartilage repair: Current needs, methods and research directions. *Semin. Cell Dev. Biol.* **2017**, *62*, 67–77.

3. Roughley, P.J.; Lee, E.R. Cartilage proteoglycans: structure and potential functions. *Microsc. Res. Tech.* **1994**, *28*, 385–397.

4. Roughley, P.J. The structure and function of cartilage proteoglycans. *Eur. Cells Mater.* **2006**, *12*, 92–101.

5. Grogan, S.P.; Miyaki, S.; Asahara, H.; D'Lima, D.D.; Lotz, M.K. Mesenchymal progenitor cell markers in human articular cartilage: Normal distribution and changes in osteoarthritis. *Arthritis Res. Ther.* **2009**, *11*, R85.

6. DeLise, A.M.; Fischer, L.; Tuan, R.S. Cellular interactions and signaling in cartilage development. *Osteoarthr. Cartil.* **2000**, *8*, 309–334.

7. Dowthwaite, G.P.; Bishop, J.C.; Redman, S.N.; Khan, I.M.; Rooney, P.; Evans, D.J.R.; Haughton, L.; Bayram, Z.; Boyer, S.; Thomson, B.; Wolfe, M.S.; Archer, C.W. The surface of articular cartilage contains a progenitor cell populations. *J. Cell Sci.* **2004**, *117*, 889–897.

8. Williams, R.; Khan, I.M.; Richardson, K.; Nelson, L.; McCarthy, H.E.; Analbelsi, T.; Singhrao, S.K.; Dowthwaite, G.P.; Jones, R.E.; Baird, D.M.; Lewis, H.; Roberts, S.; Shaw, H.M.; Dudhia, J.; Fairclough, J.; Briggs, T.; Archer, C.W. Identification and clonal characterisation of a progenitor cell sub-population in normal human articular cartilage. *PLoS One* **2010**, *5*, e13246.

9. Poole, C.A. Articular cartilage chondrons: form, function and failure. *J. Anat.* **1997**, *191*, 1–13.

10. Martel-Pelletier, J.; Boileau, C.; Pelletier, J.-P.; Roughley, P.J. Cartilage in normal and osteoarthritis conditions. *Best Pract. Res. Clin. Rheumatol.* **2008**, *22*, 351–384.

11. Venn, M.F. Chemical composition of human femoral head cartilage: Influence of topographical position and fibrillation. *Ann. Rheum. Dis.* **1979**, *38*, 57–62.

12. Watanabe, H.; Yamada, Y.; Kimata, K. Roles of aggrecan, a large chondroitin sulfate proteoglycan, in cartilage structure and function. *J. Biochem.* **1998**, *124*, 687–693.

13. Armiento, A.R.; Alini, M.; Stoddart, M.J. Articular fibrocartilage - Why does hyaline cartilage fail to repair? *Adv. Drug Deliv. Rev.* **2019**,*146*, 289–305.

14. Roughley, P.J. Articular cartilage and changes in arthritis noncollagenous proteins and proteoglycans in the extracellular matrix of cartilage. *Arthritis Res.* **2001**, *3*, 342–347.

15. Schulz, R.M.; Bader, A. Cartilage tissue engineering and bioreactor systems for the cultivation and stimulation of chondrocytes. *Eur. Biophys.* J. **2007**, *36*, 539–568.

16. Eyre, D.R.; Weis, M.A.; Wu, J.-J. Articular cartilage collagen: an irreplaceable framework? *Eur. Cell. Mater.* **2006**, *12*, 57–63.

17. Luo, Y.; Sinkeviciute, D.; He, Y.; Karsdal, M.; Henrotin, Y.; Mobasheri, A.; Önnerfjord, P.; Bay-Jensen, A. The minor collagens in articular cartilage. *Protein Cell* **2017**, *8*, 560–572.

18. Johnstone, B.; Hering, T.M.; Caplan, A.I.; Goldberg, V.M.; Yoo, J.U. In vitro chondrogenesis of bone marrow-derived mesenchymal progenitor cells. *Exp. Cell Res.* **1998**, *238*, 265–272.

19. Bi, W.; Deng, J.M.; Zhang, Z.; Behringer, R.R.; de Crombrugghe, B. Sox9 is required for cartilage formation. *Nat. Genet.* **1999**, *22*, 85–89.

20. Aydelotte, M.B.; Kuettner, K.E. Differences between sub-populations of cultured bovine articular chondrocytes. I. Morphology and cartilage matrix production. *Connect. Tissue Res.* **1988**, *18*, 205–222.

21. Archer, C.W.; McDowell, J.; Bayliss, M.T.; Stephens, M.D.; Bentley, G. Phenotypic modulation in sub-populations of human articular chondrocytes in vitro. *J. Cell Sci.* **1990**, *97 (Pt 2)*, 361–371.

22. Darling, E.M.; Zauscher, S.; Guilak, F. Viscoelastic properties of zonal articular chondrocytes measured by atomic force microscopy. *Osteoarthr. Cartil.* **2006**, *14*, 571–579.

23. Choi, J.B.; Youn, I.; Cao, L.; Leddy, H.A.; Gilchrist, C.L.; Setton, L.A.; Guilak, F. Zonal changes in the three-dimensional morphology of the chondron under compression: the relationship among

cellular, pericellular, and extracellular deformation in articular cartilage. *J. Biomech.* **2007**, *40*, 2596–2603.
24. Darling, E.M.; Athanasiou, K.A. Rapid phenotypic changes in passaged articular chondrocyte subpopulations. *J. Orthop. Res.* **2005**, *23*, 425–432.
25. Mow, V.C.; Bachrach, N.M.; Setton, L.A.; Guilak, F. Stress, Strain, Pressure and Flow Fields in Articular Cartilage and Chondrocytes. *In Cell Mechanics and Cellular Engineering*; Springer New York, **1994**; pp. 345–379.
26. Sanchez-Adams, J.; Leddy, H.A.; McNulty, A.L.; O'Conor, C.J.; Guilak, F. The Mechanobiology of Articular Cartilage: Bearing the Burden of Osteoarthritis. *Curr. Rheumatol. Rep.* **2014**, *16*, 1–9.
27. Rengel, Y.; Ospelt, C.; Gay, S. Proteinases in the joint: clinical relevance of proteinases in joint destruction. *Arthritis Res. Ther.* **2007**, *9*, 221.
28. Sophia Fox, A.J.; Bedi, A.; Rodeo, S.A. The basic science of articular cartilage: Structure, composition, and function. *Sports Health* **2009**, *1*, 461–468.
29. Weissman, I.L.; Anderson, D.J.; Gage, F. Stem and Progenitor Cells: Origins, Phenotypes, Lineage Commitments, and Transdifferentiations. *Annu. Rev. Cell Dev. Biol.* **2001**, *17*, 387–403.
30. Reubinoff, B.E.; Pera, M.F.; Fong, C.Y.; Trounson, A.; Bongso, A. Embryonic stem cell lines from human blastocysts: somatic differentiation in vitro. *Nat. Biotechnol.* **2000**, *18*, 399–404.
31. Morrison, S.J.; Shah, N.M.; Anderson, D.J. Regulatory mechanisms in stem cell biology. *Cell* **1997**, *88*, 287–298.
32. Wu, L.; Bluguermann, C.; Kyupelyan, L.; Latour, B.; Gonzalez, S.; Shah, S.; Galic, Z.; Ge, S.; Zhu, Y.; Petrigliano, F.A.; Nsair, A.; Miriuka, S.G.; Li, X.; Lyons, K.M.; Crooks, G.M.; McAllister, D.R.; Van Handel, B.; Adams, J.S.; Evseenko, D. Human developmental chondrogenesis as a basis for engineering chondrocytes from pluripotent stem cells. *Stem cell reports* **2013**, *1*, 575–589.
33. Seol, D.; McCabe, D.J.; Choe, H.; Zheng, H.; Yu, Y.; Jang, K.; Walter, M.W.; Lehman, A.D.; Ding, L.; Buckwalter, J.A.; Martin, J.A. Chondrogenic progenitor cells respond to cartilage injury. *Arthritis Rheum.* **2012**, *64*, 3626–3637.
34. Jiang, Y.; Tuan, R.S. Origin and function of cartilage stem/progenitor cells in osteoarthritis. *Nat. Rev. Rheumatol.* **2015**, *11*, 206–212.
35. Feng, G.; Yang, X.; Shang, H.; Marks, I.W.; Shen, F.H.; Katz, A.; Arlet, V.; Laurencin, C.T.; Li, X. Multipotential differentiation of human anulus fibrosus cells: an in vitro study. *J. Bone Joint Surg. Am.* **2010**, *92*, 675–685.
36. Kobayashi, S.; Takebe, T.; Zheng, Y.W.; Mizuno, M.; Yabuki, Y.; Maegawa, J.; Taniguchi, H. Presence of cartilage stem/progenitor cells in adult mice auricular perichondrium. *PLoS One* **2011**, *6*, e26393.
37. Elsaesser, A.F.; Schwarz, S.; Joos, H.; Koerber, L.; Brenner, R.E.; Rotter, N. Characterization of a migrative subpopulation of adult human nasoseptal chondrocytes with progenitor cell features and their potential for in vivo cartilage regeneration strategies. *Cell Biosci.* **2016**, *6*.
38. Yoon, M.H.; Kim, J.H.; Oak, C.H.; Jang, T.W.; Jung, M.H.; Chun, B.K.; Lee, S.J.; Heo, J.H. Tracheal cartilage regeneration by progenitor cells derived from the perichondrium. *Tissue Eng. Regen. Med.* **2013**, *10*, 286–292.
39. Srour, M.K.; Fogel, J.L.; Yamaguchi, K.T.; Montgomery, A.P.; Izuhara, A.K.; Misakian, A.L.; Lam, S.; Lakeland, D.L.; Urata, M.M.; Lee, J.S.; Mariani, F.V. Natural large-scale regeneration of rib cartilage in a mouse model. *J. Bone Miner. Res.* **2015**, *30*, 297–308.
40. Hunziker, E.B.; Kapfinger, E.; Geiss, J. The structural architecture of adult mammalian articular cartilage evolves by a synchronized process of tissue resorption and neoformation during postnatal development. *Osteoarthr. Cartil.* **2007**, *15*, 403–413.
41. Grogan, S.P.; Miyaki, S.; Asahara, H.; D'Lima, D.D.; Lotz, M.K. Mesenchymal progenitor cell markers in human articular cartilage: Normal distribution and changes in osteoarthritis. *Arthritis Res. Ther.* **2009**, *11*, 1–13.
42. Hattori, S.; Oxford, C.; Reddi, A.H. Identification of superficial zone articular chondrocyte stem/progenitor cells. *Biochem. Biophys. Res. Commun.* **2007**, *358*, 99–103.
43. Ozbey, O.; Sahin, Z.; Acar, N.; Ozcelik, F.T.; Ozenci, A.M.; Koksoy, S.; Ustunel, I. Characterization of colony-forming cells in adult human articular cartilage. *Acta Histochem.* **2014**, 116, 763–770.

44. Yu, Y.; Zheng, H.; Buckwalter, J.A.; Martin, J.A. Single cell sorting identifies progenitor cell population from full thickness bovine articular cartilage. *Osteoarthr. Cartil.* **2014**, *22*, 1318–1326.
45. De Bari, C.; Dell'Accio, F.; Tylzanowski, P.; Luyten, F.P. Multipotent mesenchymal stem cells from adult human synovial membrane. *Arthritis Rheum.* **2001**, *44*, 1928–1942.
46. Alsalameh, S.; Amin, R.; Gemba, T.; Lotz, M. Identification of Mesenchymal Progenitor Cells in Normal and Osteoarthritic Human Articular Cartilage. *Arthritis Rheum.* **2004**, *50*, 1522–1532.
47. Fickert, S.; Fiedler, J.; Brenner, R. E. Identification of subpopulations with characteristics of mesenchymal progenitor cells from human osteoarthritic cartilage using triple staining for cell surface markers. *Arthritis. Res. Ther.* **2004**, *6*, R422.
48. Joos, H.; Wildner, A.; Hogrefe, C.; Reichel, H.; Brenner, R.E. Interleukin-1 beta and tumor necrosis factor alpha inhibit migration activity of chondrogenic progenitor cells from non-fibrillated osteoarthritic cartilage. *Arthritis Res. Ther.* **2013**, *15*, R119.
49. Koelling, S.; Kruegel, J.; Irmer, M.; Path, J.R.; Sadowski, B.; Miro, X.; Miosge, N. Migratory Chondrogenic Progenitor Cells from Repair Tissue during the Later Stages of Human Osteoarthritis. *Cell Stem Cell* **2009**, *4*, 324–335.
50. Barbero, A.; Ploegert, S.; Heberer, M.; Martin, I. Plasticity of clonal populations of dedifferentiated adult human articular chondrocytes. *Arthritis Rheum.* **2003**, *48*, 1315–1325.
51. Hiraoka, K.; Grogan, S.; Olee, T.; Lotz, M. Mesenchymal progenitor cells in adult human articular cartilage. *Biorheology* **2006**, *43*, 447–454.
52. Jiang, Y.Z.; Tong, T.; Heng, B.C.; Ouyang, H.W. Cartilage injuries: Role of implantation of human stem/progenitor cells. *In Stem Cells and Cancer Stem Cells, Volume 3*; Springer Netherlands, **2012**; pp. 327–333.
53. Diaz-Romero, J.; Gaillard, J.P.; Grogan, S.P.; Nesic, D.; Trub, T.; Mainil-Varlet, P. Immunophenotypic analysis of human articular chondrocytes: Changes in surface markers associated with cell expansion in monolayer culture. *J. Cell. Physiol.* **2005**, *202*, 731–742.
54. Lee, H.J.; Choi, B.H.; Min, B.-H.; Park, S.R. Changes in surface markers of human mesenchymal stem cells during the chondrogenic differentiation and dedifferentiation processes in vitro. *Arthritis Rheum.* **2009**, *60*, 2325–2332.
55. Otsuki, S.; Grogan, S.P.; Miyaki, S.; Kinoshita, M.; Asahara, H.; Lotz, M.K. Tissue neogenesis and STRO-1 expression in immature and mature articular cartilage. *J. Orthop. Res.* **2010**, *28*, 96–102.
56. Khan, I.M.; Bishop, J.C.; Gilbert, S.; Archer, C.W. Clonal chondroprogenitors maintain telomerase activity and Sox9 expression during extended monolayer culture and retain chondrogenic potential. *Osteoarthr. Cartil.* **2009**, *17*, 518–528.
57. Hamada, T.; Sakai, T.; Hiraiwa, H.; Nakashima, M.; Ono, Y.; Mitsuyama, H.; Ishiguro, N. Surface markers and gene expression to characterize the differentiation of monolayer expanded human articular chondrocytes. *Nagoya J. Med. Sci.* **2013**, *75*, 101–111.
58. Pizzute, T.; Lynch, K.; Pei, M. Impact of Tissue-Specific Stem Cells on Lineage-Specific Differentiation: A Focus on the Musculoskeletal System. *Stem Cell Rev. Reports* **2015**, *11*, 119–132.
59. Hunter, W. Of the structure and diseases of articulating cartilages. *Philos. Trans. R. Soc. London* **1743**, *42*, 514–521.
60. Radin, E.L.; Ehrlich, M.G.; Chernack, R.; Abernethy, P.; Paul, I.L.; Rose, R.M. Effect of repetitive impulsive loading on the knee joints of rabbits. *Clin. Orthop. Relat. Res.* **1978**, *131*, 288–293.
61. Mankin, H.J.; Mow, V.C.; Buckwalter, J.A.; Iannotti, J.P.; Ratcliffe, A. Form and function of articular cartilage. *In Orthopaedic basic science*; Simon SR editor; American Academy of Orthopaedic Surgeons: Rosemont, IL, **1994**; pp. 1–44.
62. Buckwalter, J. A.; Mow, V. C.; Ratcliffe, A. Restoration of Injured or Degenerated Articular Cartilage. *J. Am. Acad. Orthop. Surg*. **1994**, *2*, 192–201.
63. Furukawa, T.; Eyre, D.R.; Koide, S.; Glimcher, M.J. Biochemical studies on repair cartilage resurfacing experimental defects in the rabbit knee. *J. Bone Joint Surg. Am.* **1980**, *62*, 79–89.
64. Woolf, A.D. Global burden of osteoarthritis and musculoskeletal diseases. *BMC Musculoskelet. Disord.* **2015**, *16*.
65. Lories, R.J.; Luyten, F.P. The bone-cartilage unit in osteoarthritis. *Nat. Rev. Rheumatol.* **2011**, *7*, 43–49.

66. Brandt, K.D.; Myers, S.L.; Burr, D.; Albrecht, M. Osteoarthritic changes in canine articular cartilage, subchondral bone, and synovium fifty-four months after transection of the anterior cruciate ligament. *Arthritis Rheum.* **1991**, *34*, 1560–1570.
67. Goldring, M.B. Articular Cartilage Degradation in Osteoarthritis. *HSS J.* **2012**, *8*, 7–9.
68. Oettmeier, R.; Abendroth, K. Osteoarthritis and bone: osteologic types of osteoarthritis of the hip. *Skeletal Radiol.* **1989**, *18*, 165–174.
69. Yuan, X.L.; Meng, H.Y.; Wang, Y.C.; Peng, J.; Guo, Q.Y.; Wang, A.Y.; Lu, S.B. Bone-cartilage interface crosstalk in osteoarthritis: Potential pathways and future therapeutic strategies. *Osteoarthr. Cartil.* **2014**, *22*, 1077–1089.
70. Kapoor, M.; Martel-Pelletier, J.; Lajeunesse, D.; Pelletier, J.P.; Fahmi, H. Role of proinflammatory cytokines in the pathophysiology of osteoarthritis. *Nat. Rev. Rheumatol.* **2011**, *7*, 33–42.
71. Martel-Pelletier, J.; Welsch, D.J.; Pelletier, J.P. Metalloproteases and inhibitors in arthritic diseases. *Best Pract. Res. Clin. Rheumatol.* **2001**, *15*, 805–829.
72. McCulloch, K.; Litherland, G.J.; Rai, T.S. Cellular senescence in osteoarthritis pathology. *Aging Cell* **2017**, *16*, 210–218.
73. Pierce, G.F.; Tarpley, J.E.; Tseng, J.; Bready, J.; Chang, D.; Kenney, W.C.; Rudolph, R.; Robson, M.C.; Vande Berg, J.; Reid, P. Detection of platelet-derived growth factor (PDGF)-AA in actively healing human wounds treated with recombinant PDGF-BB and absence of PDGF in chronic nonhealing wounds. *J. Clin. Invest.* **1995**, *96*, 1336–1350.
74. Zhang, D.; Johnson, L.J.; Hsu, H.-P.; Spector, M. Cartilaginous deposits in subchondral bone in regions of exposed bone in osteoarthritis of the human knee: histomorphometric study of PRG4 distribution in osteoarthritic cartilage. *J. Orthop. Res.* **2007**, *25*, 873–883.
75. Lotz, M.K.; Otsuki, S.; Grogan, S.P.; Sah, R.; Terkeltaub, R.; D'Lima, D. Cartilage cell clusters. *Arthritis Rheum.* **2010**, *62*, 2206–2218.
76. Jayasuriya, C.T.; Chen, Q. Potential benefits and limitations of utilizing chondroprogenitors in cell-based cartilage therapy. *Connect. Tissue Res.* **2015**, *56*, 265–271.
77. Jayasuriya, C.T.; Hu, N.; Li, J.; Lemme, N.; Terek, R.; Ehrlich, M.G.; Chen, Q. Molecular characterization of mesenchymal stem cells in human osteoarthritis cartilage reveals contribution to the OA phenotype. *Sci. Rep.* **2018**, *8*, 1–14.
78. Tong, W.; Geng, Y.; Huang, Y.; Shi, Y.; Xiang, S.; Zhang, N.; Qin, L.; Shi, Q.; Chen, Q.; Dai, K.; Zhang, X. In Vivo Identification and Induction of Articular Cartilage Stem Cells by Inhibiting NF-κB Signaling in Osteoarthritis. *Stem Cells* **2015**, *33*, 3125–3137.
79. Muhammad, H.; Schminke, B.; Bode, C.; Roth, M.; Albert, J.; Von Der Heyde, S.; Rosen, V.; Miosge, N. Human migratory meniscus progenitor cells are controlled via the TGF-β pathway. *Stem Cell Rep.* **2014**, *3*, 789–803.
80. Fellows, C.R.; Williams, R.; Davies, I.R.; Gohil, K.; Baird, D.M.; Fairclough, J.; Rooney, P.; Archer, C.W.; Khan, I.M. Characterisation of a divergent progenitor cell sub-populations in human osteoarthritic cartilage: The role of telomere erosion and replicative senescence. *Sci. Rep.* **2017**, *7*, 41421.
81. Medvedeva, E. V; Grebenik, E.A.; Gornostaeva, S.N.; Telpuhov, V.I.; Lychagin, A. V; Timashev, P.S.; Chagin, A.S. Repair of Damaged Articular Cartilage: Current Approaches and Future Directions. *Int. J. Mol. Sci.* **2018**, *19*, 2366.
82. McAlindon, T.E.; Bannuru, R.R.; Sullivan, M.C.; Arden, N.K.; Berenbaum, F.; Bierma-Zeinstra, S.M.; Hawker, G.A.; Henrotin, Y.; Hunter, D.J.; Kawaguchi, H.; Kwoh, K.; Lohmander, S.; Rannou, F.; Roos, E.M.; Underwood, M. OARSI recommendations for the management of hip and knee osteoarthritis, Part II: OARSI evidence-based, expert consensus guidelines. *Osteoarthr. Cartil.* **2014**, *22*, 363–388.
83. Wernecke, C.; Braun, H.J.; Dragoo, J.L. The effect of intra-articular corticosteroids on articular cartilage: A systematic review. *Orthop. J. Sport. Med.* **2015**, *3*, 1–7.
84. Estades-Rubio, F.J.; Reyes-Martín, A.; Morales-Marcos, V.; García-Piriz, M.; García-Vera, J.J.; Perán, M.; Marchal, J.A.; Montañez-Heredia, E. Knee Viscosupplementation: Cost-Effectiveness Analysis between Stabilized Hyaluronic Acid in a Single Injection versus Five Injections of Standard Hyaluronic Acid. *Int. J. Mol. Sci.* **2017**, *18*, 658.

85. Fraser, J.R.E.; Laurent, T.C.; Laurent, U.B.G. Hyaluronan: Its nature, distribution, functions and turnover. *In Proceedings of the Journal of Internal Medicine*; Blackwell Publishing Ltd, **1997**; Vol. 242, pp. 27–33.
86. Rutjes, A.W.S.; Jüni, P.; da Costa, B.R.; Trelle, S.; Nüesch, E.; Reichenbach, S. Viscosupplementation for osteoarthritis of the knee: a systematic review and meta-analysis. *Ann. Intern. Med.* **2012**, *157*, 180–191.
87. Sakata, R.; Reddi, A.H. Platelet-Rich Plasma Modulates Actions on Articular Cartilage Lubrication and Regeneration. *Tissue Eng. Part B. Rev.* **2016**, *22*, 408–419.
88. Shahid, M.; Kundra, R. Platelet-rich plasma (PRP) for knee disorders. *EFORT Open Rev.* **2017**, *2*, 28–34.
89. Montañez-Heredia, E.; Irízar, S.; Huertas, P.J.; Otero, E.; Del Valle, M.; Prat, I.; Díaz-Gallardo, M.S.; Perán, M.; Marchal, J.A.; Hernandez-Lamas, M.D.C. Intra-articular injections of platelet-rich plasma versus hyaluronic acid in the treatment of osteoarthritic knee pain: A randomized clinical trial in the context of the Spanish national health care system. *Int. J. Mol. Sci.* **2016**, *17*, 1064.
90. Steadman, J.R.; Rodkey, W.G.; Rodrigo, J.J. Microfracture: surgical technique and rehabilitation to treat chondral defects. *Clin. Orthop. Relat. Res.* **2001**, S362–S369.
91. Mithoefer, K.; McAdams, T.; Williams, R.J.; Kreuz, P.C.; Mandelbaum, B.R. Clinical efficacy of the microfracture technique for articular cartilage repair in the knee: an evidence-based systematic analysis. *Am. J. Sports Med.* **2009**, *37*, 2053–2063.
92. Hangody, L.; Kish, G.; Kárpáti, Z.; Udvarhelyi, I.; Szigeti, I.; Bély, M. Mosaicplasty for the Treatment of Articular Cartilage Defects: Application in Clinical Practice. *Orthopedics* **1998**, *21*, 751–756.
93. Hangody, L.; Füles, P. Autologous osteochondral mosaicplasty for the treatment of full-thickness defects of weight-bearing joints: ten years of experimental and clinical experience. *J. Bone Joint Surg. Am.* **2003**, *85-A Suppl 2*, 25–32.
94. Brittberg, M.; Lindahl, A.; Nilsson, A.; Ohlsson, C.; Isaksson, O.; Peterson, L. Treatment of deep cartilage defects in the knee with autologous chondrocyte transplantation. *N. Engl. J. Med.* **1994**, *331*, 889–895.
95. Goyal, D.; Goyal, A.; Keyhani, S.; Lee, E.H.; Hui, J.H.P. Evidence-based status of second- and third-generation autologous chondrocyte implantation over first generation: a systematic review of level I and II studies. *Arthroscopy* **2013**, *29*, 1872–1878.
96. Brittberg, M.; Recker, D.; Ilgenfritz, J.; Saris, D.B.F.; SUMMIT Extension Study Group Matrix-Applied Characterized Autologous Cultured Chondrocytes Versus Microfracture: Five-Year Follow-up of a Prospective Randomized Trial. *Am. J. Sports Med.* **2018**, *46*, 1343–1351.
97. Mistry, H.; Connock, M.; Pink, J.; Shyangdan, D.; Clar, C.; Royle, P.; Court, R.; Biant, L.C.; Metcalfe, A.; Waugh, N. Autologous chondrocyte implantation in the knee: systematic review and economic evaluation. *Health Technol. Assess.* **2017**, *21*, 1–294.
98. Harris, J.D.; Siston, R.A.; Brophy, R.H.; Lattermann, C.; Carey, J.L.; Flanigan, D.C. Failures, re-operations, and complications after autologous chondrocyte implantation - a systematic review. *Osteoarthr. Cartil.* **2011**, *19*, 779–791.
99. Jacobi, M.; Villa, V.; Magnussen, R.A.; Neyret, P. MACI - a new era? *Sports Med. Arthrosc. Rehabil. Ther. Technol.* **2011**, *3*, 10.
100. Huang, B.J.; Hu, J.C.; Athanasiou, K.A. Cell-based tissue engineering strategies used in the clinical repair of articular cartilage. *Biomaterials* **2016**, *98*, 1–22.
101. Mao, Y.; Hoffman, T.; Wu, A.; Kohn, J. An Innovative Laboratory Procedure to Expand Chondrocytes with Reduced Dedifferentiation. *Cartilage* **2018**, *9*, 202–211.
102. Caron, M.M.J.; Emans, P.J.; Coolsen, M.M.E.; Voss, L.; Surtel, D.A.M.; Cremers, A.; van Rhijn, L.W.; Welting, T.J.M. Redifferentiation of dedifferentiated human articular chondrocytes: comparison of 2D and 3D cultures. *Osteoarthr. Cartil.* **2012**, *20*, 1170–1178.
103. Yaeger, P.C.; Masi, T.L.; de Ortiz, J.L.; Binette, F.; Tubo, R.; McPherson, J.M. Synergistic action of transforming growth factor-beta and insulin-like growth factor-I induces expression of type II collagen and aggrecan genes in adult human articular chondrocytes. *Exp. Cell Res.* **1997**, *237*, 318–325.
104. Bianco, P.; Robey, P.G. Marrow stromal stem cells. *J. Clin. Invest.* **2000**, *105*, 1663–1668.
105. Murphy, J.M.; Fink, D.J.; Hunziker, E.B.; Barry, F.P. Stem cell therapy in a caprine model of osteoarthritis. *Arthritis Rheum.* **2003**, *48*, 3464–3474.

106. Wakitani, S.; Imoto, K.; Yamamoto, T.; Saito, M.; Murata, N.; Yoneda, M. Human autologous culture expanded bone marrow mesenchymal cell transplantation for repair of cartilage defects in osteoarthritic knees. *Osteoarthr. Cartil.* **2002**, *10*, 199–206.
107. Richter, W. Cell-based cartilage repair: illusion or solution for osteoarthritis. *Curr. Opin. Rheumatol.* **2007**, *19*, 451–456.
108. Lee, S.Y.; Nakagawa, T.; Reddi, A.H. Mesenchymal progenitor cells derived from synovium and infrapatellar fat pad as a source for superficial zone cartilage tissue engineering: analysis of superficial zone protein/lubricin expression. *Tissue Eng. Part A* **2010**, *16*, 317–325.
109. Siclari, A.; Mascaro, G.; Gentili, C.; Cancedda, R.; Boux, E. A cell-free scaffold-based cartilage repair provides improved function hyaline-like repair at one year. *Clin. Orthop. Relat. Res.* **2012**, *470*, 910–919.
110. Kreuz, P.C.; Gentili, C.; Samans, B.; Martinelli, D.; Krüger, J.P.; Mittelmeier, W.; Endres, M.; Cancedda, R.; Kaps, C. Scaffold-assisted cartilage tissue engineering using infant chondrocytes from human hip cartilage. *Osteoarthr. Cartil.* **2013**, *21*, 1997–2005.
111. Bistolfi, A.; Ferracini, R.; Galletta, C.; Tosto, F.; Sgarminato, V.; Digo, E.; Vernè, E.; Massè, A. Regeneration of articular cartilage: Scaffold used in orthopedic surgery. A short handbook of available products for regenerative joints surgery. *Clin. Sci. Res. Reports* **2017**, *1*, 1–7.
112. Visser, J.; Peters, B.; Burger, T.J.; Boomstra, J.; Dhert, W.J.A.; Melchels, F.P.W.; Malda, J. Biofabrication of multi-material anatomically shaped tissue constructs. *Biofabrication* **2013**, *5*, 035007.
113. Kesti, M.; Eberhardt, C.; Pagliccia, G.; Kenkel, D.; Grande, D.; Boss, A.; Zenobi-Wong, M. Bioprinting Complex Cartilaginous Structures with Clinically Compliant Biomaterials. *Adv. Funct. Mater.* **2015**, *25*, 7406–7417.
114. Burdick, J.A.; Prestwich, G.D. Hyaluronic acid hydrogels for biomedical applications. *Adv. Mater.* **2011**, *23*, H41–H56.
115. Li, C.; Chik, T.-K.; Ngan, A.H.W.; Chan, S.C.H.; Shum, D.K.Y.; Chan, B.P. Correlation between compositional and mechanical properties of human mesenchymal stem cell-collagen microspheres during chondrogenic differentiation. *Tissue Eng. Part A* **2011**, *17*, 777–788.
116. Gawaz, M.; Vogel, S. Platelets in tissue repair: Control of apoptosis and interactions with regenerative cells. *Blood* **2013**, *122*, 2550–2554.
117. Marx, R.E. Platelet-rich plasma (PRP): what is PRP and what is not PRP? *Implant Dent.* **2001**, *10*, 225–228.
118. Boswell, S.G.; Cole, B.J.; Sundman, E.A.; Karas, V.; Fortier, L.A. Platelet-rich plasma: A milieu of bioactive factors. *Arthrosc. - J. Arthrosc. Relat. Surg.* **2012**, *28*, 429–439.
119. Pietrzak, W.S.; Eppley, B.L. Platelet rich plasma: Biology and new technology. *J. Craniofac. Surg.* **2005**, *16*, 1043–1054.
120. Weiser, L.; Bhargava, M.; Attia, E.; Torzilli, P.A. Effect of serum and platelet-derived growth factor on chondrocytes grown in collagen gels. *Tissue Eng.* **1999**, *5*, 533–544.
121. Fortier, L.A.; Hackett, C.H.; Cole, B.J. The Effects of Platelet-Rich Plasma on Cartilage: Basic Science and Clinical Application. *Oper. Tech. Sports Med.* **2011**, *19*, 154–159.
122. Wang, W.; Rigueur, D.; Lyons, K.M. TGFβ signaling in cartilage development and maintenance. *Birth Defects Res. Part C - Embryo Today Rev.* **2014**, 102, 37–51.
123. Grimaud, E.; Heymann, D.; Rédini, F. Recent advances in TGF-β effects on chondrocyte metabolism potential therapeutic roles of TGF-β in cartilage disorders. *Cytokine Growth Factor Rev.* **2002**, *13*, 241–257.
124. Sundman, E.A.; Cole, B.J.; Karas, V.; Della Valle, C.; Tetreault, M.W.; Mohammed, H.O.; Fortier, L.A. The anti-inflammatory and matrix restorative mechanisms of platelet-rich plasma in osteoarthritis. *Am. J. Sports Med.* **2014**, *42*, 35–41.
125. Bendinelli, P.; Matteucci, E.; Dogliotti, G.; Corsi, M.M.; Banfi, G.; Maroni, P.; Desiderio, M.A. Molecular basis of anti-inflammatory action of platelet-rich plasma on human chondrocytes: mechanisms of NF-κB inhibition via HGF. *J. Cell. Physiol.* **2010**, *225*, 757–766.
126. Backly, R. El; Ulivi, V.; Tonachini, L.; Cancedda, R.; Descalzi, F.; Mastrogiacomo, M. Platelet lysate induces in vitro wound healing of human keratinocytes associated with a strong proinflammatory response. *Tissue Eng. - Part A* **2011**, *17*, 1787–1800.

127. Ruggiu, A.; Ulivi, V.; Sanguineti, F.; Cancedda, R.; Descalzi, F. The effect of Platelet Lysate on osteoblast proliferation associated witha transient increase of the inflammatory response in bone regeneration. *Biomaterials* **2013**, *34*, 9318–9330.
128. Pereira, R.C.; Scaranari, M.; Benelli, R.; Strada, P.; Reis, R.L.; Cancedda, R.; Gentili, C. Dual effect of platelet lysate on human articular cartilage: A maintenance of chondrogenic potential and a transient proinflammatory activity followed by an inflammation resolution. *Tissue Eng. - Part A* **2013**, *19*, 1476–1488.
129. Romaldini, A.; Ulivi, V.; Nardini, M.; Mastrogiacomo, M.; Cancedda, R.; Descalzi F. Platelet Lysate Inhibits NF-κB Activation and Induces Proliferation and an Alert State in Quiescent Human Umbilical Vein Endothelial Cells Retaining Their Differentiation Capability. *Cells* **2019**, *8*, 331.
130. Dai, W.-L.; Zhou, A.-G.; Zhang, H.; Zhang, J. Efficacy of Platelet-Rich Plasma in the Treatment of Knee Osteoarthritis: A Meta-analysis of Randomized Controlled Trials. *Arthroscopy* **2017**, *33*, 659–670.
131. Shen, L.; Yuan, T.; Chen, S.; Xie, X.; Zhang, C. The temporal effect of platelet-rich plasma on pain and physical function in the treatment of knee osteoarthritis: Systematic review and meta-analysis of randomized controlled trials. *J. Orthop. Surg. Res.* **2017**, *12*, 16.
132. Muraglia, A.; Ottonello, C.; Spanò, R.; Dozin, B.; Strada, P.; Grandizio, M.; Cancedda, R.; Mastrogiacomo, M. Biological activity of a standardized freeze-dried platelet derivative to be used as cell culture medium supplement. *Platelets* **2014**, *25*, 211–220.
133. Muraglia, A.; Todeschi, M.R.; Papait, A.; Poggi, A.; Spanò, R.; Strada, P.; Cancedda, R.; Mastrogiacomo, M. Combined platelet and plasma derivatives enhance proliferation of stem/progenitor cells maintaining their differentiation potential. *Cytotherapy* **2015**, *17*, 1793–1806.
134. Muraglia, A.; Nguyen, V.T.; Nardini, M.; Mogni, M.; Coviello, D.; Dozin, B.; Strada, P.; Baldelli, I.; Formica, M.; Cancedda, R.; Mastrogiacomo, M. Culture medium supplements derived from human platelet and plasma: Cell commitment and proliferation support. *Front. Bioeng. Biotechnol.* **2017**, *5*, 66.
135. Van Nguyen, T.; Cancedda, R.; Descalzi, F. Platelet lysate activates quiescent cell proliferation and reprogramming in human articular cartilage: Involvement of hypoxia inducible factor 1. *J. Tissue Eng. Regen. Med.* **2018**, *12*, e1691–e1703.
136. Gaissmaier, C.; Fritz, J.; Krackhardt, T.; Flesch, I.; Aicher, W.K.; Ashammakhi, N. Effect of human platelet supernatant on proliferation and matrix synthesis of human articular chondrocytes in monolayer and three-dimensional alginate cultures. *Biomaterials* **2005**, *26*, 1953–1960.
137. Kaps, C.; Loch, A.; Haisch, A.; Smolian, H.; Burmester, G.R.; Häupl, T.; Sittinger, M. Human platelet supernatant promotes proliferation but not differentiation of articular chondrocytes. *Med. Biol. Eng. Comput.* **2002**, *40*, 485–490.
138. Hildner, F.; Eder, M.J.; Hofer, K.; Aberl, J.; Redl, H.; van Griensven, M.; Gabriel, C.; Peterbauer-Scherb, A. Human platelet lysate successfully promotes proliferation and subsequent chondrogenic differentiation of adipose-derived stem cells: A comparison with articular chondrocytes. *J. Tissue Eng. Regen. Med.* **2015**, *9*, 808–818.
139. Sykes, J.G.; Kuiper, J.H.; Richardson, J.B.; Roberts, S.; Wright, K.T.; Kuiper, N.J. Impact of human platelet lysate on the expansion and chondrogenic capacity of cultured human chondrocytes for cartilage cell therapy. *Eur. Cells Mater.* **2018**, *35*, 255–267.
140. Ozbolat, I.T. Bioprinting scale-up tissue and organ constructs for transplantation. *Trends Biotechnol.* **2015**, *33*, 395–400.
141. Klebe, R.J. Cytoscribing: A method for micropositioning cells and the construction of two- and three-dimensional synthetic tissues. *Exp. Cell Res.* **1988**, *179*, 362–373.
142. Mironov, V.; Reis, N.; Derby, B. Bioprinting: a beginning. *Tissue Eng.* **2006**, *12*, 631–634.
143. Vijayavenkataraman, S. A Perspective on Bioprinting Ethics. *Artif. Organs* **2016**, *40*, 1033–1038.
144. Ozbolat, I.T. Scaffold-Based or Scaffold-Free Bioprinting: Competing or Complementing Approaches? J. *Nanotechnol. Eng. Med.* **2015**, *6*, 024701.
145. Ozbolat, I.T.; Peng, W.; Ozbolat, V. Application areas of 3D bioprinting. *Drug Discov. Today* **2016**, *21*, 1257–1271.
146. Thoma, C.R.; Zimmermann, M.; Agarkova, I.; Kelm, J.M.; Krek, W. 3D cell culture systems modeling tumor growth determinants in cancer target discovery. *Adv. Drug Deliv. Rev.* **2014**, *69*, 29–41.

147. Ma, X.; Qu, X.; Zhu, W.; Li, Y.-S.; Yuan, S.; Zhang, H.; Liu, J.; Wang, P.; Lai, C.S.E.; Zanella, F.; Feng, G.S.; Sheikh, F.; Chien, S.; Chen, S. Deterministically patterned biomimetic human iPSC-derived hepatic model via rapid 3D bioprinting. *Proc. Natl. Acad. Sci. U. S. A.* **2016**, *113*, 2206–2211.
148. Murphy, S. V.; Atala, A. 3D bioprinting of tissues and organs. *Nat. Biotechnol.* **2014**, *32*, 773–785.
149. Donderwinkel, I.; Van Hest, J.C.M.; Cameron, N.R. Bio-inks for 3D bioprinting: Recent advances and future prospects. *Polym. Chem.* **2017**, *8*, 4451–4471.
150. Peng, W.; Unutmaz, D.; Ozbolat, I.T. Bioprinting towards Physiologically Relevant Tissue Models for Pharmaceutics. *Trends Biotechnol.* **2016**, *34*, 722–732.
151. Gudapati, H.; Dey, M.; Ozbolat, I. A comprehensive review on droplet-based bioprinting: Past, present and future. *Biomaterials* **2016**, *102*, 20–42.
152. Seol, Y.-J.; Kang, H.-W.; Lee, S.J.; Atala, A.; Yoo, J.J. Bioprinting technology and its applications. *Eur. J. Cardiothorac. Surg.* **2014**, *46*, 342–348.
153. Markstedt, K.; Mantas, A.; Tournier, I.; Martínez Ávila, H.; Hägg, D.; Gatenholm, P. 3D Bioprinting Human Chondrocytes with Nanocellulose-Alginate Bioink for Cartilage Tissue Engineering Applications. *Biomacromolecules* **2015**, *16*, 1489–1496.
154. Barron, J.A.; Ringeisen, B.R.; Kim, H.; Spargo, B.J.; Chrisey, D.B. Application of laser printing to mammalian cells. *In Proceedings of the Thin Solid Films*; **2004**; Vol. 453–454, pp. 383–387.
155. Mandrycky, C.; Wang, Z.; Kim, K.; Kim, D.H. 3D bioprinting for engineering complex tissues. *Biotechnol. Adv.* **2016**, *34*, 422–434.
156. Yue, Z.; Liu, X.; Coates, P.T.; Wallace, G.G. Advances in printing biomaterials and living cells: implications for islet cell transplantation. *Curr. Opin. Organ Transplant.* **2016**, *21*, 467–475.
157. Furth, M.E.; Atala, A.; Van Dyke, M.E. Smart biomaterials design for tissue engineering and regenerative medicine. *Biomaterials* **2007**, *28*, 5068–5073.
158. Hospodiuk, M.; Dey, M.; Sosnoski, D.; Ozbolat, I.T. The bioink: A comprehensive review on bioprintable materials. *Biotechnol. Adv.* **2017**, *35*, 217–239.
159. Lutolf, M.P. Biomaterials: Spotlight on hydrogels. *Nat. Mater.* **2009**, *8*, 451–453.
160. Zhu, J.; Marchant, R.E. Design properties of hydrogel tissue-engineering scaffolds. *Expert Rev. Med. Devices* **2011**, *8*, 607–626.
161. Nicodemus, G.D.; Bryant, S.J. Cell encapsulation in biodegradable hydrogels for tissue engineering applications. *Tissue Eng. Part B. Rev.* **2008**, *14*, 149–165.
162. Billiet, T.; Vandenhaute, M.; Schelfhout, J.; Van Vlierberghe, S.; Dubruel, P. A review of trends and limitations in hydrogel-rapid prototyping for tissue engineering. *Biomaterials* **2012**, *33*, 6020–6041.
163. Unagolla, J.M.; Jayasuriya, A.C. Hydrogel-based 3D bioprinting: A comprehensive review on cell-laden hydrogels, bioink formulations, and future perspectives. *Appl. Mater. Today* **2019**, 100479.
164. Malda, J.; Visser, J.; Melchels, F.P.; Jüngst, T.; Hennink, W.E.; Dhert, W.J. a; Groll, J.; Hutmacher, D.W. Engineering hydrogels for biofabrication. *Adv. Mater.* **2013**, *25*, 5011–5028.
165. Schuurman, W.; Levett, P.A.; Pot, M.W.; van Weeren, P.R.; Dhert, W.J.A.; Hutmacher, D.W.; Melchels, F.P.W.; Klein, T.J.; Malda, J. Gelatin-methacrylamide hydrogels as potential biomaterials for fabrication of tissue-engineered cartilage constructs. *Macromol. Biosci.* **2013**, *13*, 551–561.
166. Aguado, B.A.; Mulyasasmita, W.; Su, J.; Lampe, K.J.; Heilshorn, S.C. Improving viability of stem cells during syringe needle flow through the design of hydrogel cell carriers. *Tissue Eng. Part A* **2012**, *18*, 806–815.
167. Fedorovich, N.E.; Schuurman, W.; Wijnberg, H.M.; Prins, H.-J.; van Weeren, P.R.; Malda, J.; Alblas, J.; Dhert, W.J.A. Biofabrication of osteochondral tissue equivalents by printing topologically defined, cell-laden hydrogel scaffolds. *Tissue Eng. Part C. Methods* **2012**, *18*, 33–44.
168. Guvendiren, M.; Lu, H.D.; Burdick, J.A. Shear-thinning hydrogels for biomedical applications. *Soft Matter* **2012**, *8*, 260–272.
169. Rezende, R.A.; Bartolo, P.J.; Mendes, A.; Filho, R.M. Rheological behavior of alginate solutions for biomanufacturing. *J. Appl. Polym. Sci.* **2009**, *113*, 3866–3871.
170. Paxton, N.; Smolan, W.; Böck, T.; Melchels, F.; Groll, J.; Jungst, T. Proposal to assess printability of bioinks for extrusion-based bioprinting and evaluation of rheological properties governing bioprintability. *Biofabrication* **2017**, *9*, 044107.
171. Hunt, N.C.; Grover, L.M. Cell encapsulation using biopolymer gels for regenerative medicine. *Biotechnol. Lett.* **2010**, *32*, 733–742.

172. Tako, M.; Nakamura, S. Gelation mechanism of agarose. *Carbohydr. Res.* **1988**, *180*, 277–284.
173. Duarte Campos, D.F.; Blaeser, A.; Korsten, A.; Neuss, S.; Jäkel, J.; Vogt, M.; Fischer, H. The stiffness and structure of three-dimensional printed hydrogels direct the differentiation of mesenchymal stromal cells toward adipogenic and osteogenic lineages. *Tissue Eng. Part A* **2015**, *21*, 740–756.
174. Lee, W.; Lee, V.; Polio, S.; Keegan, P.; Lee, J.-H.; Fischer, K.; Park, J.-K.; Yoo, S.-S. On-demand three-dimensional freeform fabrication of multi-layered hydrogel scaffold with fluidic channels. *Biotechnol. Bioeng.* **2010**, *105*, 1178–1186.
175. Ozbolat, I.T.; Hospodiuk, M. Current advances and future perspectives in extrusion-based bioprinting. *Biomaterials* **2016**, *76*, 321–343.
176. Jungst, T.; Smolan, W.; Schacht, K.; Scheibel, T.; Groll, J. Strategies and Molecular Design Criteria for 3D Printable Hydrogels. *Chem. Rev.* **2016**, *116*, 1496–1539.
177. Ab-Rahim, S.; Selvaratnam, L.; Raghavendran, H.R.B.; Kamarul, T. Chondrocyte-alginate constructs with or without TGF-β1 produces superior extracellular matrix expression than monolayer cultures. *Mol. Cell. Biochem.* **2013**, *376*, 11–20.
178. Ozbolat, I.T.; Chen, H.; Yu, Y. Development of "Multi-arm Bioprinter" for hybrid biofabrication of tissue engineering constructs. Robot. *Comput. Integr. Manuf.* **2014**, *30*, 295–304.
179. Zhang, Y.; Yu, Y.; Akkouch, A.; Dababneh, A.; Dolati, F.; Ozbolat, I.T. In vitro study of directly bioprinted perfusable vasculature conduits. *Biomater. Sci.* **2015**, *3*, 134–143.
180. Cohen, D.L.; Lo, W.; Tsavaris, A.; Peng, D.; Lipson, H.; Bonassar, L.J. Increased mixing improves hydrogel homogeneity and quality of three-dimensional printed constructs. *Tissue Eng. Part C.* Methods **2011**, *17*, 239–248.
181. Ferreira, A.M.; Gentile, P.; Chiono, V.; Ciardelli, G. Collagen for bone tissue regeneration. *Acta Biomater.* **2012**, *8*, 3191–3200.
182. Smith, C.M.; Stone, A.L.; Parkhill, R.L.; Stewart, R.L.; Simpkins, M.W.; Kachurin, A.M.; Warren, W.L.; Williams, S.K. Three-dimensional bioassembly tool for generating viable tissue-engineered constructs. *Tissue Eng.* **2004**, *10*, 1566–1576.
183. Homenick, C.M.; De Silveira, G.; Sheardown, H.; Adronov, A. Pluronics as crosslinking agents for collagen: Novel amphiphilic hydrogels. *Polym. Int.* **2011**, *60*, 458–465.
184. Deitch, S.; Kunkle, C.; Cui, X.; Boland, T.; Dean, D. Collagen Matrix Alignment Using Inkjet Printer Technology. *MRS Proc.* **2008**, *1094*.
185. Yanez, M.; Rincon, J.; Dones, A.; De Maria, C.; Gonzales, R.; Boland, T. In vivo assessment of printed microvasculature in a bilayer skin graft to treat full-thickness wounds. *Tissue Eng. - Part A* **2015**, *21*, 224–233.
186. Gruene, M.; Pflaum, M.; Hess, C.; Diamantouros, S.; Schlie, S.; Deiwick, A.; Koch, L.; Wilhelmi, M.; Jockenhoevel, S.; Haverich, A.; Chichkov, B. Laser printing of three-dimensional multicellular arrays for studies of cell-cell and cell-environment interactions. *Tissue Eng. Part C. Methods* **2011**, *17*, 973–982.
187. Chiou, B. Sen; Avena-Bustillos, R.J.; Bechtel, P.J.; Jafri, H.; Narayan, R.; Imam, S.H.; Glenn, G.M.; Orts, W.J. Cold water fish gelatin films: Effects of cross-linking on thermal, mechanical, barrier, and biodegradation properties. *Eur. Polym. J.* **2008**, *44*, 3748–3753.
188. Sakai, S.; Hirose, K.; Taguchi, K.; Ogushi, Y.; Kawakami, K. An injectable, in situ enzymatically gellable, gelatin derivative for drug delivery and tissue engineering. *Biomaterials* **2009**, *30*, 3371–3377.
189. Hellio, D.; Djabourov, M. Physically and chemically crosslinked gelatin gels. *In Proceedings of the Macromolecular Symposia*; **2006**; Vol. 241, pp. 23–27.
190. Boland, T.; Tao, X.; Damon, B.J.; Manley, B.; Kesari, P.; Jalota, S.; Bhaduri, S. Drop-on-demand printing of cells and materials for designer tissue constructs. *Mater. Sci. Eng. C* **2007**, *27*, 372–376.
191. Schiele, N.R.; Koppes, R.A.; Corr, D.T.; Ellison, K.S.; Thompson, D.M.; Ligon, L.A.; Lippert, T.K.M.; Chrisey, D.B. Laser direct writing of combinatorial libraries of idealized cellular constructs: Biomedical applications. *Appl. Surf. Sci.* **2009**, *255*, 5444–5447.
192. Zhong, S.P.; Campoccia, D.; Doherty, P.J.; Williams, R.L.; Benedetti, L.; Williams, D.F. Biodegradation of hyaluronic acid derivatives by hyaluronidase. *Biomaterials* **1994**, *15*, 359–365.
193. Nichol, J.W.; Koshy, S.T.; Bae, H.; Hwang, C.M.; Yamanlar, S.; Khademhosseini, A. Cell-laden microengineered gelatin methacrylate hydrogels. *Biomaterials* **2010**, *31*, 5536–5544.

194. Mesa, M.; Sierra, L.; Patarin, J.; Guth, J.L. Morphology and porosity characteristics control of SBA-16 mesoporous silica. Effect of the triblock surfactant Pluronic F127 degradation during the synthesis. *Solid State Sci.* **2005**, *7*, 990–997.
195. Gong, C.Y.; Shi, S.; Dong, P.W.; Zheng, X.L.; Fu, S.Z.; Guo, G.; Yang, J.L.; Wei, Y.Q.; Qian, Z.Y. In vitro drug release behavior from a novel thermosensitive composite hydrogel based on Pluronic f127 and poly(ethylene glycol)-poly(epsilon-caprolactone)-poly(ethylene glycol) copolymer. *BMC Biotechnol.* **2009**, *9*, 8.
196. Wu, W.; Deconinck, A.; Lewis, J.A. Omnidirectional printing of 3D microvascular networks. *Adv. Mater.* **2011**, *23*, H178–H183.
197. Lin, C.-C.; Anseth, K.S. PEG hydrogels for the controlled release of biomolecules in regenerative medicine. *Pharm. Res.* **2009**, *26*, 631–643.
198. Bertassoni, L.E.; Cardoso, J.C.; Manoharan, V.; Cristino, A.L.; Bhise, N.S.; Araujo, W.A.; Zorlutuna, P.; Vrana, N.E.; Ghaemmaghami, A.M.; Dokmeci, M.R.; Khademhosseini, A. Direct-write bioprinting of cell-laden methacrylated gelatin hydrogels. *Biofabrication* ***2014***, *6*, 024105.
199. Cui, X.; Breitenkamp, K.; Finn, M.G.; Lotz, M.; D'Lima, D.D. Direct human cartilage repair using three-dimensional bioprinting technology. *Tissue Eng. - Part A* **2012**, *18*, 1304–1312.
200. Hribar, K.C.; Soman, P.; Warner, J.; Chung, P.; Chen, S. Light-assisted direct-write of 3D functional biomaterials. *Lab Chip* **2014**, *14*, 268–275.
201. Jessop, Z.M.; Al-Sabah, A.; Gardiner, M.D.; Combellack, E.; Hawkins, K.; Whitaker, I.S. 3D bioprinting for reconstructive surgery: Principles, applications and challenges. *J. Plast. Reconstr. Aesthet. Surg.* **2017**, *70*, 1155–1170.
202. Mironov, V. Toward human organ printing: Charleston Bioprinting Symposium. *Asaio J.* **2006**, *52*, e27–e30.
203. Xu, T.; Binder, K.W.; Albanna, M.Z.; Dice, D.; Zhao, W.; Yoo, J.J.; Atala, A. Hybrid printing of mechanically and biologically improved constructs for cartilage tissue engineering applications. *Biofabrication* **2013**, *5*, 015001.
204. Ma, B.; Leijten, J.C.H.; Wu, L.; Kip, M.; van Blitterswijk, C.A.; Post, J.N.; Karperien, M. Gene expression profiling of dedifferentiated human articular chondrocytes in monolayer culture. *Osteoarthr. Cartil.* **2013**, *21*, 599–603.
205. Dominici, M.; Le Blanc, K.; Mueller, I.; Slaper-Cortenbach, I.; Marini, F.; Krause, D.; Deans, R.; Keating, A.; Prockop, D.; Horwitz, E. Minimal criteria for defining multipotent mesenchymal stromal cells. The International Society for Cellular Therapy position statement. *Cytotherapy* **2006**, *8*, 315–317.
206. Brini, A.T.; Niada, S.; Lambertini, E.; Torreggiani, E.; Arrigoni, E.; Lisignoli, G.; Piva, R. Chondrogenic potential of human mesenchymal stem cells and expression of Slug transcription factor. *J. Tissue Eng. Regen. Med.* **2015**, *9*, 740–744.
207. Visser, J.; Gawlitta, D.; Benders, K.E.M.; Toma, S.M.H.; Pouran, B.; van Weeren, P.R.; Dhert, W.J.A.; Malda, J. Endochondral bone formation in gelatin methacrylamide hydrogel with embedded cartilage-derived matrix particles. *Biomaterials* **2015**, *37*, 174–182.
208. Vermonden, T.; Censi, R.; Hennink, W.E. Hydrogels for protein delivery. *Chem. Rev.* **2012**, *112*, 2853–2888.
209. Poldervaart, M.T.; Wang, H.; van der Stok, J.; Weinans, H.; Leeuwenburgh, S.C.G.; Öner, F.C.; Dhert, W.J.A.; Alblas, J. Sustained release of BMP-2 in bioprinted alginate for osteogenicity in mice and rats. *PLoS One* **2013**, *8*, e72610.
210. Pati, F.; Jang, J.; Ha, D.H.; Won Kim, S.; Rhie, J.W.; Shim, J.H.; Kim, D.H.; Cho, D.W. Printing three-dimensional tissue analogues with decellularized extracellular matrix bioink. *Nat. Commun.* **2014**, *5*.
211. Fedorovich, N.E.; Schuurman, W.; Wijnberg, H.M.; Prins, H.-J.; van Weeren, P.R.; Malda, J.; Alblas, J.; Dhert, W.J.A. Biofabrication of osteochondral tissue equivalents by printing topologically defined, cell-laden hydrogel scaffolds. *Tissue Eng. Part C. Methods* **2012**, *18*, 33–44.
212. Carlier, A.; Skvortsov, G.A.; Hafezi, F.; Ferraris, E.; Patterson, J.; Koç, B.; Van Oosterwyck, H. Computational model-informed design and bioprinting of cell-patterned constructs for bone tissue engineering. *Biofabrication* **2016**, *8*, 025009.

213. Tatman, P.D.; Gerull, W.; Sweeney-Easter, S.; Davis, J.I.; Gee, A.O.; Kim, D.-H. Multiscale Biofabrication of Articular Cartilage: Bioinspired and Biomimetic Approaches. *Tissue Eng. Part B. Rev.* **2015**, *21*, 543–559.
214. Keriquel, V.; Guillemot, F.; Arnault, I.; Guillotin, B.; Miraux, S.; Amédée, J.; Fricain, J.-C.; Catros, S. In vivo bioprinting for computer- and robotic-assisted medical intervention: preliminary study in mice. *Biofabrication* **2010**, *2*, 014101.
215. Onofrillo, C.; Duchi, S.; O'Connell, C.D.; Blanchard, R.; O'Connor, A.J.; Scott, M.; Wallace, G.G.; Choong, P.F.M.; Di Bella, C. Biofabrication of human articular cartilage: a path towards the development of a clinical treatment. *Biofabrication* **2018**, *10*, 045006.
216. Vinod, E.; Boopalan, P.R.J.V.C.; Sathishkumar, S. Reserve or Resident Progenitors in Cartilage? Comparative Analysis of Chondrocytes versus Chondroprogenitors and Their Role in Cartilage Repair. *Cartilage* **2018**, *9*, 171–182.
217. Gentili, C.; Cancedda, R. Cartilage and bone extracellular matrix. *Curr. Pharm. Des.* **2009**, *15*, 1334–1348.
218. Loeser, R.F.; Goldring, S.R.; Scanzello, C.R.; Goldring, M.B. Osteoarthritis: a disease of the joint as an organ. *Arthritis Rheum.* **2012**, *64*, 1697–1707.
219. Hunziker, E.B.; Lippuner, K.; Keel, M.J.B.; Shintani, N. An educational review of cartilage repair: precepts & practice--myths & misconceptions--progress & prospects. *Osteoarthr. Cartil.* **2015**, *23*, 334–350.
220. Huey, D.J.; Hu, J.C.; Athanasiou, K.A. Unlike bone, cartilage regeneration remains elusive. *Science* **2012**, *338*, 917–921.
221. Johnstone, B.; Hering, T.M.; Caplan, A.I.; Goldberg, V.M.; Yoo, J.U. In vitro chondrogenesis of bone marrow-derived mesenchymal progenitor cells. *Exp. Cell Res.* **1998**, *238*, 265–272.
222. Wakitani, S.; Imoto, K.; Yamamoto, T.; Saito, M.; Murata, N.; Yoneda, M. Human autologous culture expanded bone marrow mesenchymal cell transplantation for repair of cartilage defects in osteoarthritic knees. *Osteoarthr. Cartil.* **2002**, *10*, 199–206.
223. Pretzel, D.; Linss, S.; Rochler, S.; Endres, M.; Kaps, C.; Alsalameh, S.; Kinne, R.W. Relative percentage and zonal distribution of mesenchymal progenitor cells in human osteoarthritic and normal cartilage. *Arthritis Res. Ther.* **2011**, *13*, R64.
224. Jones, E.A.; Crawford, A.; English, A.; Henshaw, K.; Mundy, J.; Corscadden, D.; Chapman, T.; Emery, P.; Hatton, P.; McGonagle, D. Synovial fluid mesenchymal stem cells in health and early osteoarthritis: detection and functional evaluation at the single-cell level. *Arthritis Rheum.* **2008**, *58*, 1731–1740.
225. Mueller, M.B.; Tuan, R.S. Functional characterization of hypertrophy in chondrogenesis of human mesenchymal stem cells. *Arthritis Rheum.* **2008**, *58*, 1377–1388.
226. Hamada, T.; Sakai, T.; Hiraiwa, H.; Nakashima, M.; Ono, Y.; Mitsuyama, H.; Ishiguro, N. Surface markers and gene expression to characterize the differentiation of monolayer expanded human articular chondrocytes. *Nagoya J. Med. Sci.* **2013**, *75*, 101–111.
227. Kon, E.; Filardo, G.; Di Martino, A.; Marcacci, M. Platelet-rich plasma (PRP) to treat sports injuries: evidence to support its use. *Knee Surg. Sports Traumatol. Arthrosc.* **2011**, *19*, 516–527.
228. Romaldini, A.; Mastrogiacomo, M.; Cancedda, R.; Descalzi, F. Platelet Lysate Activates Human Subcutaneous Adipose Tissue Cells by Promoting Cell Proliferation and Their Paracrine Activity Toward Epidermal Keratinocytes. *Front. Bioeng. Biotechnol.* **2018**, *6*, 203.
229. Lucarelli, E.; Beccheroni, A.; Donati, D.; Sangiorgi, L.; Cenacchi, A.; Del Vento, A.M.; Meotti, C.; Bertoja, A.Z.; Giardino, R.; Fornasari, P.M.; Mercuri, M.; Picci, P. Platelet-derived growth factors enhance proliferation of human stromal stem cells. *Biomaterials* **2003**, *24*, 3095–3100.
230. Krüger, J.P.; Hondke, S.; Endres, M.; Pruss, A.; Siclari, A.; Kaps, C. Human platelet-rich plasma stimulates migration and chondrogenic differentiation of human subchondral progenitor cells. *J. Orthop. Res.* **2012**, *30*, 845–852.
231. Cancedda, R.; Bollini, S.; Descalzi, F.; Mastrogiacomo, M.; Tasso, R. Learning from Mother Nature: Innovative Tools to Boost Endogenous Repair of Critical or Difficult-to-Heal Large Tissue Defects. *Front. Bioeng. Biotechnol.* **2017**, *5*, 1–13.
232. Cole, B.J.; Karas, V.; Hussey, K.; Pilz, K.; Fortier, L.A. Hyaluronic Acid Versus Platelet-Rich Plasma: A Prospective, Double-Blind Randomized Controlled Trial Comparing Clinical Outcomes and Effects

on Intra-articular Biology for the Treatment of Knee Osteoarthritis. *Am. J. Sports Med.* **2017**, *45*, 339–346.
233. Siclari, A.; Mascaro, G.; Gentili, C.; Kaps, C.; Cancedda, R.; Boux, E. Cartilage repair in the knee with subchondral drilling augmented with a platelet-rich plasma-immersed polymer-based implant. *Knee Surg. Sports Traumatol. Arthrosc.* **2014**, *22*, 1225–1234.
234. Akeda, K.; An, H.S.; Okuma, M.; Attawia, M.; Miyamoto, K.; Thonar, E.J.-M.A.; Lenz, M.E.; Sah, R.L.; Masuda, K. Platelet-rich plasma stimulates porcine articular chondrocyte proliferation and matrix biosynthesis. *Osteoarthr. Cartil.* **2006**, *14*, 1272–1280.
235. van Buul, G.M.; Koevoet, W.L.M.; Kops, N.; Bos, P.K.; Verhaar, J.A.N.; Weinans, H.; Bernsen, M.R.; van Osch, G.J.V.M. Platelet-rich plasma releasate inhibits inflammatory processes in osteoarthritic chondrocytes. *Am. J. Sports Med.* **2011**, *39*, 2362–2370.
236. Zhang, Y.; Morgan, B.J.; Smith, R.; Fellows, C.R.; Thornton, C.; Snow, M.; Francis, L.W.; Khan, I.M. Platelet-rich plasma induces post-natal maturation of immature articular cartilage and correlates with LOXL1 activation. *Sci. Rep.* **2017**, *7*, 1–12.
237. Sellberg, F.; Berglund, E.; Ronaghi, M.; Strandberg, G.; Löf, H.; Sommar, P.; Lubenow, N.; Knutson, F.; Berglund, D. Composition of growth factors and cytokines in lysates obtained from fresh versus stored pathogen-inactivated platelet units. *Transfus. Apher. Sci.* **2016**, *55*, 333–337.
238. Wiese, C.; Rolletschek, A.; Kania, G.; Blyszczuk, P.; Tarasov, K. V.; Tarasova, Y.; Wersto, R.P.; Boheler, K.R.; Wobus, A.M. Nestin expression - A property of multi-lineage progenitor cells? *Cell. Mol. Life Sci.* **2004**, *61*, 2510–2522.
239. Debacq-Chainiaux, F.; Erusalimsky, J.D.; Campisi, J.; Toussaint, O. Protocols to detect senescence-associated beta-galactosidase (SA-betagal) activity, a biomarker of senescent cells in culture and in vivo. *Nat. Protoc.* **2009**, *4*, 1798–1806.
240. Shin, S.I.; Freedman, V.H.; Risser, R.; Pollack, R. Tumorigenicity of virus transformed cells in nude mice is correlated specifically with anchorage independent growth in vitro. *Proc. Natl. Acad. Sci. U. S. A.* **1975**, *72*, 4435–4439.
241. Sherr, C.J. Growth factor-regulated G1 cyclins. *Stem Cells* **1994**, *12 Suppl 1*, 47–55.
242. Kienzle, G.; von Kempis, J. Vascular cell adhesion molecule 1 (CD106) on primary human articular chondrocytes: functional regulation of expression by cytokines and comparison with intercellular adhesion molecule 1 (CD54) and very late activation antigen 2. *Arthritis Rheum.* **1998**, *41*, 1296–1305.
243. Bernal, A.; Arranz, L. Nestin-expressing progenitor cells: function, identity and therapeutic implications. *Cell. Mol. Life Sci.* **2018**, *75*, 2177–2195.
244. Mignone, J.L.; Kukekov, V.; Chiang, A.-S.; Steindler, D.; Enikolopov, G. Neural stem and progenitor cells in nestin-GFP transgenic mice. *J. Comp. Neurol.* **2004**, *469*, 311–224.
245. Pereira, R.C.; Benelli, R.; Canciani, B.; Scaranari, M.; Daculsi, G.; Cancedda, R.; Gentili, C. Beta-tricalcium phosphate ceramic triggers fast and robust bone formation by human mesenchymal stem cells. *J. Tissue Eng. Regen. Med.* **2019**, *13*, 1007–1018.
246. Sanchez, C.; Bay-Jensen, A.C.; Pap, T.; Dvir-Ginzberg, M.; Quasnichka, H.; Barrett-Jolley, R.; Mobasheri, A.; Henrotin, Y. Chondrocyte secretome: a source of novel insights and exploratory biomarkers of osteoarthritis. *Osteoarthr. Cartil.* **2017**, *25*, 1199–1209.
247. Summers, K.L.; O'Donnell, J.L.; Hoy, M.S.; Peart, M.; Dekker, J.; Rothwell, A.; Hart, D.N. Monocyte-macrophage antigen expression on chondrocytes. *J. Rheumatol.* **1995**, *22*, 1326–1334.
248. Orazizadeh, M.; Salter, D.M. CD147 (extracellular matrix metalloproteinase inducer-emmprin) expression by human articular chondrocytes. *Iran. Biomed. J.* **2008**, *12*, 153–158.
249. Iliopoulos, D.; Malizos, K.N.; Oikonomou, P.; Tsezou, A. Integrative microRNA and proteomic approaches identify novel osteoarthritis genes and their collaborative metabolic and inflammatory networks. *PLoS One* **2008**, *3*, e3740.
250. Schwab, W.; Gavlik, J. M.; Beichler, T.; Funk, R. H. W.; Albrecht, S.; Magdolen, V.; Luther, T.; Kasper, M.; Shakibaei, M. Expression of the urokinase-type plasminogen activator receptor in human articular chondrocytes: association with caveolin and β 1-integrin. *Histochem. Cell Biol.*, **2001**, *115*, 317–323.
251. Oh, H.; Chun, C.-H.; Chun, J.-S. Dkk-1 expression in chondrocytes inhibits experimental osteoarthritic cartilage destruction in mice. *Arthritis Rheum.* **2012**, *64*, 2568–2578.

252. Bonyadi Rad, E.; Musumeci, G.; Pichler, K.; Heidary, M.; Szychlinska, M.A.; Castrogiovanni, P.; Marth, E.; Böhm, C.; Srinivasaiah, S.; Krönke, G.; Weinberg, A.; Schäfer, U. Runx2 mediated Induction of Novel Targets ST2 and Runx3 Leads to Cooperative Regulation of Hypertrophic Differentiation in ATDC5 Chondrocytes. *Sci. Rep.* **2017**, *7*, 17947.

253. Lotz, M.; Moats, T.; Villiger, P.M. Leukemia inhibitory factor is expressed in cartilage and synovium and can contribute to the pathogenesis of arthritis. *J. Clin. Invest.* **1992**, *90*, 888–896.

254. Yao, Y.; Deng, Q.; Song, W.; Zhang, H.; Li, Y.; Yang, Y.; Fan, X.; Liu, M.; Shang, J.; Sun, C.; Tang, Y.; Jin, X.; Liu, H.; Huang, B.; Zhou, Y. MIF Plays a Key Role in Regulating Tissue-Specific Chondro-Osteogenic Differentiation Fate of Human Cartilage Endplate Stem Cells under Hypoxia. *Stem Cell Reports* **2016**, *7*, 249–262.

255. Hatfield, J.T.; Anderson, P.J.; Powell, B.C. Retinol-binding protein 4 is expressed in chondrocytes of developing mouse long bones: implications for a local role in formation of the secondary ossification center. *Histochem. Cell Biol.* **2013**, *139*, 727–734.

256. Scotece, M.; Koskinen-Kolasa, A.; Moilanen, T.; Moilanen, E.; Vuolteenaho, K. Novel adipokine associated with osteoarthritis: retinol binding protein 4 is produced by cartilage and correlates withmatrix metalloproteinasesin osteoarthritis patients. *Osteoarthr. Cartil.* **2018**, *26*, S126–S127.

257. Rai, V.; Dietz, N.E.; Dilisio, M.F.; Radwan, M.M.; Agrawal, D.K. Vitamin D attenuates inflammation, fatty infiltration, and cartilage loss in the knee of hyperlipidemic microswine. *Arthritis Res. Ther.* **2016**, *18*, 203.

258. Sandell, L.J.; Xing, X.; Franz, C.; Davies, S.; Chang, L.W.; Patra, D. Exuberant expression of chemokine genes by adult human articular chondrocytes in response to IL-1β. *Osteoarthr. Cartil.* **2008**, *16*, 1560–1571.

259. Pattappa, G.; Peroglio, M.; Sakai, D.; Mochida, J.; Benneker, L.M.; Alini, M.; Grad, S. CCL5/RANTES is a key chemoattractant released by degenerative intervertebral discs in organ culture. *Eur. Cell. Mater.* **2014**, *27*, 124–136.

260. Mazzetti, I.; Magagnoli, G.; Paoletti, S.; Uguccioni, M.; Olivotto, E.; Vitellozzi, R.; Cattini, L.; Facchini, A.; Borzì, R.M. A Role for Chemokines in the Induction of Chondrocyte Phenotype Modulation. *Arthritis Rheum.* **2004**, *50*, 112–122.

261. Hopper, N.; Henson, F.; Brooks, R.; Ali, E.; Rushton, N.; Wardale, J. Peripheral blood derived mononuclear cells enhance osteoarthritic human chondrocyte migration. *Arthritis Res. Ther.* **2015**, *17*.

262. Fiedler, J.; Röderer, G.; Günther, K.P.; Brenner, R.E. BMP-2, BMP-4, and PDGF-bb stimulate chemotactic migration of primary human mesenchymal progenitor cells. *J. Cell. Biochem.* **2002**, *87*, 305–312.

263. Fiedler, J.; Brill, C.; Blum, W.F.; Brenner, R.E. IGF-I and IGF-II stimulate directed cell migration of bone-marrow-derived human mesenchymal progenitor cells. *Biochem. Biophys. Res. Commun.* **2006,** *345*, 1177–1183.

264. Chatterjee, M.; Gawaz, M. Platelet-derived CXCL12 (SDF-1α): Basic mechanisms and clinical implications. *J. Thromb. Haemost.* **2013**, *11*, 1954–1967.

265. Ulivi, V.; Tasso, R.; Cancedda, R.; Descalzi, F. Mesenchymal stem cell paracrine activity is modulated by platelet lysate: Induction of an inflammatory response and secretion of factors maintaining macrophages in a proinflammatory phenotype. *Stem Cells Dev.* **2014**, *23*, 1858–1869.

266. Vinod, E.; Kachroo, U.; Ozbey, O.; Sathishkumar, S.; Boopalan, P.R.J.V.C. Comparison of human articular chondrocyte and chondroprogenitor cocultures and monocultures: To assess chondrogenic potential and markers of hypertrophy. *Tissue Cell* **2019**, *57*, 42–48.

267. Chen, J.H.; Ozanne, S.E.; Hales, C.N. Analysis of expression of growth factor receptors in replicatively and oxidatively senescent human fibroblasts. *FEBS Lett.* **2005**, *579*, 6388–6394.

268. Itahana, K.; Dimri, G.P.; Hara, E.; Itahana, Y.; Zou, Y.; Desprez, P.Y.; Campisi, J. A role for p53 in maintaining and establishing the quiescence growth arrest in human cells. *J. Biol. Chem.* **2002**, *277*, 18206–18214.

269. Jeon, O.H.; Kim, C.; Laberge, R.-M.; Demaria, M.; Rathod, S.; Vasserot, A.P.; Chung, J.W.; Kim, D.H.; Poon, Y.; David, N.; Baker, D.J.; van Deursen, J.M.; Campisi, J.; Elisseeff, J.H. Local clearance of senescent cells attenuates the development of post-traumatic osteoarthritis and creates a pro-regenerative environment. *Nat. Med.* **2017**, *23*, 775–781.

270. Kienzle, G.; Von Kempis, J. Vascular cell adhesion molecule 1 (CD106) on primary human articular chondrocytes: Functional regulation of expression by cytokines and comparison with intercellular adhesion molecule 1 (CD54) and very late activation antigen 2. *Arthritis Rheum.* **1998**, *41*, 1296–1305.
271. Jiang, Y.; Cai, Y.; Zhang, W.; Yin, Z.; Hu, C.; Tong, T.; Lu, P.; Zhang, S.; Neculai, D.; Tuan, R.S.; Ouyang, H.W. Human Cartilage-Derived Progenitor Cells From Committed Chondrocytes for Efficient Cartilage Repair and Regeneration. *Stem Cells Transl. Med.* **2016**, *5*, 733–744.
272. Su, X.; Zuo, W.; Wu, Z.; Chen, J.; Wu, N.; Ma, P.; Xia, Z.; Jiang, C.; Ye, Z.; Liu, S.; Zhou, G.; Wan, C.; Qiu, G. CD146 as a new marker for an increased chondroprogenitor cell sub-population in the later stages of osteoarthritis. *J. Orthop. Res.* **2015**, *33*, 84–91.
273. Méndez-Ferrer, S.; Michurina, T. V.; Ferraro, F.; Mazloom, A.R.; MacArthur, B.D.; Lira, S.A.; Scadden, D.T.; Ma'ayan, A.; Enikolopov, G.N.; Frenette, P.S. Mesenchymal and haematopoietic stem cells form a unique bone marrow niche. *Nature* **2010**, *466*, 829–834.
274. Fellows, C.R.; Khan, I.M.; Archer, C.W. Articular cartilage contains a nestin positive stem cell population. *Eur. Cell Mater.* **2014**, *28*, 55.
275. Dell'Accio, F.; De Bari, C.; Luyten, F.P. Molecular markers predictive of the capacity of expanded human articular chondrocytes to form stable cartilage in vivo. *Arthritis Rheum.* **2001**, *44*, 1608–1619.
276. Oda, T.; Sakai, T.; Hiraiwa, H.; Hamada, T.; Ono, Y.; Nakashima, M.; Ishizuka, S.; Matsukawa, T.; Yamashita, S.; Tsuchiya, S.; Ishiguro, N.Osteoarthritis-derived chondrocytes are a potential source of multipotent progenitor cells for cartilage tissue engineering. *Biochem. Biophys. Res. Commun.* **2016**, *479*, 469–475.
277. Wang, K.; Li, J.; Li, Z.; Wang, B.; Qin, Y.; Zhang, N.; Zhang, H.; Su, X.; Wang, Y.; Zhu, H. Chondrogenic Progenitor Cells Exhibit Superiority Over Mesenchymal Stem Cells and Chondrocytes in Platelet-Rich Plasma Scaffold-Based Cartilage Regeneration. *Am. J. Sports Med.* **2019**.
278. De Luca, P.; Kouroupis, D.; Viganò, M.; Perucca-Orfei, C.; Kaplan, L.; Zagra, L.; de Girolamo, L.; Correa, D.; Colombini, A. Human Diseased Articular Cartilage Contains a Mesenchymal Stem Cell-Like Population of Chondroprogenitors with Strong Immunomodulatory Responses. *J. Clin. Med.* **2019**, *8*, 423.
279. De Seny, D.; Cobraiville, G.; Charlier, E.; Neuville, S.; Lutteri, L.; Goff, C. Le; Malaise, D.; Malaise, O.; Chapelle, J.P.; Relic, B.; Malaise, M.G. Apolipoprotein-A1 as a damage-associated molecular patterns protein in osteoarthritis: Ex vivo and in vitro pro-inflammatory properties. *PLoS One* **2015**, *10*, e0122904.
280. Gómez, R.; Conde, J.; Scotece, M.; Gómez-Reino, J.J.; Lago, F.; Gualillo, O. What's new in our understanding of the role of adipokines in rheumatic diseases? *Nat. Rev. Rheumatol.* **2011**, *7*, 528–536.
281. Vallabhaneni, K.C.; Tkachuk, S.; Kiyan, Y.; Shushakova, N.; Haller, H.; Dumler, I.; Eden, G. Urokinase receptor mediates mobilization, migration, and differentiation of mesenchymal stem cells. *Cardiovasc. Res.* **2011**, *90*, 113–121.
282. Bodine, P.V.N. Wnt signaling control of bone cell apoptosis. *Cell Res.* **2008**, *18*, 248–253.
283. Wu, J.; Huang, J.F.; Qin, X.X.; Hu, F.; Chen, Z.F.; Zheng, Y.; Liu, Y.X.; Cai, X.H. Platelet-rich plasma inhibits Wnt/β-catenin signaling in rabbit cartilage cells activated by IL-1β. *Int. Immunopharmacol.* **2018**, *55*, 282–289.
284. Paralkar, V.M.; Vail, A.L.; Grasser, W.A.; Brown, T.A.; Xu, H.; Vukicevic, S.; Ke, H.Z.; Qi, H.; Owen, T.A.; Thompson, D.D. Cloning and characterization of a novel member of the transforming growth factor-β/bone morphogenetic protein family. *J. Biol. Chem.* **1998**, *273*, 13760–13767.
285. Higgins, P.J.; Czekay, R.P.; Wilkins-Port, C.E.; Higgins, S.P.; Freytag, J.; Overstreet, J.M.; Klein, R.M.; Higgins, C.E.; Samarakoon, R. PAI-1: An integrator of cell signaling and migration. *Int. J. Cell Biol.* **2011**.
286. Liu, W.; Liu, D.; Zheng, J.; Shi, P.; Chou, P.-H.; Oh, C.; Chen, D.; An, H.S.; Chee, A. Annulus fibrosus cells express and utilize C-C chemokine receptor 5 (CCR5) for migration. *Spine J.* **2017**, *17*, 720–726.
287. Kucia, M.; Reca, R.; Miekus, K.; Wanzeck, J.; Wojakowski, W.; Janowska-Wieczorek, A.; Ratajczak, J.; Ratajczak, M.Z. Trafficking of Normal Stem Cells and Metastasis of Cancer Stem Cells Involve Similar Mechanisms: Pivotal Role of the SDF-1-CXCR4 Axis. *Stem Cells* **2005**, *23*, 879–894.

288. Zhong, L.; Huang, X.; Rodrigues, E.D.; Leijten, J.C.H.; Verrips, T.; El Khattabi, M.; Karperien, M.; Post, J.N. Endogenous DKK1 and FRZB Regulate Chondrogenesis and Hypertrophy in Three-Dimensional Cultures of Human Chondrocytes and Human Mesenchymal Stem Cells. *Stem Cells Dev.* **2016**, *25*, 1808–1817.
289. Lian, J.B.; McKee, M.D.; Todd, A.M.; Gerstenfeld, L.C. Induction of bone-related proteins, osteocalcin and osteopontin, and their matrix ultrastructural localization with development of chondrocyte hypertrophy in vitro. *J. Cell. Biochem.* **1993**, *52*, 206–219.
290. Martel-Pelletier, J.; Cloutier, J.M.; Pelletier, J.P. Cathepsin B and cysteine protease inhibitors in human osteoarthritis. *J. Orthop. Res.* **1990**, *8*, 336–344.
291. Herlihy, S.E.; Brown, M.L.; Pilling, D.; Weeks, B.R.; Myers, L.K.; Gomer, R.H. Role of the Neutrophil Chemorepellent Soluble Dipeptidyl Peptidase IV in Decreasing Inflammation in a Murine Model of Arthritis. *Arthritis Rheumatol.* **2015**, *67*, 2634–2638.
292. Jayasuriya, C.T.; Twomey-Kozak, J.; Newberry, J.; Desai, S.; Feltman, P.; Franco, J.R.; Li, N.; Terek, R.; Ehrlich, M.G.; Owens, B.D. Human Cartilage-Derived Progenitors Resist Terminal Differentiation and Require CXCR4 Activation to Successfully Bridge Meniscus Tissue Tears. *Stem Cells* **2019**, *37*, 102–114.
293. Poole, A.R.; Kojima, T.; Yasuda, T.; Mwale, F.; Kobayashi, M.; Laverty, S. Composition and structure of articular cartilage: a template for tissue repair. *Clin. Orthop. Relat. Res.* **2001**, *391*, S26–S33.
294. Buckwalter, J.A.; Mankin, H.J. Articular cartilage: tissue design and chondrocyte-matrix interactions. *Instr. Course Lect.* **1998**, *47*, 477–486.
295. Sophia Fox, A.J.; Bedi, A.; Rodeo, S.A. The basic science of articular cartilage: Structure, composition, and function. *Sports Health* **2009**, *1*, 461–468.
296. Heijink, A.; Gomoll, A.H.; Madry, H.; Drobnič, M.; Filardo, G.; Espregueira-Mendes, J.; van Dijk, C.N. Biomechanical considerations in the pathogenesis of osteoarthritis of the knee. K*nee Surgery, Sport. Traumatol. Arthrosc.* **2012**, *20*, 423–435.
297. Steadman, J.R.; Rodkey, W.G.; Singleton, S.B.; Briggs, K.K. Microfracture technique for full-thickness chondral defects: Technique and clinical results. *Oper. Tech. Orthop.* **1997**, *7*, 300–304.
298. Brittberg, M.; Lindahl, A.; Nilsson, A.; Ohlsson, C.; Isaksson, O.; Peterson, L. Treatment of deep cartilage defects in the knee with autologous chondrocyte transplantation. *N. Engl. J. Med.* **1994**, *331*, 889–895.
299. Roberts, S.; Menage, J.; Sandell, L.J.; Evans, E.H.; Richardson, J.B. Immunohistochemical study of collagen types I and II and procollagen IIA in human cartilage repair tissue following autologous chondrocyte implantation. *Knee* **2009**, *16*, 398–404.
300. Frank, R.M.; Cotter, E.J.; Nassar, I.; Cole, B. Failure of bone marrow stimulation techniques. *Sports Med. Arthrosc.* **2017**, *25*, 2–9.
301. Steinert, A.F.; Ghivizzani, S.C.; Rethwilm, A.; Tuan, R.S.; Evans, C.H.; Nöth, U. Major biological obstacles for persistent cell-based regeneration of articular cartilage. *Arthritis Res. Ther.* **2007**, *9*, 213.
302. Holtzer, H.; Abbott, J.; Lash, J.; Holtzer, S. The loss of phenotypic traits by differentiated cells in vitro, I. Dedifferentiation of cartilage cells. *Proc. Natl. Acad. Sci.* **1960**, *46*, 1533–1542.
303. Lin, Z.; Fitzgerald, J.B.; Xu, J.; Willers, C.; Wood, D.; Grodzinsky, A.J.; Zheng, M.H. Gene expression profiles of human chondrocytes during passaged monolayer cultivation. *J. Orthop. Res.* **2008**, *26*, 1230–1237.
304. Von Der Mark, K.; Gauss, V.; Von Der Mark, H.; Müller, P. Relationship between cell shape and type of collagen synthesised as chondrocytes lose their cartilage phenotype in culture. *Nature* **1977**, *267*, 531–532.
305. Mandl, E.W.; Jahr, H.; Koevoet, J.L.M.; Van Leeuwen, J.P.T.M.; Weinans, H.; Verhaar, J.A.N.; Van Osch, G.J.V.M. Fibroblast growth factor-2 in serum-free medium is a potent mitogen and reduces dedifferentiation of human ear chondrocytes in monolayer culture. *Matrix Biol.* **2004**, *23*, 231–241.
306. Van Osch, G.J.V.M.; Marijnissen, W.J.C.M.; Van Der Veen, S.W.; Verwoerd-Verhoef, H.L. The Potency of Culture-Expanded Nasal Septum Chondrocytes for Tissue Engineering of Cartilage. *Am. J. Rhinol.* **2001**, *15*, 187–192.

307. Schulze-Tanzil, G.; De Souza, P.; Villegas Castrejon, H.; John, T.; Merker, H.J.; Scheid, A.; Shakibaei, M. Redifferentiation of dedifferentiated human chondrocytes in high-density cultures. *Cell Tissue Res.* **2002**, *308*, 371–379.
308. Demoor, M.; Ollitrault, D.; Gomez-Leduc, T.; Bouyoucef, M.; Hervieu, M.; Fabre, H.; Lafont, J.; Denoix, J.M.; Audigié, F.; Mallein-Gerin, F.; Legendre, F.; Galera, P. Cartilage tissue engineering: Molecular control of chondrocyte differentiation for proper cartilage matrix reconstruction. *Biochim. Biophys. Acta - Gen. Subj.* **2014**, *1840*, 2414–2440.
309. Markway, B.D.; Cho, H.; Johnstone, B. Hypoxia promotes redifferentiation and suppresses markers of hypertrophy and degeneration in both healthy and osteoarthritic chondrocytes. *Arthritis Res. Ther.* **2013**, *15*, R92.
310. Lin, Z.; Willers, C.; Xu, J.; Zheng, M.-H. The chondrocyte: biology and clinical application. *Tissue Eng.* **2006**, *12*, 1971–1984.
311. Caron, M.M.J.; Emans, P.J.; Coolsen, M.M.E.; Voss, L.; Surtel, D.A.M.; Cremers, A.; van Rhijn, L.W.; Welting, T.J.M. Redifferentiation of dedifferentiated human articular chondrocytes: comparison of 2D and 3D cultures. *Osteoarthr. Cartil.* **2012**, *20*, 1170–1178.
312. Parreno, J.; Nabavi Niaki, M.; Andrejevic, K.; Jiang, A.; Wu, P.H.; Kandel, R.A. Interplay between cytoskeletal polymerization and the chondrogenic phenotype in chondrocytes passaged in monolayer culture. *J. Anat.* **2017**, *230*, 234–248.
313. Benya, P.D.; Shaffer, J.D. Dedifferentiated chondrocytes reexpress the differentiated collagen phenotype when cultured in agarose gels. *Cell* **1982**, *30*, 215–224.
314. Buschmann, M.D.; Gluzband, Y.A.; Grodzinsky, A.J.; Kimura, J.H.; Hunziker, E.B. Chondrocytes in agarose culture synthesize a mechanically functional extracellular matrix. *J. Orthop. Res.* **1992**, *10*, 745–758.
315. Perka, C.; Spitzer, R.S.; Lindenhayn, K.; Sittinger, M.; Schultz, O. Matrix-mixed culture: new methodology for chondrocyte culture and preparation of cartilage transplants. *J. Biomed. Mater. Res.* **2000**, *49*, 305–311.
316. Bianchi, V.J.; Lee, A.; Anderson, J.; Parreno, J.; Theodoropoulos, J.; Backstein, D.; Kandel, R. Redifferentiated Chondrocytes in Fibrin Gel for the Repair of Articular Cartilage Lesions. *Am. J. Sports Med.* **2019,** *47*, 2348–2359.
317. Aurich, M.; Hofmann, G.O.; Best, N.; Rolauffs, B. Induced Redifferentiation of Human Chondrocytes from Articular Cartilage Lesion in Alginate Bead Culture After Monolayer Dedifferentiation: An Alternative Cell Source for Cell-Based Therapies? *Tissue Eng. Part A* **2018**, *24*, 275–286.
318. Häuselmann, H.J.; Masuda, K.; Hunziker, E.B.; Neidhart, M.; Mok, S.S.; Michel, B.A.; Thonar, E.J. Adult human chondrocytes cultured in alginate form a matrix similar to native human articular cartilage. *Am. J. Physiol.* **1996**, *271*, C742–C752.
319. Grigolo, B.; Lisignoli, G.; Piacentini, A.; Fiorini, M.; Gobbi, P.; Mazzotti, G.; Duca, M.; Pavesio, A.; Facchini, A. Evidence for redifferentiation of human chondrocytes grown on a hyaluronan-based biomaterial (HYAFF®11): Molecular, immunohistochemical and ultrastructural analysis. *Biomaterials* **2002**, *23*, 1187–1195.
320. Zhang, Z.; McCaffery, J.M.; Spencer, R.G.S.; Francomano, C.A. Hyaline cartilage engineered by chondrocytes in pellet culture: Histological, immunohistochemical and ultrastructural analysis in comparison with cartilage explants. *J. Anat.* **2004**, *205*, 229–237.
321. Giannoni, P.; Pagano, A.; Maggi, E.; Arbicò, R.; Randazzo, N.; Grandizio, M.; Cancedda, R.; Dozin, B. Autologous chondrocyte implantation (ACI) for aged patients: Development of the proper cell expansion conditions for possible therapeutic applications. *Osteoarthr. Cartil.* **2005**, *13*, 589–600.
322. Yang, J.; Zhang, Y.S.; Yue, K.; Khademhosseini, A. Cell-laden hydrogels for osteochondral and cartilage tissue engineering. *Acta Biomater.* **2017**, *57*, 1–25.
323. Kang, H.-W.; Lee, S.J.; Ko, I.K.; Kengla, C.; Yoo, J.J.; Atala, A. A 3D bioprinting system to produce human-scale tissue constructs with structural integrity. *Nat. Biotechnol.* **2016**, *34*, 312–319.
324. Spanò, R.; Muraglia, A.; Todeschi, M.R.; Nardini, M.; Strada, P.; Cancedda, R.; Mastrogiacomo, M. Platelet-rich plasma-based bioactive membrane as a new advanced wound care tool. *J. Tissue Eng. Regen. Med.* **2018**, *12*, e82–e96.

325. Barbosa, I.; Garcia, S.; Barbier-Chassefière, V.; Caruelle, J.-P.; Martelly, I.; Papy-García, D. Improved and simple micro assay for sulfated glycosaminoglycans quantification in biological extracts and its use in skin and muscle tissue studies. *Glycobiology* **2003**, *13*, 647–653.
326. Lee, K.Y.; Mooney, D.J. Alginate: Properties and biomedical applications. *Prog. Polym. Sci.* **2012**, *37*, 106–126.
327. Mehta, S.; Watson, J.T. Platelet rich concentrate: basic science and current clinical applications. *J. Orthop. Trauma* **2008**, *22*, 432–438.
328. Eppley, B.L.; Woodell, J.E.; Higgins, J. Platelet quantification and growth factor analysis from platelet-rich plasma: Implications for wound healing. *Plast. Reconstr. Surg.* **2004**, *114*, 1502–1508.
329. Murphy, M.B.; Blashki, D.; Buchanan, R.M.; Yazdi, I.K.; Ferrari, M.; Simmons, P.J.; Tasciotti, E. Adult and umbilical cord blood-derived platelet-rich plasma for mesenchymal stem cell proliferation, chemotaxis, and cryo-preservation. *Biomaterials* **2012**, *33*, 5308–5316.
330. Sampson, S.; Gerhardt, M.; Mandelbaum, B. Platelet rich plasma injection grafts for musculoskeletal injuries: a review. *Curr. Rev. Musculoskelet. Med.* **2008**, *1*, 165–174.
331. Faramarzi, N.; Yazdi, I.K.; Nabavinia, M.; Gemma, A.; Fanelli, A.; Caizzone, A.; Ptaszek, L.M.; Sinha, I.; Khademhosseini, A.; Ruskin, J.N.; Tamayol, A. Patient-Specific Bioinks for 3D Bioprinting of Tissue Engineering Scaffolds. *Adv. Healthc. Mater.* **2018**, *7*, e1701347.
332. Nurden, A.T. Platelets, inflammation and tissue regeneration. *Thromb. Haemost.* **2011**, *105 Suppl 1*, S13–S33.
333. Toyoda, T.; Isobe, K.; Tsujino, T.; Koyata, Y.; Ohyagi, F.; Watanabe, T.; Nakamura, M.; Kitamura, Y.; Okudera, H.; Nakata, K.; Kawase, T. Direct activation of platelets by addition of $CaCl_2$ leads coagulation of platelet-rich plasma. *Int. J. Implant Dent.* **2018**, *4*, 23.
334. Qiu, M.; Chen, D.; Shen, C.; Shen, J.; Zhao, H.; He, Y. Platelet-rich plasma-loaded poly(D,L-lactide)-poly(ethylene glycol)-poly(D,L-lactide) hydrogel dressing promotes full-thickness skin wound healing in a rodent model. *Int. J. Mol. Sci.* **2016**, *17*, 1001.
335. Khansari, S.; Duzyer, S.; Sinha-Ray, S.; Hockenberger, A.; Yarin, A.L.; Pourdeyhimi, B. Two-stage desorption-controlled release of fluorescent dye and vitamin from solution-blown and electrospun nanofiber mats containing porogens. *Mol. Pharm.* **2013**, *10*, 4509–4526.
336. Martínez Ávila, H.; Schwarz, S.; Rotter, N.; Gatenholm, P. 3D bioprinting of human chondrocyte-laden nanocellulose hydrogels for patient-specific auricular cartilage regeneration. *Bioprinting* **2016**, *1*, 22–35.
337. Nuernberger, S.; Cyran, N.; Albrecht, C.; Redl, H.; Vécsei, V.; Marlovits, S. The influence of scaffold architecture on chondrocyte distribution and behavior in matrix-associated chondrocyte transplantation grafts. *Biomaterials* **2011**, *32*, 1032–1040.
338. Schuh, E.; Hofmann, S.; Stok, K.; Notbohm, H.; Müller, R.; Rotter, N. Chondrocyte redifferentiation in 3D: The effect of adhesion site density and substrate elasticity. *J. Biomed. Mater. Res. - Part A* **2012**, *100 A*, 38–47.
339. Isogai, N.; Kusuhara, H.; Ikada, Y.; Ohtani, H.; Jacquet, R.; Hillyer, J.; Lowder, E.; Landis, W.J. Comparison of different chondrocytes for use in tissue engineering of cartilage model structures. *Tissue Eng.* **2006**, *12*, 691–703.
340. Elder, S.; Thomason, J. Effect of Platelet-Rich Plasma on Chondrogenic Differentiation in Three-Dimensional Culture. *Open Orthop. J.* **2014**, *8*, 78–84.
341. Morales, T.I.; Roberts, A.B. Transforming growth factor β regulates the metabolism of proteoglycans in bovine cartilage organ cultures. *J. Biol. Chem.* **1988**, *263*, 12828–12831.
342. Coricor, G.; Serra, R. TGF-β regulates phosphorylation and stabilization of Sox9 protein in chondrocytes through p38 and Smad dependent mechanisms. *Sci. Rep.* **2016**, *6*, 38616.
343. Levato, R.; Webb, W.R.; Otto, I.A.; Mensinga, A.; Zhang, Y.; van Rijen, M.; van Weeren, R.; Khan, I.M.; Malda, J. The bio in the ink: cartilage regeneration with bioprintable hydrogels and articular cartilage-derived progenitor cells. *Acta Biomater.* **2017**, *61*, 41–53.
344. Zhou, G.; Jiang, H.; Yin, Z.; Liu, Y.; Zhang, Q.; Zhang, C.; Pan, B.; Zhou, J.; Zhou, X.; Sun, H.; Li, D.; He, A.; Zhang, Z.; Zhang, W.; Liu, W.; Cao, Y. In Vitro Regeneration of Patient-specific Ear-shaped Cartilage and Its First Clinical Application for Auricular Reconstruction. *EBioMedicine* **2018**, *28*, 287–302.